1996

Biological conversion of hydrogen sulfide to elemental sulfur in a suspended-growth continuous stirred-tank reactor.

Paul Frederick. Henshaw
University of Windsor

NOTICE

AVIS

The quality of this microform is heavily dependent upon the quality of the original thesis submitted for microfilming. Every effort has been made to ensure the highest quality of reproduction possible.

If pages are missing, contact the university which granted the degree.

Some pages may have indistinct print especially if the original pages were typed with a poor typewriter ribbon or if the university sent us an inferior photocopy.

Reproduction in full or in part of this microform is governed by the Canadian Copyright Act, R.S.C. 1970, c. C-30, and subsequent amendments.

La qualité de cette microforme dépend grandement de la qualité de la thèse soumise au microfilmage. Nous avons tout fait pour assurer une qualité supérieure de reproduction.

S'il manque des pages, veuillez communiquer avec l'université qui a conféré le grade.

La qualité d'impression de certaines pages peut laisser à désirer, surtout si les pages originales ont été dactylographiées à l'aide d'un ruban usé ou si l'université nous a fait parvenir une photocopie de qualité inférieure.

La reproduction, même partielle, de cette microforme est soumise à la Loi canadienne sur le droit d'auteur, SRC 1970, c. C-30, et ses amendements subséquents.

Biological Conversion of Hydrogen Sulfide to Elemental Sulfur in a Suspended-Growth Continuous Stirred-Tank Reactor

by

Paul F. Henshaw
B.Sc., B.Eng., M.A.Sc.

A Dissertation Submitted to the
Faculty of Graduate Studies and Research
through the Department of Civil & Environmental Engineering
in Partial Fulfillment of the Requirements for
the Degree of Doctor of Philosophy
at the University of Windsor

Windsor, Ontario, Canada

December 1995

Canada

Name _____

*Dissertation Abstracts International and Masters Abstracts International are arranged by broad, general subject categories.
Please select the one subject which most nearly describes the content of your dissertation or thesis. Enter the corresponding
four-digit code in the spaces provided.*

CHEMICAL ENGINEERING
SUBJECT TERM

| 0 | 5 | 4 | 2 |

UMI
SUBJECT CODE

Subject Categories

THE HUMANITIES AND SOCIAL SCIENCES

COMMUNICATIONS AND THE ARTS
Architecture 0729
Art History 0377
Cinema 0900
Dance 0378
Fine Arts 0357
Information Science 0723
Journalism 0391
Library Science 0399
Mass Communications 0708
Music 0413
Speech Communication 0459
Theater 0465

EDUCATION
General 0515
Administration 0514
Adult and Continuing 0516
Agricultural 0517
Art 0273
Bilingual and Multicultural 0282
Business 0688
Community College 0275
Curriculum and Instruction 0727
Early Childhood 0518
Elementary 0524
Finance 0277
Guidance and Counseling 0519
Health 0680
Higher 0745
History of 0520
Home Economics 0278
Industrial 0521
Language and Literature 0279
Mathematics 0280
Music 0522
Philosophy of 0998
Physical 0523

Psychology 0525
Reading 0535
Religious 0527
Sciences 0714
Secondary 0533
Social Sciences 0534
Sociology of 0340
Special 0529
Teacher Training 0530
Technology 0710
Tests and Measurements 0288
Vocational 0747

LANGUAGE, LITERATURE AND LINGUISTICS
Language
    General 0679
    Ancient 0289
    Linguistics 0290
    Modern 0291
Literature
    General 0401
    Classical 0294
    Comparative 0295
    Medieval 0297
    Modern 0298
    African 0316
    American 0591
    Asian 0305
    Canadian (English) 0352
    Canadian (French) 0355
    English 0593
    Germanic 0311
    Latin American 0312
    Middle Eastern 0315
    Romance 0313
    Slavic and East European 0314

PHILOSOPHY, RELIGION AND THEOLOGY
Philosophy 0422
Religion
    General 0318
    Biblical Studies 0321
    Clergy 0319
    History of 0320
    Philosophy of 0322
Theology 0469

SOCIAL SCIENCES
American Studies 0323
Anthropology
    Archaeology 0324
    Cultural 0326
    Physical 0327
Business Administration
    General 0310
    Accounting 0272
    Banking 0770
    Management 0454
    Marketing 0338
Canadian Studies 0385
Economics
    General 0501
    Agricultural 0503
    Commerce-Business 0505
    Finance 0508
    History 0509
    Labor 0510
    Theory 0511
Folklore 0358
Geography 0366
Gerontology 0351
History
    General 0578

Ancient 0579
Medieval 0581
Modern 0582
Black 0328
African 0331
Asia, Australia and Oceania 0332
Canadian 0334
European 0335
Latin American 0336
Middle Eastern 0333
United States 0337
History of Science 0585
Law 0398
Political Science
    General 0615
    International Law and
        Relations 0616
    Public Administration 0617
Recreation 0814
Social Work 0452
Sociology
    General 0626
    Criminology and Penology 0627
    Demography 0938
    Ethnic and Racial Studies 0631
    Individual and Family
        Studies 0628
    Industrial and Labor
        Relations 0629
    Public and Social Welfare 0630
    Social Structure and
        Development 0700
    Theory and Methods 0344
Transportation 0709
Urban and Regional Planning 0999
Women's Studies 0453

THE SCIENCES AND ENGINEERING

BIOLOGICAL SCIENCES
Agriculture
    General 0473
    Agronomy 0285
    Animal Culture and
        Nutrition 0475
    Animal Pathology 0476
    Food Science and
        Technology 0359
    Forestry and Wildlife 0478
    Plant Culture 0479
    Plant Pathology 0480
    Plant Physiology 0817
    Range Management 0777
    Wood Technology 0746
Biology
    General 0306
    Anatomy 0287
    Biostatistics 0308
    Botany 0309
    Cell 0379
    Ecology 0329
    Entomology 0353
    Genetics 0369
    Limnology 0793
    Microbiology 0410
    Molecular 0307
    Neuroscience 0317
    Oceanography 0416
    Physiology 0433
    Radiation 0821
    Veterinary Science 0778
    Zoology 0472
Biophysics
    General 0786
    Medical 0760

EARTH SCIENCES
Biogeochemistry 0425
Geochemistry 0996

Geodesy 0370
Geology 0372
Geophysics 0373
Hydrology 0388
Mineralogy 0411
Paleobotany 0345
Paleoecology 0426
Paleontology 0418
Paleozoology 0985
Palynology 0427
Physical Geography 0368
Physical Oceanography 0415

HEALTH AND ENVIRONMENTAL SCIENCES
Environmental Sciences 0768
Health Sciences
    General 0566
    Audiology 0300
    Chemotherapy 0992
    Dentistry 0567
    Education 0350
    Hospital Management 0769
    Human Development 0758
    Immunology 0982
    Medicine and Surgery 0564
    Mental Health 0347
    Nursing 0569
    Nutrition 0570
    Obstetrics and Gynecology 0380
    Occupational Health and
        Therapy 0354
    Ophthalmology 0381
    Pathology 0571
    Pharmacology 0419
    Pharmacy 0572
    Physical Therapy 0382
    Public Health 0573
    Radiology 0574
    Recreation 0575

Speech Pathology 0460
Toxicology 0383
Home Economics 0386

PHYSICAL SCIENCES
Pure Sciences
Chemistry
    General 0485
    Agricultural 0749
    Analytical 0486
    Biochemistry 0487
    Inorganic 0488
    Nuclear 0738
    Organic 0490
    Pharmaceutical 0491
    Physical 0494
    Polymer 0495
    Radiation 0754
Mathematics 0405
Physics
    General 0605
    Acoustics 0986
    Astronomy and
        Astrophysics 0606
    Atmospheric Science 0608
    Atomic 0748
    Electronics and Electricity 0607
    Elementary Particles and
        High Energy 0798
    Fluid and Plasma 0759
    Molecular 0609
    Nuclear 0610
    Optics 0752
    Radiation 0756
    Solid State 0611
Statistics 0463

Applied Sciences
Applied Mechanics 0346
Computer Science 0984

Engineering
    General 0537
    Aerospace 0538
    Agricultural 0539
    Automotive 0540
    Biomedical 0541
    Chemical 0542
    Civil 0543
    Electronics and Electrical 0544
    Heat and Thermodynamics 0348
    Hydraulic 0545
    Industrial 0546
    Marine 0547
    Materials Science 0794
    Mechanical 0548
    Metallurgy 0743
    Mining 0551
    Nuclear 0552
    Packaging 0549
    Petroleum 0765
    Sanitary and Municipal 0554
    System Science 0790
Geotechnology 0428
Operations Research 0796
Plastics Technology 0795
Textile Technology 0994

PSYCHOLOGY
General 0621
Behavioral 0384
Clinical 0622
Developmental 0620
Experimental 0623
Industrial 0624
Personality 0625
Physiological 0989
Psychobiology 0349
Psychometrics 0632
Social 0451

ABSTRACT

A biological process employing green sulfur bacteria was investigated to remove sulfide ($S^=$) from industrial wastewaters and convert it to elemental sulfur. This research is unique in that dissolved sulfide was present in the liquid influent fed into a continuous-flow photosynthetic bioreactor.

A suspended-growth once-through continuous-flow stirred-tank bioreactor was successfully operated under five different experimental conditions. For the first three experiments, concentrated nutrient solution and sulfide stock solution were pumped separately into a 13.7 L reactor at a hydraulic retention time of 45 hours and $S^=$ loading rates of 2.1, 4.4, and 5.6 mg/h·L. At the lowest loading rate, nearly all influent $S^=$ was oxidized to sulfate. The middle loading rate resulted in complete conversion of $S^=$ to S^0. Steady state conditions were not achieved at the highest loading rate, resulting in the accumulation of $S^=$ in the bioreactor.

In two more experiments, nutrient medium and $S^=$ stock solution were separately fed into a 12.0 L bioreactor at $S^=$ loading rates of 3.2 and 2.7 mg/h·L, and hydraulic retention times of 173 and 99 hours respectively. In these trials, the loading rates were adjusted to maintain a residual of $S^=$ in the bioreactor, and consequently, there was nearly complete conversion of the consumed $S^=$ to S^0.

A parameter was developed to relate the experiments of this dissertation with those reported in the literature, where smaller reactors and higher bacterial concentrations were used in batch reactors fed with $H_2S_{(g)}$. This parameter described the capacity of the bioreactor to consume $S^=$, and was calculated as the product of the radiant flux per unit

reactor volume and the bacteriochlorophyll concentration.

Three predictive models were developed for the bioreactor. In the yield-based model, a yield coefficient was used to link the increase in bacteriochlorophyll with the consumption of $S^=$. Poor correlations between the rates of reaction and the concentrations of the reactant sulfur species led to the conclusion that a reaction pathway-based model was not appropriate for this system. An empirical model was proposed to relate the reactor volume, $S^=$ loading rate, reactor irradiation and bacteriochlorophyll concentration.

ACKNOWLEDGEMENTS

TABLE OF CONTENTS

NOMENCLATURE

Sulfur, as used in this dissertation, refers to the sixteenth element of the Periodic Table in whatever form it may occur. In this dissertation, it also refers to the sum of measurements of all forms of sulfur, *i.e.* the "total sulfur". The inorganic species of sulfur in order of increasing valence are: sulfide, elemental sulfur, thiosulfate, sulfite, and sulfate.

Sulfide is the most reduced form of inorganic sulfur (valence -II). Sulfide is a component of metal bearing ores (eg. pyrite FeS_2). Hydrogen sulfide (H_2S) is a gas at room temperature and soluble in water (4.1 g/L). Sodium sulfide (Na_2S) is a hygroscopic solid which is highly soluble in water (47 g/L). When dissolved in water, H_2S and Na_2S exist in equilibrium with bisulfide (HS^-) and the sulfide ($S^=$) ions. At pH = 7, the sulfide is present as 48% $H_2S_{(aq)}$ and 52% HS^-. The analytical method used in this dissertation measured the amount of sulfide ion in solution as well as that associated with hydrogen (HS^-, H_2S). Thus, in this dissertation, the term sulfide ($S^=$) refers to the *total* amount of sulfide in solution whether it occurred as sulfide ion, bisulfide ion or hydrogen sulfide.

Elemental sulfur is the desired end-product of this bioprocess. The valence of elemental sulfur is zero. Although the chemical formula S^0 is used interchangeably with the term elemental sulfur in this dissertation, the sulfur molecule produced biologically is an orthorhombic crystal with formula S_8 (Truper, 1967). The density of elemental sulfur is 2.1 kg/L. It is hydrophobic and almost insoluble in water (solubility = 5 x 10^{-6} M; Chen and Morris, 1972).

Thiosulfate is a partially oxidized form of sulfur. The valence of sulfur within

thiosulfite is II. In this dissertation, the term thiosulfate ($S_2O_3^-$) refers to all forms of thiosulfate including the thiosulfate ion.

Sulfite is another partially oxidized form of sulfur. The valence of the sulfur is IV. In this dissertation, the term sulfite (SO_3^-) refers to all forms of sulfite including the sulfite ion.

Sulfate is the most oxidized form of inorganic sulfur (sulfur valence VI). It is the end product of complete biochemical sulfide oxidation. In this dissertation, the term sulfate (SO_4^-) refers to all forms of sulfate including the sulfate ion.

Illuminance is the rate of visible light incident upon a unit area of a given surface, expressed in units of lux. Illuminance refers only to light and contains the luminance efficiency weighting factor necessitated by the nonlinear wavelength-response of the human eye (CRC, 1979).

Irradiance is a measure of the rate of energy falling on a given area. The units are Watts per metre squared (W/m^2). All wavelengths are equally weighted (CRC, 1979).

Radiant flux, by analogy to the term luminous flux, is the rate of total electromagnetic energy striking a surface. The unit of radiant flux is the Watt (W).

Attached-growth (fixed-film) is a type of bioreactor in which the bacterial cells are grown attached to a surface.

Suspended-growth (free-cell) is a type of bioreactor in which the bacterial cells are kept in suspension and not attached to a surface.

LIST OF ABBREVIATIONS

ACS   American Chemical Society

bchl   bacteriochlorophyll, the coloured pigment in photosynthetic bacteria

BOD   biochemical oxygen demand

C. thio.   *Chlorobium limicola* forma specialis *thiosulfatophilum*

CNS   concentrated nutrient solution (Section 3.2.2)

CSTR   continuous (flow) stirred-tank reactor

GSB   green sulfur bacteria

IC   ion chromatography

HPLC   high performance liquid chromatography

HRT   hydraulic retention time (also referred to as the liquid retention time, and detention time in the literature)

NM   nutrient medium (Section 3.2.2)

PRC   photochemical reaction centre (Section 2.1.2)

r_A rate of formation of chemical A (mg/h·L)

$-r_A$ rate of consumption of chemical A (mg/h·L)

SSC   sulfur species characterization (Section 4.1.3)

SSS   sulfide stock solution (Section 3.2.2)

TES   trace element solution (Section 3.2.2)

VSS   volatile suspended solids

[A]   concentration of chemical A (mg/L)

CHAPTER ONE

INTRODUCTION

The aim of alchemy - on the physical plane at least - was to take a raw material and through long and complicated chemical processes to manufacture the Philosophers' Stone. The Stone had in itself the power of perfecting matter and when a small quantity of it was mixed with other materials, it would turn them into gold.

Biedermann (1983)

1.1 General

Like the medieval alchemist, who toiled to transform lead into gold, the modern environmental engineer would like to process waste toxins into valuable products. Specifically, this dissertation examines the development of a continuous process which can convert toxic sulfide into valuable elemental sulfur.

1.2 The Problem of Sulfide

For Canadians, pollution is more often the cause of water problems than absolute scarcity of water supply (SCC, 1988). Inorganic compounds of sulfur are receiving increasing attention as water pollutants.

Chemically, sulfide ($S^=$) is the most reduced species of sulfur. Hydrogen sulfide (H_2S) gas is highly toxic and malodorous (Cadena & Peters, 1988). For humans, its odour threshold is 0.13 ppm (MSDS, 1988) and it is fatal at concentrations higher than 13 ppm (Cadena & Peters, 1988). Sulfide has a high oxygen demand of 2 mole O_2/mole sulfide and thus may cause significant depletion of oxygen in receiving waters (Kobayashi *et al.*, 1983).

Sources of sulfide to lakes and rivers include anaerobic digestion of organic matter

containing sulfur, heavy water plants (Gulens *et al.*, 1982) and petroleum refineries. Anaerobic decomposition of wastewater releases $H_2S_{(g)}$ which is oxidized to sulfuric acid at the crown of sanitary sewers, leading to the corrosion of concrete pipes and appurtenances (Gaudy & Gaudy, 1980). Anaerobic digestion of pulp mill effluent containing sulfite (Salkinoja *et al.*, 1985) is also a sulfide source.

Crude oil containing malodorous compounds (H_2S, mercaptans) is termed "sour" crude (MOE, 1987). Sour gas contains $H_2S_{(g)}$. Fuel gases must be treated for H_2S removal to minimize the sulfur dioxide formed while burning the gas (Sittig, 1978). Petroleum refineries also produce hydrogen sulfide in hydrocrackers, thermal crackers, gas recovery units, hydro-desulphurization units and steam (ethylene) crackers (MOE, 1987).

1.3 Regulations

In Canada, refinery wastewaters containing sulfide must meet the Federal Refinery Effluent Regulations and Guidelines. Currently the upper limit is 0.3 kg $S^=/1000$ m^3 of oil refined/day for refineries that commenced operations on or after Nov.1, 1973. Refineries that were operating before that date are subject to the guidelines of 0.6 kg $S^=/1000$ m^3 of oil refined/day (Losier, 1990).

Under the Municipal Industrial Strategy for Abatement (MISA) Program, Ontario refineries are required to measure weekly the sulfide concentration in a 24 hour composite sample of their process effluent. Each refinery has a load limit based on its reference production rate, which works out to a monthly average concentration of less than 0.2 mg $S^=$ per litre wastewater. In addition, the maximum daily concentration cannot exceed 0.3 mg $S^=/L$ (MOE, 1992).

1.4 Sulfide Control

Sulfide can be chemically oxidized to sulfate by hypochlorites, chlorine, potassium permanganate, hydrogen peroxide and oxygen. Hydrogen peroxide and oxygen react slowly with sulfide but produce no chemical residue. Hypochlorite and chlorine react to form chloride ions. Permanganate leaves behind manganese oxide. At pH values greater than 7, the product of the oxidation is always sulfate (Cadena & Peters, 1988). Chemical oxidizers are expensive and energy intensive (Kobayashi et al., 1983).

The full conversion of H_2S to sulfate produces sulfuric acid (H_2SO_4) which has to be neutralized before discharge. Although non-toxic, sulfates discharged in large quantities to surface waters can lead to excess mineralization (Maree & Strydom, 1985). Domestic wastewater typically contains 20 to 50 mg $SO_4^=$/L (Metcalf and Eddy, 1991). In Ontario, the aesthetic objective for sulfate in drinking water is 500 mg $SO_4^=$/L to avoid a laxative effect at higher levels (MOEE, 1994). Finally, even if sulfate could be refined into commercial H_2SO_4 it would have been worth \$36/ton in 1978. Elemental sulfur was worth \$110/ton (Cork, 1978) to \$300/ton (Kim & Chang, 1991).

The partial oxidation of H_2S to S^0 instead of $SO_4^=$ has several advantages. Elemental sulfur is an easily handled and transported noncorrosive solid containing more sulfur per unit mass than any other form. Also, the agricultural use of elemental sulfur as a nutrient and fungicide is increasing. Elemental sulfur has also been added to sewage sludge prior to aerobic digestion. The sulfuric acid produced, leached heavy metals from the biosolids making them more suitable for application on agricultural land (Ravishankar et al., 1992). However, the main use of elemental sulfur is as a feedstock for the chemical, fertilizer

and materials manufacturing industries (West & Duncan, 1974).

For these reasons, petroleum refineries recover H_2S liberated in their processes by converting it to elemental sulfur. Sulfur recovery from sour gas is most commonly done by the Claus process (Cork *et al.*, 1986). In the first step of the Claus process, H_2S is partially burned to SO_2 with air. The H_2S/SO_2 mixture is then reacted over a bauxite catalyst to yield S^0 and water. Normally 90-95% of the H_2S is converted to S^0. The remaining H_2S is either incinerated to SO_2 or converted to sulfur in a tail gas treating unit (Sittig, 1978).

Sulfur can also be recovered from sour water. Petroleum refinery operations produce sour water whenever steam is condensed in the presence of gases containing H_2S (Sittig, 1978). Condensates from gas separators may contain up to 5000 mg $S^=/L$ (Nemerov, 1978). The H_2S can be removed by the process of sour water stripping. Steam is contacted with heated sour water in the sour water stripper. Sour gas containing some steam leaves the top of the stripper and then is partly condensed. Condensate and sour gas are separated in the surge tank. The sour gas is then sent to a sulfur recovery plant (Sittig, 1978). The water from the bottom of the stripping column contains about 80 mg H_2S/L and is directed to the wastewater treatment plant where H_2S may escape from open channels or be oxidized to $SO_4^=$ in the aeration tank.

Sour water can also be treated by the Holmes-Stretford process which oxidizes H_2S to S^0 using a vanadium catalyst in water. Over 99% of the H_2S is removed in this process (Vasan, 1978).

The chemical processes for sulfur recovery are expensive because of the need to

4

replace poisoned and expired catalysts, contaminated reactor liquids and corroded reaction vessels (Cork et al., 1986). In addition, gas streams leaving the Claus process require further treatment to meet environmental regulations (Cork et al.,1986; Vasan, 1978).

Some of these disadvantages can be overcome through the use of a biological sulfide removal process. The original intent of this research was to develop a biological process to remove the $S^=$ remaining in the water from the bottom of the sour water stripper. This would reduce the oxygen demand on the wastewater treatment plant, and possibly the sulfide load to the receiving water body. The operating costs of this process can be offset by the sale of elemental sulfur.

Taking a broader view, a process which biologically converts $H_2S_{(aq)}$ to S^0 can potentially replace either the Holmes-Stretford process or the combination of sour water stripper and Claus sulfur recovery processes.

1.5 Objective

The objective of this research was to develop a continuous flow bioprocess to remove sulfide dissolved in wastewater and convert it to elemental sulfur.

1.6 Scope

The scope of this study was to:

- select and calibrate appropriate analytical methods for different sulfur species and confirm that other sulfur species did not interfere in the analysis;

- demonstrate and quantify the production of elemental sulfur from sulfide in a continuous biological reactor;

- compare the operation of this continuous biological reactor with other biological

sulfide removal systems reported in the literature; and

- develop a model to predict the conversion of sulfide to elemental sulfur in a continuous biological reactor.

CHAPTER TWO

LITERATURE REVIEW

The 'great work' laid a heavy burden on those who attempted it. It involved... the reading of almost impossibly difficult books - a task which had to be repeated many times until, slowly and painfully, the hidden meaning loomed up through the mists of symbolism.

Biedermann (1983)

2.1 Bacteria Used in Bioreactors

Conversions between different species of sulfur can be accomplished by naturally occurring bacteria. These transformations are localized in a sulfuretum (Figure 2.1). Several ecological niches for bacteria are formed by the combination of oxygen concentration, light, sulfur, carbon dioxide and organic material. Of interest to this project are the chemoautotrophs and the photoautotrophs both of which oxidize $S^=$ to S^0 and further to $SO_4^=$. At the water surface, the chemoautotrophs use the energy released in the spontaneous reaction of H_2S or S^0 with dissolved oxygen (or nitrate) to form $SO_4^=$. In the upper anaerobic zone, the photoautotrophs use infra-red light energy to perform the same oxidation. In the photoautotrophs, the electrons that are removed when $S^=$ or S^0 is oxidized are transferred to the carbon in CO_2, reducing it to cell material. In the case of the chemoautotrophs, carbon and O_2 or nitrate (NO_3^-) receive electrons. The sulfide or elemental sulfur is thus termed the "electron donor" for the reaction.

The desirable bacterium for the bioprocess under investigation should readily convert H_2S to S^0, require a minimum of nutrient inputs, and produce S^0 that is easily separable from the biomass.
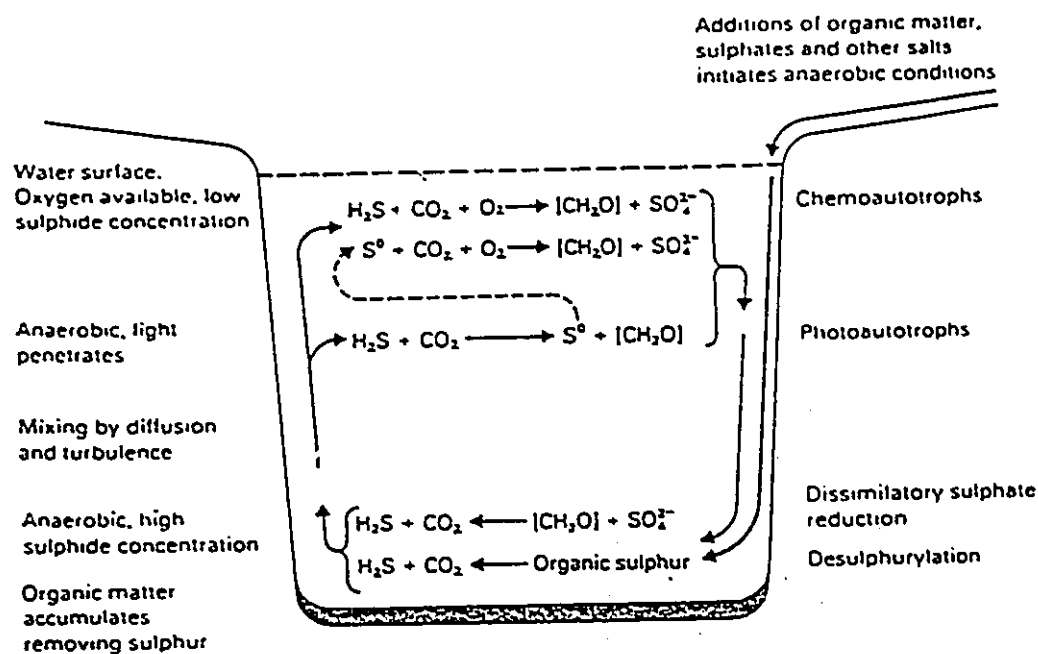
7

Additions of organic matter, sulphates and other salts initiates anaerobic conditions

Water surface. Oxygen available. low sulphide concentration

$H_2S + CO_2 + O_2 \rightarrow [CH_2O] + SO_4^{2-}$
$S^0 + CO_2 + O_2 \rightarrow [CH_2O] + SO_4^{2-}$

Chemoautotrophs

Anaerobic. light penetrates

$H_2S + CO_2 \rightarrow S^0 + [CH_2O]$

Photoautotrophs

Mixing by diffusion and turbulence

Anaerobic. high sulphide concentration

$H_2S + CO_2 \leftarrow [CH_3O] + SO_4^{2-}$

$H_2S + CO_2 \leftarrow$ Organic sulphur

Dissimilatory sulphate reduction

Desulphurylation

Organic matter accumulates removing sulphur

FIGURE 2.1 Bacterial interactions in a sulfuretum (Anderson, 1978)

2.1.1 Chemoautotrophs

The chemoautotrophs that participate in the sulfur cycle are termed the "colourless sulfur bacteria" because they have no photosynthetic pigments. The *Thiobacteria* belong to this group and deposit elemental sulfur extracellularly (outside the cell), making it easier to separate from the bacteria.

Rozek (1978) patented a process for oxidizing sulfide in sulfur mine wastewater. Inorganic nutrients and *Thiobacillus thioparus* were added to the wastewater containing up to 35 mg S⁼/L. After oxidation, the water surface was covered with a layer of elemental sulfur and bacterial cells.

Thiobacillus was found in the "charge" of a fixed-film upflow bioreactor used to treat

8

sulfide-rich wastewater from Soviet spas. In this case, gravel was used as the support on which the bacterial film grew. The flow of water through the reactor was upward from perforated distribution pipes at the bottom of the cylindrical reactor. Air was bubbled from another set of distribution pipes at the bottom. The raw water containing 28 to 56 mg $S^=$/L was treated to contain less than 1 mg $S^=$/L resulting in a removal efficiency of approximately 100% (Table 2.1). Most of the sulfide was oxidized to $SO_4^=$, with less than 1% ending up in the exhaust air stream. S^0 production was not quantified (Ass *et al.*, 1983).

Thiobacillus denitrificans was used to remove H_2S from gas streams (Sublette & Sylvester, 1987a). A free-cell (suspended-growth) continuous stirred-tank reactor (CSTR) was used. Sterile nutrient medium containing nitrate was pumped into the reactor and medium and cells were pumped out. The flow rate of liquid was set to give hydraulic retention times (HRTs) of either 34 or 17 hours in the reactor. A mixture of H_2S, CO_2 and N_2 gases was sparged through the reactor. Measurements of concentrations in the reactor were taken after 5 reactor volumes of liquid had gone through. Ninety-four percent of the H_2S bubbled into the reactor was removed.

In a similar experiment, Sublette (1987) used 1.44 and 2.0 L suspended-growth CSTRs where air was bubbled in as the electron acceptor and nitrate was absent from the reactor-medium. In continuous reactor operation, the steady state sulfide concentration was less than 1 μM in the liquid and less than 0.05 μM in the outlet gas. The steady state elemental sulfur concentration in the reactor was less than 1 mg/L, and the sulfate liquid concentration indicated that all of the sulfide was converted to sulfate.

TABLE 2.1 Continuous sulfide removal using chemoautotrophs.

Reference	Configuration	Vol. (L)	Influent [H_2S]	$S^=$ loading (mg/h·L)	Eff. rem. (%)	Eff. con. (%)
Ass et al. (1983)	FF, U, air	47	30-60 mg/L in liquid	21-96	~100	NQ
Sublette & Sylvester (1987a)	SG, CSTR, NO_3^-	1.44	0.20-0.32 mM in gas	32-74	94	NQ
Sublette (1987)	SG, CSTR, air	1.44	0.27-0.32 mM in gas	38-51	~100	<0.2
		2.0		32-33	~100	<0.2
Sublette & Sylvester (1987b)	SG, CSTR, NO_3^-	1.44	? in gas	58	~100	0
Buisman et al. (1990a)	FF, CSTR, O_2	5.5	100 mg/L in liquid	129	97	83 SNM
	SG, CSTR, O_2		55 mg/L in liquid	7.9	~100	~100 SNM
Buisman et al. (1990b)	FF, CSTR, O_2	8.3	35-174 mg/L in liquid	104-521	100-60	50-58 SNM
	FF, biorotor, O_2	3	45-203 mg/L in liquid	208-938	100-69	50-69 SNM
	FF, U, O_2	20	45-225 mg/L in liquid	208-1040	100-73	60-73 SNM
Lizama & Sankey (1993)	FF, CC, air	0.34	0.17 mM in gas	19-38	77-69	NQ

FF= fixed-film, SG= suspended-growth, U= upflow, CC= countercurrent contactor, electron acceptor: air= O_2 in air, O_2= pure oxygen and NO_3^-= nitrate, Vol.= wet volume of reactor, Eff.rem.= removal efficiency (($S^=_{in}-S^=_{out}$)/$S^=_{in}$), Eff.con.= conversion efficiency ($S^0_{out}/S^=_{in}$), NQ = not quantified, SNM = results by subtraction since S^0 not measured.

10

An additional experiment was performed by contaminating one of the nitrate-fed CSTR's with heterotrophic bacteria (Sublette & Sylvester, 1987b). Although the sulfide loading rate was slightly higher than in previous experiments (Table 2.1), no elemental sulfur was detected in the reactor at any time, even though sulfide consumption was approximately 100%.

Recently, *Thiobacillus* has been demonstrated to convert sulfide to S^0 (Buisman *et al.*, 1990a). *Thiobacillus* growth was promoted from an initial inoculum of ditch mud in a fixed-film aerobic continuously fed CSTR. The biomass support particles were suspended above the mixing paddle by a screen. Sodium sulfide and inorganic nutrients were added to tap water and pH stabilized before being fed into the reactor. Pure oxygen was added to a gas recirculation loop which was bubbled into the bottom of the reactor. At a dissolved oxygen concentration of 0.7 mg/L, and influent concentrations of 100 mg $S^=$/L and 8 mg S/L as $SO_4^=$ respectively, concentrations of 6 mg $S^=$/L and 18 mg S/L as $SO_4^=$ were measured in the effluent. By subtraction, it was concluded that 83 mg S^0/L were present in the effluent, although S^0 was never measured. The experiment was repeated using a free-cell suspension and a longer HRT. Complete removal of the $S^=$ was achieved with no $SO_4^=$ production. Therefore 100% conversion to S^0 was achieved. Buisman (1990a) concluded that at the same $S^=$ and oxygen bulk concentrations, the $SO_4^=$ production rate in the suspended-growth reactor was lower than in the fixed-film reactor. According to Buisman and co-workers (1990a), this occurred because the oxygen diffused faster than the sulfide into the pores of the fixed-film medium. At a certain depth into the pore, oxygen and bacteria were available to oxidize $S^=$, but $S^=$ was not available so

instead S^0 was oxidized to $SO_4^=$.

Subsequently, Buisman *et al.* (1990b) tested three continuous-flow reactor configurations: fixed-film CSTR, biorotor (a rotating cage partly immersed in the reactor liquid) and a fixed-film upflow reactor with fine-bubble diffusion. The sulfide loadings in these experiments were the highest of any studies where colourless sulfur bacteria were used (Table 2.1). For each reactor, the sulfide loading was varied. At low loadings, all of the influent $S^=$ was removed but only 50 to 60% was converted to elemental sulfur. At high loadings, $S^=$ removal was 60 to 73% but all of the sulfide removed was converted to S^0. Therefore, there was a compromise between effluent sulfide concentration and sulfate formation. Complete conversion of all of the *removed* sulfide to S^0 was achieved only when sulfide appeared in the effluent. On the other hand, a zero sulfide effluent concentration was realised only when sulfate appeared in the effluent.

Poor performance was achieved in a countercurrent column contactor inoculated with *T. thiooxidans* (Lizama, 1993). Air mixed with H_2S was passed into the bottom of a column containing glass beads as a fixed-film support while liquid nutrient medium was sprayed on top and recirculated from the bottom. The apparatus was operated with and without gas recirculation through the column. Although the sulfide loading rates were relatively low (Table 2.1), only 69 to 77% of the sulfide was removed in the gas flow-through mode.

The fixed-film pure oxygen supplied reactors have been shown to remove all of the sulfide while converting the majority of the removed sulfide to elemental sulfur (Buisman, 1990a, 1990b). The S^0 concentration in the effluent of such a reactor needs to be

.

measured explicitly to quantify the amount of sulfur produced. Elemental sulfur yields reported may include S^0 trapped in the biomass support which would not be available for commercial use.

2.1.2 Photoautotrophs

The purple and green sulfur bacteria contain bacteriochlorophylls (bchl) which are responsible for light harvesting and transferring energy to the photochemical reaction centre (Stanier et al., 1986). The type and abundance of these photosynthetic pigments give the bacteria their characteristic colour. The purple sulfur bacteria are motile and elemental sulfur granules formed from sulfide oxidation are found inside the cells. Bacteria of the genus Chromatium are included in this group. The green sulfur bacteria (GSB) are strictly anaerobic non-motile bacteria which oxidize sulfide and deposit S^0 extracellularly (Roy & Trudinger, 1970). The GSB include the genus Chlorobium which in turn includes the species Chlorobium limicola and Chlorobium limicola forma specialis thiosulfatophilum (referred to here as C. limicola and C. thio. respectively).

Photosynthetic green plants use the energy of light to oxidize reduced oxygen ($O^=$) to gaseous oxygen (O_2) while reducing CO_2 to carbohydrates (CH_2O).

$$2nH_2O + nCO_2 \rightarrow nO_2 + n(CH_2O) + nH_2O \qquad [2\text{-}1]$$
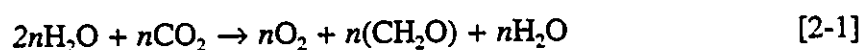
By comparison, GSB use light energy to oxidize sulfide ($S^=$) to elemental sulfur (S^0) while reducing CO_2 to carbohydrates.

$$2nH_2S + nCO_2 \rightarrow 2nS^0 + n(CH_2O) + nH_2O \qquad [2\text{-}2]$$
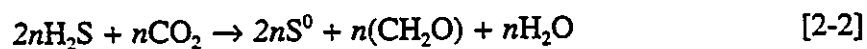
This process is termed anoxygenic photosynthesis since no oxygen is formed. The light that is absorbed by the GSB's photochemical reaction centre (PRC) is utilised in two

ways. In the process called *cyclic photophosphorylation*, the PRC is excited to a higher state by light energy. On relaxation to its normal energy state, a chemical potential is formed across an internal membrane of the bacterial cell. This chemical potential is used to form adenosine triphosphate, ATP, an energy storing molecule. In the second process termed *noncyclic photophosphorylation*, the excited PRC forces nicotinamide adenine dinucleotide phosphate, $NADP^+$, to accept two electrons and become NADPH, an electron storing molecule. The electrons removed from the excited PRC are replaced by those from an electron donor like sulfide or elemental sulfur (Stanier *et al.*, 1986). In green sulfur bacteria, carbon dioxide is combined with carbohydrates in the *reversed citric acid cycle* to eventually yield a six-carbon sugar (Madigan & Brock, 1988). Overall, 10 NADPH and 7 ATP are required to manufacture one glucose molecule from CO_2. In order to efficiently use the light energy to assimilate CO_2, the rates of cyclic and noncyclic photophosphorylation would have to be co-ordinated so that the NADPH to ATP ratio is maintained.

Although sulfide is the electron donor for phototrophic growth, it is also inhibitory at high concentrations. Van Gemerden (1984) observed that *C. thio.* was inhibited to one half its maximum specific growth rate at a sulfide concentration of 3 to 4 mM (96 to 128 mg/L). Mathers & Cork (1985) noted that low growth rates of *C. thio.* occurred in sulfide concentrations above 6 mM (192 mg/L). Henshaw (1990) calculated that the growth of GSB was zero at 300 mg $S^=$/L.

Maree and Strydom (1985) used an upflow anaerobic packed-bed reactor in series with a photosynthetic reactor to remove sulfate from mine wastewater. Sulfate was

14

reduced to H_2S in the first reactor, and purple and green sulfur bacteria precipitated S^0 in the second reactor. Assuming that all of the sulfate consumed in the first reactor was converted to sulfide, over 90% of the sulfide produced in the first reactor was removed in the second reactor. The elemental sulfur yield, retention time and light intensity in the photosynthetic reactor were not quantified. Subsequent research concentrated on the sulfate removal phase and sulfide was either air-stripped (Maree *et al.*, 1986), not quantified (Maree & Strydom, 1987), or gas stripped and chemically oxidized to elemental sulfur (Maree & Hill, 1989).

Kobayashi *et al.* (1983) tested a fixed-film upflow photosynthetic reactor and a phototube (plug-flow reactor) for removal of H_2S from anaerobic filters. *Chlorobium* was identified as the common organism in the phototube. At a HRT of 24 hours, the upflow reactor removed 81 to 92% of the sulfide but elemental sulfur was not detected in the effluent. In the phototube, sulfide removal was 100%, most of which was achieved in the first 2 m of the 12.8 m reactor (Table 2.2). Even though there was ample capacity in the phototube to remove sulfide, only 8 to 12% of the influent sulfide was converted to elemental sulfur. The sum of concentrations of $SO_4^=$ and S^0 in the phototube effluent did not equal the concentration of sulfide in the influent, indicating the formation of some other species of sulfur or accumulation of elemental sulfur within the tube.

Cork (1978) tested *Chromatium vinosum* and *C. thio.* in the photosynthetic reactor of a two-stage bioprocess. Sulfate was reduced to H_2S by *Desulfovibrio desulfuricans* in the first stage. Hydrogen sulfide gas was carried by an inert gas into the second stage photosynthetic reactor for production of S^0. Over 90% of the influent sulfate was

15

TABLE 2.2 Continuous sulfide removal using photoautotrophs.

Refer-ence	Config-uration	Vol. (L)	Influent [H_2S]	$S^=$ loading (mg/h·L)	Eff. rem. (%)	Eff. con. (%)	Irrad-iance (W/m²)	Rad flx (W)
Kobayashi (1983)	FF, U	8	16 mg/L in liquid	0.59 -1.27	92 -81	~0	NQ	NQ
	FF, plug	0.1	24-19 mg/L in liquid	102 -125	100	8 -12	NQ	NQ
Cork (1984b)	SG, CSTR	0.8	4.1 mM in gas	62	100	?	ID	2.8
Cork et al. (1985)	SG, CSTR	0.8	? in gas	109 -74	100	95 -93	2000 -150	29-2.1
Maka & Cork (1990)	SG, CSTR	0.8	1-2 mM in gas	32 -64	100 -90	97 -90	139	2
Kim et al. (1991a)	SG, CSTR	4	2.1 mM in gas	61	99.5	35	490	122
Kim et al. (1992)	SG, CSTR	4	2.1 mM in gas	64	100	63	714	178

FF= fixed-film, SG= suspended-growth, Vol.= wet volume of reactor, Eff.rem.= removal efficiency (($S^=_{in}$-$S^=_{out}$)/$S^=_{in}$), Eff.con.= conversion efficiency (S^0_{out}/$S^=_{in}$), Rad flx = radiant flux, NQ = not quantified, ID = insufficient data to calculate.

converted into S^0. *C. thio.* was found to be superior to *Chromatium vinosum* in the following categories:

- production of S^0 per unit time

- ratio of S^0 produced to other oxidized forms of sulfur produced

- ratio of S^0 produced to sulfate input (into the first stage)

- tolerance to high sulfide concentration (>4 mM (128 mg/L))

- extracellular production of S^0

Cork claimed that the extracellular S^0 could be easily isolated by differential centrifugation (Cork, 1978) or rotary filtration (Cork, 1987). The optimum pH and temperature were found to be 7.0 and 30°C respectively for *C. thio.* growth. This process was later patented (Cork, 1984a) as a means of removing sulfate from copper mining wastewater.

Cork (1987) also patented a process for 95 to 98% removal of H_2S from natural gas streams containing 0.1 to 65% H_2S. The natural gas was to be bubbled through a nutrient medium containing *C. thio.*

The gas-fed photosynthetic batch reactor was optimized by modulating the influent gas flow so as to have zero H_2S in the effluent (Cork, 1984b). The influent gas was 9% H_2S, 17% CO_2 and 74% N_2 for three experiments performed at light levels of 2.8, 1.9 and 1.1 Watts. Sulfide did not accumulate in the reactor at the highest level of light input. Sulfide began to accumulate after 50 hours when the reactor was irradiated with 1.9 W of white light. With 1.1 W of light, sulfide accumulated only for the first 30 hours, then reached a plateau at 7 mM.At slightly higher sulfide loadings, all of the $H_2S_{(g)}$ that was

sparged into a fed-gas batch reactor was consumed and 93 to 95% was converted to elemental sulfur (Cork *et al.*, 1985). The concept of the "van Niel curve" was proposed wherein the light absorbance was coupled to the consumption of sulfide. On a molecular level, the reverse citric acid cycle requires NADPH and ATP to assimilate CO_2. It appears that *C. thio.* has a mechanism whereby the rates of cyclic and noncyclic photophosphorylation are balanced to produce the proper ratio of NADPH to ATP. The total rate of photophosphorylation is dependant on the amount of light energy received by the PRC. At a given light input, the rate of noncyclic photophosphorylation is fixed so that the number of two-electron yielding $S^=$ to S^0 conversions is also fixed. At higher sulfide concentrations, surplus electron donor molecules are not oxidized; and at lower $S^=$ concentrations, full use is made of the insufficient number of electron donor molecules by oxidizing $S^=$ to $SO_4^=$ for a yield of 8 electrons. Thus a plot of reactor feed rate as a function of irradiance (W/m^2) for the reactor system used by Cork *et al.* (1985) resulted in the curve shown in Figure 2.2. At any point on the curve, the sulfide fed to the reactor was fully consumed and no sulfate was produced. At a condition to the left of the curve (Region I) light was insufficient and sulfide accumulated. To the right of the curve (Region II) the overabundance of light produced sulfate.

Maka and Cork (1990) investigated the effects of light quantity, light intensity and quality (spectrum) of light on H_2S metabolism in a gas fed-batch reactor. The *in situ* absorption spectrum of *C. thio.* contains peaks at wavelengths of 760 and 460 nm. One could postulate that the optimum sulfide use per unit of energy would be achieved if the bacteria can function with light supplied at only 760 nm. In addition, the use of infrared
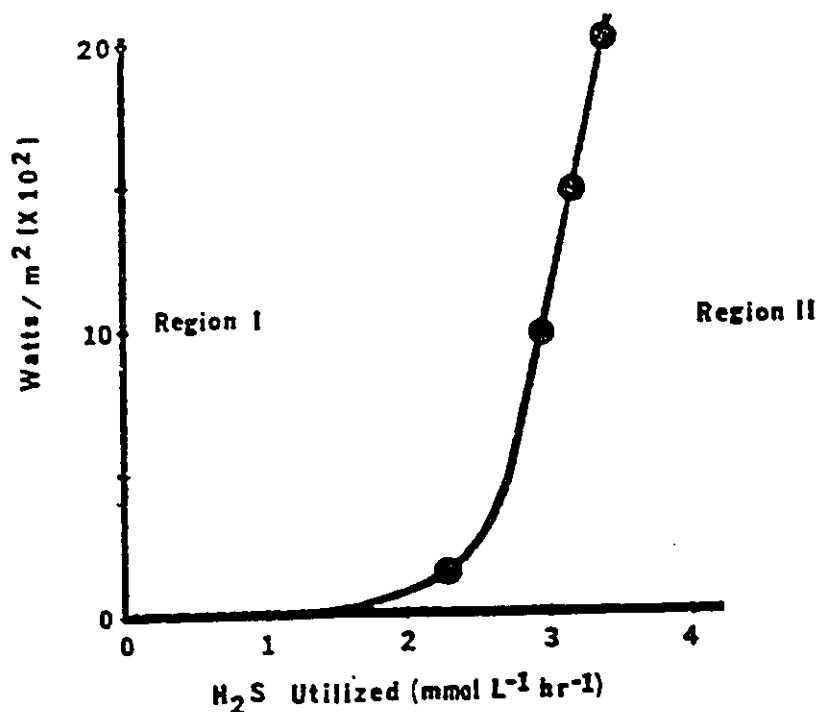
18

FIG. 3. Mass balance curve of regulated sulfur oxidation (>90% H_2S to S^0 mass balance). Region I shows oxidative sulfur metabolism, and region II shows inhibition of growth and sulfur metabolism.

FIGURE 2.2 The van Niel curve (Cork *et al.*, 1985)

light (>700 nm) in the reactor would give GSB an advantage in competing against algae or other bacteria which require higher-energy white light.

In the first experiment, the intensity of the light source was varied, keeping the exposed area of the reactor constant at a loading of 32 mg S⁻/h·L. A high irradiance resulted in removal of all of the sulfide, over half of which was converted to sulfate. At low irradiance, sulfide was not fully oxidized and accumulated in the reactor. Between these limits, there was a condition where neither sulfide nor sulfate were found in the reactor, and elemental sulfur and thiosulfate were the only products. This is the condition

described by the van Niel curve. For white light (380 to 900 nm) this optimum condition resulted in 60% of the influent H_2S becoming S^0, and 40% becoming $S_2O_3^-$. For infrared light (700 to 900 nm) the optimum favoured sulfur production, 97:3 ($S^0:S_2O_3^=$). The optimum for infrared light also occurred at a lower irradiance (219 W/m^2) than white light (406 W/m^2). This demonstrated two more ways in which infrared light was superior to white light for elemental sulfur production.

In a second set of experiments, the radiant flux (W) received by the reactor remained constant but the exposed reactor surface area was varied over a four-fold range. Under white light of 6.7 W, "over-oxidation" to sulfate occurred at large surface areas. An infrared radiant flux of 1.5 W resulted in no $S^=$ or $SO_4^=$ in the reactor at any surface area, although the ratio of $S^0:S_2O_3^=$ varied from 98:2 at 0.0144 m^2 area to 87:11 at 0.0032 m^2 area. For white light, the smaller window may have limited the exposure time of each bacterium to light, allowing only the first oxidation to elemental sulfur, whereas with ample light and a large surface area, the prolonged exposure of the bacterium to light resulted in further oxidation to sulfate. In the case of infrared light, a similar phenomenon may have occurred, with thiosulfate being an intermediate in the pathway to sulfate formation.

Finally, Maka and Cork compared the quantum requirements of *C. thio.* at different wavelength ranges of light. The ratio of the number of photons absorbed to the number of molecules of S^0 produced was lowest (17) in the middle wavelengths between 535 and 660 nm. The second lowest photon requirement of 59, occurred at the broad band infrared (700 to 900 nm). The specific wavelength of 760 nm had a quantum requirement

of 47. And the ultraviolet (350 to 535 nm) and red (660 to 700 nm) regions of the spectrum both had quantum requirements of 200 photons/molecule S^0. Maka and Cork concluded that the greater the inherent energy of the photon, the greater the oxidation of sulfur; however, light at 760 nm seems to be the exception to this rule.

From Maka and Cork's data, the sulfide loading appears to be more related to the radiant flux (W) than the irradiance (W/m^2). Figure 2.3 shows the van Niel curve plotted with radiant flux as the independent variable. The data shown were considered to be "on the curve" (*i.e.* complete conversion to S^0), because the percentage of $S^=$ plus the percentage of $SO_4^=$ in the reactor at the end of each experiment was less than 4% of the total sulfur. Further analysis of this plot confirms the superiority of infrared light as an energy source for *C. thio.*. For the same light wattage, infrared light supports a higher sulfide loading than white light.

Henshaw (1990) demonstrated the sequential conversion of $S^=$ to S^0 to $SO_4^=$ in sterile 9 L batch reactors. Up to 90% conversion of $S^=$ to S^0 was achieved and there was an inverse correlation between $S^=$ to S^0 conversion and pH, between pH values of 6.9 and 7.5. Thiosulfate was not measured in these experiments.

Kim *et al.* (1991, 1992, 1993) and Kim and Chang (1991) applied several innovations to maximize the S^0 yield for gas-fed batch reactors employing *C. thio.*, operating at 30°C and pH of 6.8 to 6.9. Light emitting diodes (LED's) illuminating the surface of a 4 L reactor at wavelengths of 690 to 770 nm were shown to have a 19-fold increase in H_2S removal/cell/irradiance over incandescent bulbs (Kim *et al.*, 1991). However, because of the low total power, the specific growth rate and H_2S removal/cell
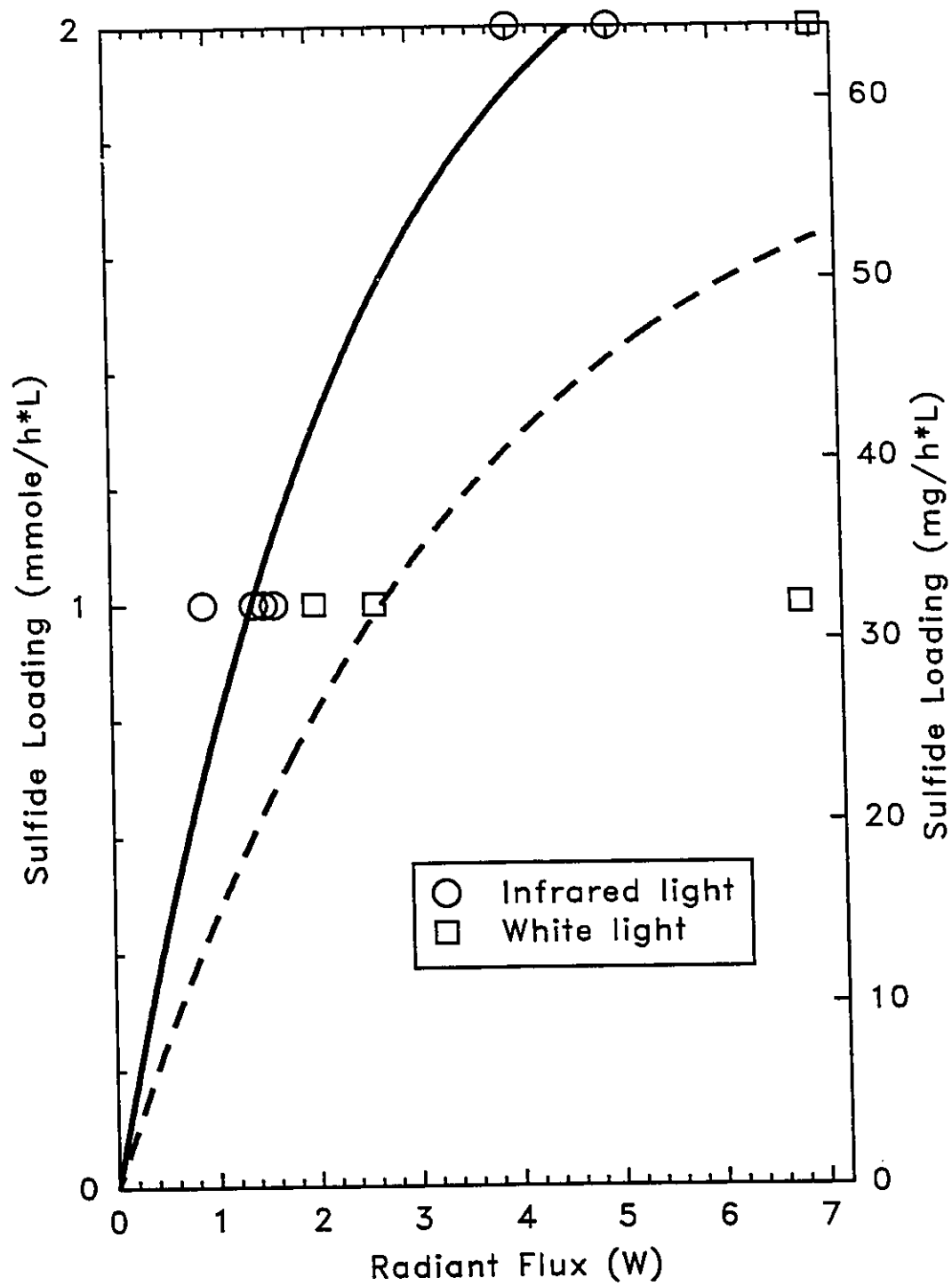
FIGURE 2.3 Sulfide Loading as a function of radiant flux (Maka and Cork, 1990)

were slightly lower than that for the incandescent source.

Kim and Chang (1991) realised that elemental sulfur from *C. thio.* metabolism was itself scattering light destined for the bacteria. Two reactor configuration changes were made to remedy this: immobilizing the bacteria in transparent beads, and recycling the reactor contents through a sulfur settler. The immobilization of *C. thio.* in 3.5 mm diameter strontium alginate beads resulted in a 30% reduction in the light energy requirement as compared to a suspended-growth reactor at the same H_2S removal rate. The S^0 produced accumulated in the beads and after 60 hours the H_2S removal rate decreased. In addition, the author stated that sulfur recovery from the beads would be almost impossible. In the second approach, the reactor contents were pumped through a conical elemental sulfur settler followed by a filtering screen. Some of the filtrate from the screen was disposed of and the remainder was supplemented with fresh medium before being re-introduced into the reactor. Total S^0 production was not quantified. The final steady state concentration of the S^0 in the reactor was 500 mg/L, and 80 to 90% of the S^0 was removed in the settler. The loading rate on this system reached 76.8 mg $S^=$/h·L and the removal rate of this system per unit concentration of protein exceeded that of the suspended-growth reactor without recycle. In comparing non-recycle reactors of 2 L and 4 L, the larger had a removal rate only 1.3 times that of the smaller due to greater light scattering by suspended elemental sulfur in the larger reactor. The reactor loading for the free-cell reactor could not be calculated from the information given.

Loading rates for 2 L and 4 L gas-fed semi-batch reactors ranged from 25 to 212 mg $S^=$/h·L in other experiments (Kim *et al.*, 1992). For a 4 L reactor, illuminated at

35,000 lux (714 W/m^2) and fed 64 mg S$^=$/h·L, the removal of sulfide was 100% but elemental sulfur production (calculated as the concentration of S^0 in the reactor divided by the cumulative mass of sulfide input to the reactor per reactor volume) was 63%. The radiant flux was 178 W if the exposed reactor area can be assumed to be 0.249 m^2 (Kim et al., 1991). The van Niel curves for 2 L and 4 L reactors were given and a model was proposed to compensate for the effects of light scattering and absorption by suspended elemental sulfur and bacteria.

The control of illuminance using a model-based algorithm was demonstrated using a 4 L reactor (Kim et al., 1993). During start-up, illuminance was increased step-wise as the H$_2$S$_{(g)}$ flow rate was increased.

Suspended-growth CSTRs have shown the best results for production of elemental sulfur while completely removing sulfide (Cork et al., 1985, Maka & Cork, 1990). The plug-flow reactor has been shown to remove sulfide at high hydraulic loadings (Kobayashi et al., 1983). Decreasing the volume of reactor may result in a higher S^0 yield.

2.1.3 Summary

In comparison to photoautotrophs, chemotrophic bacteria have demonstrated the removal of sulfide at higher sulfide loadings (>100 mg/h·L). In addition, the successful chemotrophic reactors have been fixed-film types. With the chemotrophic bacteria attached to the biomass support, the excreted S^0 was presumably flushed away with the liquid flowing through the reactor. However, due to the faster diffusion of oxygen over sulfide, oxidation of elemental sulfur to sulfate in the pores of the fixed-film support medium occurred to some extent.

The advantages of using phototrophic bacteria to produce elemental sulfur from sulfide are the higher percentage conversion of $S^=$ to S^0, and the ability to quickly and automatically control the oxidation rate of sulfide by varying the light intensity. Caution must be exercised in comparing liquid-fed continuous-flow bioreactors operated with chemotrophs to gas-fed semi-batch bioreactors operated with phototrophs. For phototrophs, the reactor must be designed to allow the maximum penetration of light, an uncommon characteristic for bioreactor design. The use of a fixed-film photoreactor seems unlikely (in spite of the success of Kobayashi's phototube) because of the difficulty in finding a transparent, oxygen impermeable biomass supporting medium.

In sour water the H_2S is present in the liquid phase. While dissolved in water, H_2S is less likely to be an environmental or safety hazard than H_2S gas. Thus, it is advantageous to convert sulfide directly to S^0 while in the liquid phase. The use of a suspended-growth photoreactor, fed with dissolved sulfide, has not been reported in the literature.

2.2 Bioreactor System

The throughput of any biological treatment process can be increased if more bacteria are available in the reactor to consume the substrate. By analogy, a higher consumption of sulfide can be achieved by increasing the concentration of bacteria in this bioreactor. This can be achieved by recirculating some of the reactor effluent biomass back into the reactor as shown in Figure 2.4. It is desirable to separate elemental sulfur from the recirculated stream for three reasons. Firstly, S^0 has a commercial value which can be realized only if it is separated and purified. Secondly, S^0 in the bioreactor blocks the
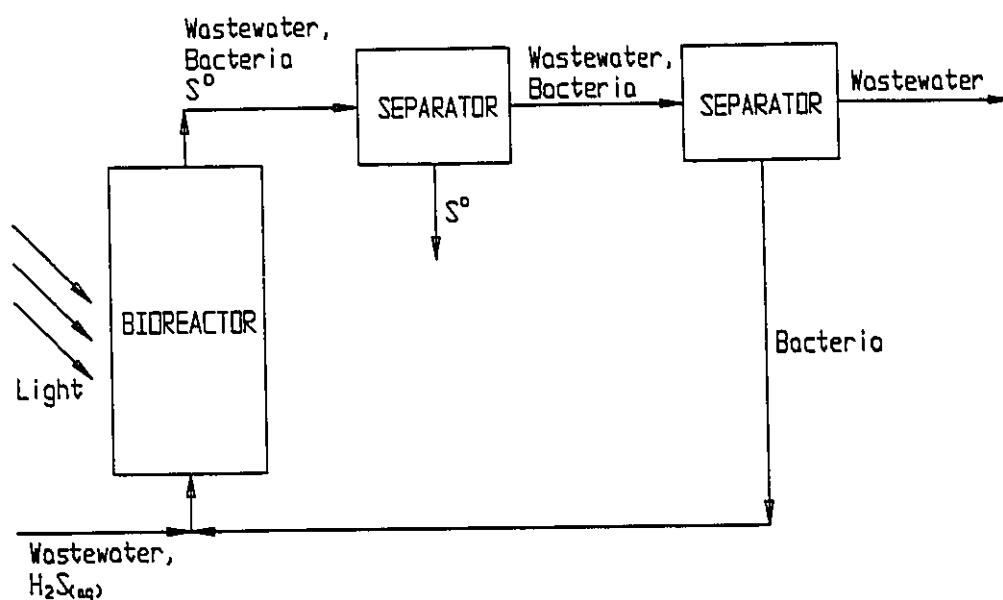
FIGURE 2.4 Schematic of a proposed bioreactor system using phototrophic bacteria.

available light needed by these photosynthetic bacteria. Finally, S^0 is an alternate electron

donor to green sulfur bacteria and recirculating it into the bioreactor may result in further

oxidation of the elemental sulfur to sulfate, decreasing the yield of S^0 from the process.

2.2.1 Separation of Elemental Sulfur

Separation of the elemental sulfur from the bacteria and wastewater by gravity

settling, filtration, centrifugation and floatation have been tested on laboratory scales.

2.2.1.1 Gravity Settling

A solid particle within a liquid settles if its weight is greater than the sum of the

buoyant force and the drag force opposing downward motion. Cork (1984b) has reported

that elemental sulfur settled from bioreactor contents within 24 hours. Kim and Chang

(1991) successfully used a settling unit to remove some S^0 from the recycle stream of a

gas-fed bioreactor, claiming it removed 80 to 90% of the elemental sulfur. A standard column test was used by Ly (1990) to determine the settling characteristics of S^0 and GSB. In separate experiments, 90% of the elemental sulfur settled out of a 1 m depth of column in 9 minutes whereas only 7% of the GSB settled in that time. Even after settling for 14 hours, the maximum removal of bacteria from suspension was 38%. However, when settled together, the S^0 settled at the same rate as the bacteria, the rate being intermediate between the individual settling rates of S^0 and bacteria. Forty-three percent of both the elemental sulfur and GSB were removed after 26 minutes. The reported elemental sulfur removal values in the combined experiment were lower than the actual S^0 removal, since S^0 was measured at only one depth in the column. In spite of this, the adhesion of the elemental sulfur to GSB precludes the use of simple settling as a means of separating elemental sulfur from the bacteria in a continuous bioreactor system.

2.2.1.2 Effect of pH on Settling Process

Preliminary tests revealed that increasing the pH of the contents of a batch bioreactor caused the suspended material to aggregate and settle rapidly. A standard column test was performed by Diemer (1991) to quantify this effect. At the optimum pH of 8.6, 67% of the elemental sulfur was settled from a mixed suspension compared to 27% of the GSB. Thus, the sediment was enriched in S^0 and recirculation of the supernatant, after neutralizing pH and concentrating the bacteria, is feasible. At higher pH values, the settling rates of S^0 and bacteria had increased, but the *difference* between the removal rates was less than in the pH=8.6 experiment. The viability of the bacteria after settling at a pH of 8.6 was not tested.

2.2.1.3 Filtration

Microphotographs of green sulfur bacteria and adjacent elemental sulfur have revealed that the diameters of the S^0 granules are greater than the short dimension of the ovoid GSB cells (Stanier *et al.*, 1986). Kim *et al.*(1992) reported average S^0 particle and GSB sizes of 9.4 μm and 1.1 μm respectively in a culture of *C. thio.*. A membrane or fibre filter might utilize this size difference to remove elemental sulfur from suspension by sieving action. In preliminary tests, all of the S^0 but only 30% of the GSB were trapped on a 5 μm pore size membrane filter. Similarly, 100% of the elemental sulfur but only 50% of the bacteria were removed by a glass fibre filter that retained particles larger than 1.2 μm. Further studies were conducted by Dantas (1992) with membrane pore sizes ranging from 1.2 to 8.0 μm. The findings of the preliminary tests could not be repeated as *all* suspended material was removed at all pore sizes. The greater removal in the latter study was attributed to longer GSB chains as a consequence of longer bacteria retention time in the reactor. Thus the batch-to-batch variation in bacterial chain length precludes filtration as a reliable method of separating bacteria and elemental sulfur.

2.2.1.4 Centrifuging

In preliminary tests, the use of a centrifuge to produce a strong separating force, was shown to accomplish a good separation of 90:10 (% S^0 removed: % GSB removed) from the contents of a batch bioreactor. This method was suggested by Cork (1987) as an alternative to filtration. Further tests by Dantas (1992) achieved an optimum separation of 87:26 when the sample was spun at 143 gravities for 8 minutes. Centrifuging at lower speeds (56 gravities) resulted in less removal (65:26) of both elemental sulfur and bacteria

from suspension and the *difference* in removal percentages was less. Extreme agitation of the sample in a household blender to break the bacteria-S^0 adhesion prior to centrifuging gave similar results and did not justify the cost of agitation on an industrial scale.

At the conditions under which S^0 separation was optimized, the low S^0 concentration resulted in a low elemental sulfur concentration in the pellet. To illustrate this, consider that the average sulfur concentration in these experiments was 19 mg/L. If 89% of the S^0 was removed from a 1 L sample, 17 mg would end up in the pellet. The average bchl concentration was 39 mg/L. If 26% of this were removed from a 1 L sample, 10 mg bchl would be in the pellet after centrifuging. Assuming 3% of the VSS in the biomass is bchl (Section A.6 in Appendix A), the VSS in the pellet would be 10 mg/0.03 = 333 mg. Therefore, the percentage of sulfur in the pellet would be only 100(17/(17+333)) = 5%.

2.2.1.5 Floatation

In a dissolved air floatation system, clarified effluent is saturated with air under pressure and then mixed with sludge at atmospheric pressure. The air bubbles released in the solution, rise through the suspension and lift hydrophobic (water-hating) particles to the surface while leaving hydrophillic (water-loving) particles in suspension. This method could potentially take advantage of the difference in surface properties between sulfur granules and bacteria. Indeed, Rozek (1978) observed elemental sulfur floating on the surface of biologically oxidized mine wastewater. Due to problems with GSB supply, preliminary investigations on the use of this technique were performed using activated sludge from a local wastewater treatment plant spiked with elemental sulfur (Neave and

LaRiviere, 1993). Using CO_2 as the dissolved gas, 30-50% of the elemental sulfur was removed whereas 80-90% of the volatile suspended solids (bacteria) were removed from suspension. This result was contra-intuitive, since one would expect the hydrophobic S^0 to be removed to a greater extent than the bacteria. A few tests were performed on dilute cultures of *C. thio.*, resulting in no significant removal of either elemental sulfur or GSB from suspension.

2.2.1.6 Summary

The poor test performance of some of these methods of separation may have been due to the inconsistent nature and low concentration of the bacteria. The tests described previously were all conducted on bacteria grown in batch reactors. Of these methods, centrifuging was the most consistent and gave the highest differential separation of S^0 and GSB. Even so, the S^0 content in the sulfur-enriched fraction after separation was low, due to the low S^0 concentration in the bioreactor.

2.2.2 Separation of Bacteria

In the continuous bioreactor system illustrated in Figure 2.4, once elemental sulfur has been separated from the bioreactor effluent, the bacteria must be concentrated so that they can be recycled into the reactor. This standard solid-liquid separation can be accomplished by any of the techniques discussed above. Of these, the least energy intensive is sedimentation. However, even under alkaline conditions, only about half of the GSB had settled from suspension (Diemer, 1991). Further tests are required to determine the best technique to separate GSB from the wastewater.

CHAPTER THREE

MATERIALS AND METHODS

The 'great work'... meant months and years of toil over stills and furnaces, difficult processes being repeated over and over again with inadequate equipment.

Biedermann (1983)

3.1 Methods of Analysis

Throughout this section deH_2O refers to Type I (APHA *et al.*, 1992) deionized water. Deaerated deionized water ($dadeH_2O$) was prepared by boiling deH_2O for 5 minutes, corking the flask, and quickly cooling it in a cold water bath.

All absorbance measurements were made with a Pye Unicam PU8600 UV/VIS spectrophotometer using a 10 mm quartz cuvette and are reported in optical density units (O.D.). An International Equipment Co. Centra 8 centrifuge with a #269 rotor was used in the sulfide, sulfate, thiosulfate and bacteriochlorophyll assays. Indicated centrifuge times include a 2 minute acceleration period.

The concentrations of all sulfur species are expressed as "mg of species *as sulfur* per litre of volume" or "mg Sp-S/L" where Sp represents the particular sulfur species being measured. In this way, the concentrations of different sulfur species can be compared on a "mass of sulfur" basis.

3.1.1 Sulfide

The method of Truper & Schegel (1964) was used.

3.1.1.1 Reagents

Zn Solution: Roughly 19.1 g zinc acetate ($Zn(CH_3COO)_2 2H_2O$) crystals and

31

0.8 L of deH$_2$O were added to a glass bottle. The solution was shaken immediately before use.

DPD Solution: Exactly 2.00 g of dimethyl-*p*-phenylenediamine sulfate (DPD) were added to 1.00 L of cooled 20% H$_2$SO$_4$ (200 mL conc. H$_2$SO$_4$ + 800 mL deH$_2$O) in a beaker and stirred. The mixture was poured into a dark glass bottle for storage.

FAS Solution: Approximately 18.1 g of ferric ammonium sulfate (FeNH$_4$(SO$_4$)$_2$·12H$_2$O) were dissolved in 200 mL deH$_2$O, then 20 mL of conc. H$_2$SO$_4$ and 0.78 L of deH$_2$O were added to the solution.

3.1.1.2 Procedure

A graduated cylinder was used to measure 20 mL of the Zn solution into a 100.0 mL volumetric flask. Samples of the reactor contents were centrifuged for 32 minutes at 2,500 rpm (1,400 gravities). The sample was drawn into a syringe or into a disposable pipette tip using an Eppendorf Digital Pipette. When a syringe was used, it was rinsed thrice with the sample and filled. The syringe or pipette was inserted into a 100.0 mL volumetric flask. Between 0.010 and 1.00 mL of sample was squeezed into the Zn solution. The volumetric flask was swirled and 10.00 mL of DPD solution followed by 0.50 mL of FAS solution were pipetted into the volumetric flask. The flask was made up to the mark with deH$_2$O, capped and inverted several times. After a waiting period of at least 30 minutes, the absorbance was measured at 670 nm against deH$_2$O.

3.1.1.3 Calculation

The O.D.$_{670}$ value was converted to S$^=$ concentration using a calibration equation obtained in the laboratory (Section A.2 in Appendix A):

$$mg \, S^-/L \text{ in sample} = \frac{100.00}{mL \text{ sample}} \left[\frac{O.D._{670} - 0.022}{1.108} \pm 0.033 \right]$$

This method has been calibrated for $S^=$ concentrations of less than 1 mg/L *in the spectrophotometer cuvette.*

3.1.2 Elemental Sulfur

Aqueous samples were extracted into chloroform ($CHCl_3$) prior to quantification by high-performance liquid chromatography (HPLC; Lauren & Watkinson, 1985).

3.1.2.1 Apparatus

HPLC equipment included Waters: 501 Solvent Delivery System, Intelligent Sample Processor (WISP) Model 712, Nova-Pak C18 column (3.9x150 mm) at room temperature, 486 Tunable Absorbance Detector, System Interface Module and Maxima 820 software. The guard column was a Zorbak ODS (4.0x12.5 mm). The eluent was methanol (Baker HPLC grade) at 1.0 mL/min. The eluent was degassed on the day of use by vacuum filtering through a 0.45 μm pore Millipore FH filter.

3.1.2.2 Procedure

A 5.00 mL sample was added to a screw-capped culture tube (Pyrex, no. 99447, 16x125 mm) containing 2.00 mL of chloroform (Aldrich HPLC grade) and 0.500 mL of 10% (v/v) nitric acid. Where S^0 concentrations were anticipated to be high, the sample was diluted with deH_2O in the screw-capped culture tube so that the total aqueous volume was 5.00 mL. Tubes were shaken with a Burrell Wrist Action Shaker (Model 75) for 15 minutes, and then centrifuged at 3,000 rpm (2,000 gravities) for 7 minutes. One millilitre of the $CHCl_3$ layer was pipetted into a WISP vial containing 3.00 mL methanol (Baker

33

HPLC grade, as received). At least one standard was injected each day when the HPLC was run. The standards were prepared by refluxing elemental sulfur (Aldrich 99.999%) in $CHCl_3$ (Aldrich HPLC grade), serially diluting with HPLC grade $CHCl_3$ then diluting 1:3 with HPLC methanol in a WISP vial. The WISP vials were inverted to mix and queued in the WISP for injection. The run time for all samples was 5 minutes.

3.1.2.3 Calculation

The calibration curve to be used depended upon the matrix of the sample. For samples of the reactor contents:

$$mg\ S^o/L = \frac{5.00}{mL\ sample}\left[\frac{Response(\mu V\cdot s) - 1{,}448.7}{7{,}273.2} \pm 0.82\right]$$

Otherwise the following three equations were used.

At 0 mg $S^=$/L,

$$mg\ S^o/L = \left[\frac{Response(\mu V\cdot s) - 1{,}730.5}{7{,}869.3} \pm 0.85\right]$$

At 148 mg $S^=$/L,

$$mg\ S^o/L = \left[\frac{Response(\mu V\cdot s) - 25{,}879.2}{8{,}394.3} \pm 2.6\right]$$

At 305 mg $S^=$/L,

$$mg\ S^o/L = \left[\frac{Response(\mu V\cdot s) - 40{,}680.6}{8{,}360.0} \pm 2.0\right]$$

A spreadsheet was used to interpolate between these equations in the following way. At elemental sulfur concentrations of 0, 100 and 200 mg/L, the responses which would have occurred at each of the sulfide values tested (0, 148 and 305 mg $S^=$/L) were calculated (9 values). The sulfide concentration in the sample was measured and used to interpolate

34

between the calculated response numbers to determine what would be the response at 0, 100 and 200 mg S^0/L at the sample sulfide concentration (3 values). Then the actual response from the HPLC measurement of the sample was used to interpolate between the responses at 0 and 100, or 100 and 200 mg S^0/L. This gave the concentration of S^0 if the sample was 5.00 mL. Dilution of the sample was then taken into account. Sample dilution was performed to keep the elemental sulfur and sulfide concentrations below 200 mg S^0/L and 305 mg $S^=$/L respectively.

3.1.3 Sulfate

The APHA *et al.* (1992) turbidimetric method was used. Because Buffer A reacted with the $S^=$ and S^0 in the sample, the turbidity of the buffered solution without barium chloride ($BaCl_2$) was subtracted from that with $BaCl_2$. Turbidity measurements were made in nephelometric turbidity units with a Hach model 43900 Ratio/XR Turbidimeter. Standard Methods (APHA *et al.*, 1992) recommends that samples with $[SO_4^-]$ in the cuvette less than ~2.5 mg $SO_4^=$-S/L be spiked with standard sulfate. However, the approach used in this dissertation was to divide the calibration curve into two linear sections (Figure A.3 in Appendix A).

3.1.3.1 Reagents

Buffer A: Approximately 30 g of magnesium chloride hexahydrate ($MgCl_2$·$6H_2O$), 5 g of sodium acetate trihydrate ($Na(CH_3COO)$·$3H_2O$), 1 g of potassium nitrate (KNO_3), and 20 mL of glacial acetic acid (CH_3COOH) were added to a 1 L plastic bottle. One (1.0) L of deH_2O was added and the bottle was capped and shaken.

3.1.3.2 Procedure

A portion of the draw from the reactor was centrifuged at 2,500 rpm (1,400 gravities) for 32 minutes. A 5.00 to 20.00 mL sample was pipetted into a 250 mL erlenmeyer flask and 95.0 to 80.0 mL of deH$_2$O and a magnetic stir bar were added. The timer was started and 20.0 mL of Buffer A were added. The mixture was stirred mildly for ½ minute and then was used to rinse and fill a turbidimetric cuvette. The turbidity (NTU$_i$) of this solution was measured at 360 ± 30 seconds. At a clock time of 120 seconds, ½ mL of BaCl$_2$ crystals were added to the erlenmeyer flask and the solution was stirred vigorously for 60 ± 2 seconds. The solution was allowed to stand, used to rinse the cuvette, and the turbidity was measured (NTU$_f$) at 480 ± 30 seconds clock time.

3.1.3.3 Calculation

The ΔNTU value was converted to SO$_4^=$-S concentration using a calibration equation developed in the laboratory (Section A.4 in Appendix A):

$$\Delta NTU = NTU_f - NTU_i$$

For ΔNTU < 25,

$$mg\ SO_4^=-S/L = \frac{120.0}{mL\ sample}\left[\frac{\Delta NTU - 0.11}{9.39} \pm 0.024\right]$$

For 25 < ΔNTU < 180,

$$mg\ SO_4^=-S/L = \frac{120.0}{mL\ sample}\left[\frac{\Delta NTU + 13.22}{14.12} \pm 1.2\right]$$

This method has been shown to be free of interference for samples with [S$^=$]+[S^0] < 128 mg/L (Henshaw, 1990).

36

3.1.4 Thiosulfate

Ion chromatography (IC; Hamilton, 1992) was used.

3.1.4.1 Apparatus

IC equipment included Waters: 510 HPLC Pump, Rheodyne 7161 Manual Injector, Hamilton PRP-X100 column (4.1x150 mm), 431 Conductivity Detector, System Interface Module and Maxima 820 software. The guard column was a Zorbak ODS (4.0x12.5 mm). The eluent was 4mM *p*-hydroxybenzoic acid (Section A.5.2) at 2.0 mL/min.

3.1.4.2 Reagents

p-hydroxybenzoic acid: A stock solution of 4.4198 g of *p*-hydroxybenzoic acid (BDH) was prepared in 200 mL methanol (Baker HPLC grade). Twenty-five millilitres of this stock solution was pipetted into a calibrated 1 L plastic bottle and made up to the mark with Milli-Q water (18 MΩ·cm). On the day of use, the eluent was degassed by filtration through a Millipore HA filter and the pH was adjusted to 8.5 using 1 M NaOH made up in Milli-Q water. The conductivity of this eluent was roughly 320-340 μS.

3.1.4.3 Procedure

Standards were made each day that thiosulfate was measured in the reactor (Section A.5.2 in Appendix A). Prior to injecting the reactor samples, standards were injected full strength, 2/5 and/or 1/5 strength into the equilibrated IC apparatus. Reactor samples were centrifuged at 2,500 rpm (1,400 gravities) for 32 minutes. The supernatant was injected directly into the IC. The run time was 30 minutes.

3.1.4.4 Calculation

The conductivity detector response was converted to thiosulfate concentration by

the following relationship:

$$mg\,S_2O_3^-\text{-}S/L = \left[\frac{Response(\mu V \cdot s) - 539{,}052}{223{,}255} \pm 13\right]$$

The detector response was a linear function of $S_2O_3^-$ concentration up to 140 mg $S_2O_3^=\text{-}S/L$.

3.1.5 Bacteria

Bacteriochlorophyll (bchl) was extracted into methanol and its absorbance was measured (Maka, 1986). The concentration of bchl was taken as an indicator of the biomass concentration, although this measure gave no indication as to the activity of the biomass.

3.1.5.1 Procedure

A glass pipette was used to dispense 10.00 mL of ACS grade methanol into a centrifuge tube. A 1.00 mL sample was transferred by disposable pipette into the methanol. The tube was capped, swirled by hand for one minute, and centrifuged at 2,500 rpm (1,400 gravities) for 10 minutes. The absorbance of the supernatant was measured at 670 nm against an ACS grade methanol blank.

3.1.5.2 Calculation

The O.D.670 value was converted to bchl concentration using the conversion given by Maka (1986):

$$mg\,bchl/L \; in \; sample = 127.9\left[\,O.D._{670}\,\right] \pm 0.66$$

The original calibration of this method (Kakidas, 1982) was used up to a 77 mg bchl/L $(O.D._{670} < 0.6)$.

3.2 Apparatus

The requirements for a continuous bioreactor system are bacteria, a liquid nutrient growth medium, a light energy source, and a reactor vessel.

3.2.1 Bacteria

Chlorobium thiosulfatophilum was ordered from the American Type Culture Collection (ATCC, Rockville, Maryland; catalogue no. 17092) and subcultured weekly into sterile growth medium (Madigan, 1988).

3.2.2 Growth Medium

The chemical requirements for growth of GSB are CO_2, sulfide and some essential minerals. These requirements are satisfied in the growth medium presented by Madigan (1988). It consists of three parts: a mineral salts solution (supplying nitrogen, phosphate, calcium, magnesium and trace elements), a bicarbonate solution, and a sulfide solution. In the continuous-flow bioreactor experiments, the components of the growth medium were split amongst several influent streams. In all, 15 experiments (5 Runs and 10 Trials) were performed. Only 5 of these maintained growing bacteria until steady state (no significant change in $S^=$ and bchl concentration) measurements could be taken (see Appendix B for a summary of the experimental history). Runs 3, 4, and 5 and Trials 9 and 10 were successful. In the Runs the influent was composed of three streams: deionized water, a concentrated nutrient solution, and a sulfide stock solution (Figure 3.1). For the Trials there were only two feeds: a nutrient medium, and a sulfide stock solution (Figure 3.2). By increasing the flow rate of all feeds, the hydraulic retention time (HRT) was changed. By increasing the flow of the sulfide stock solution relative to the total
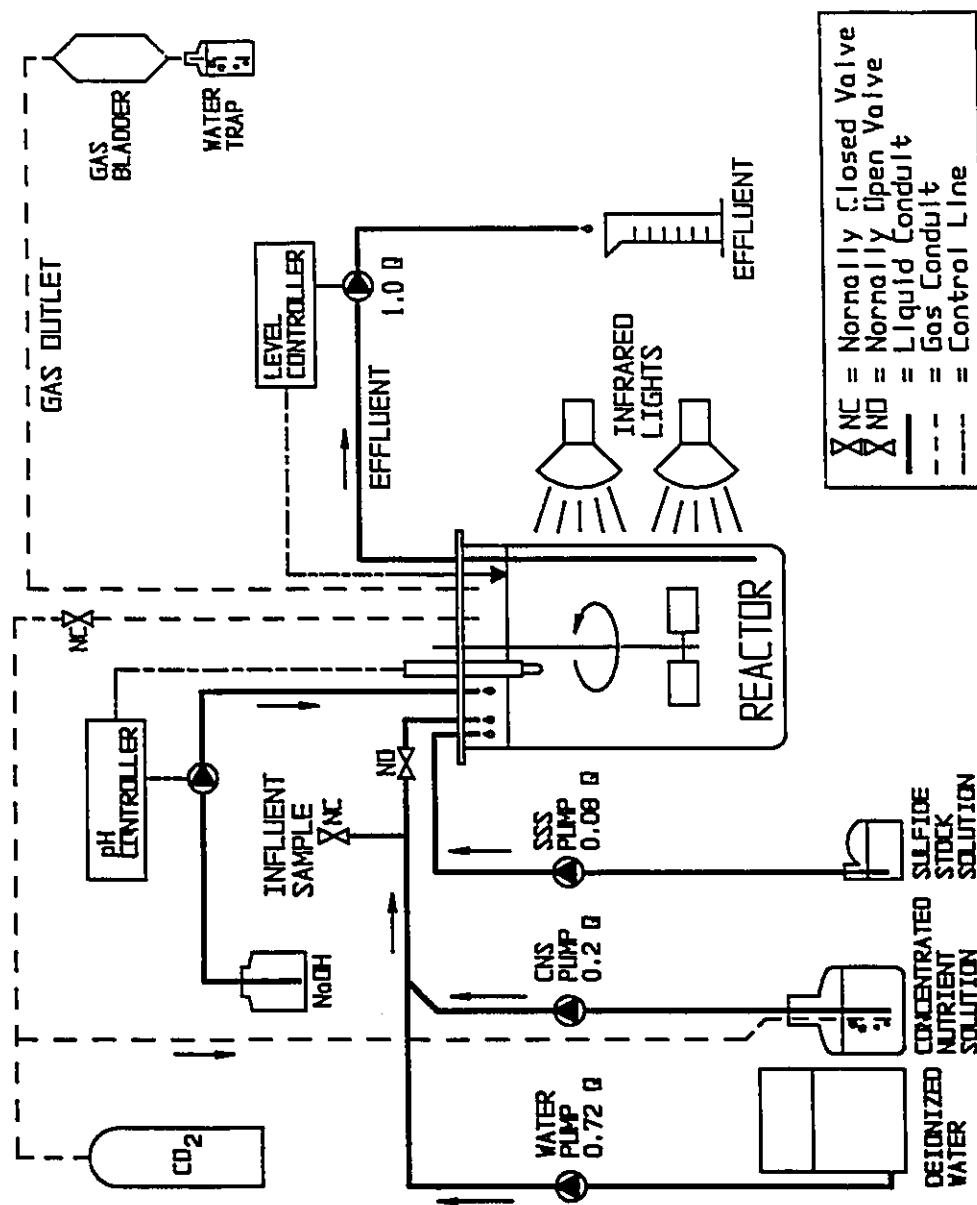
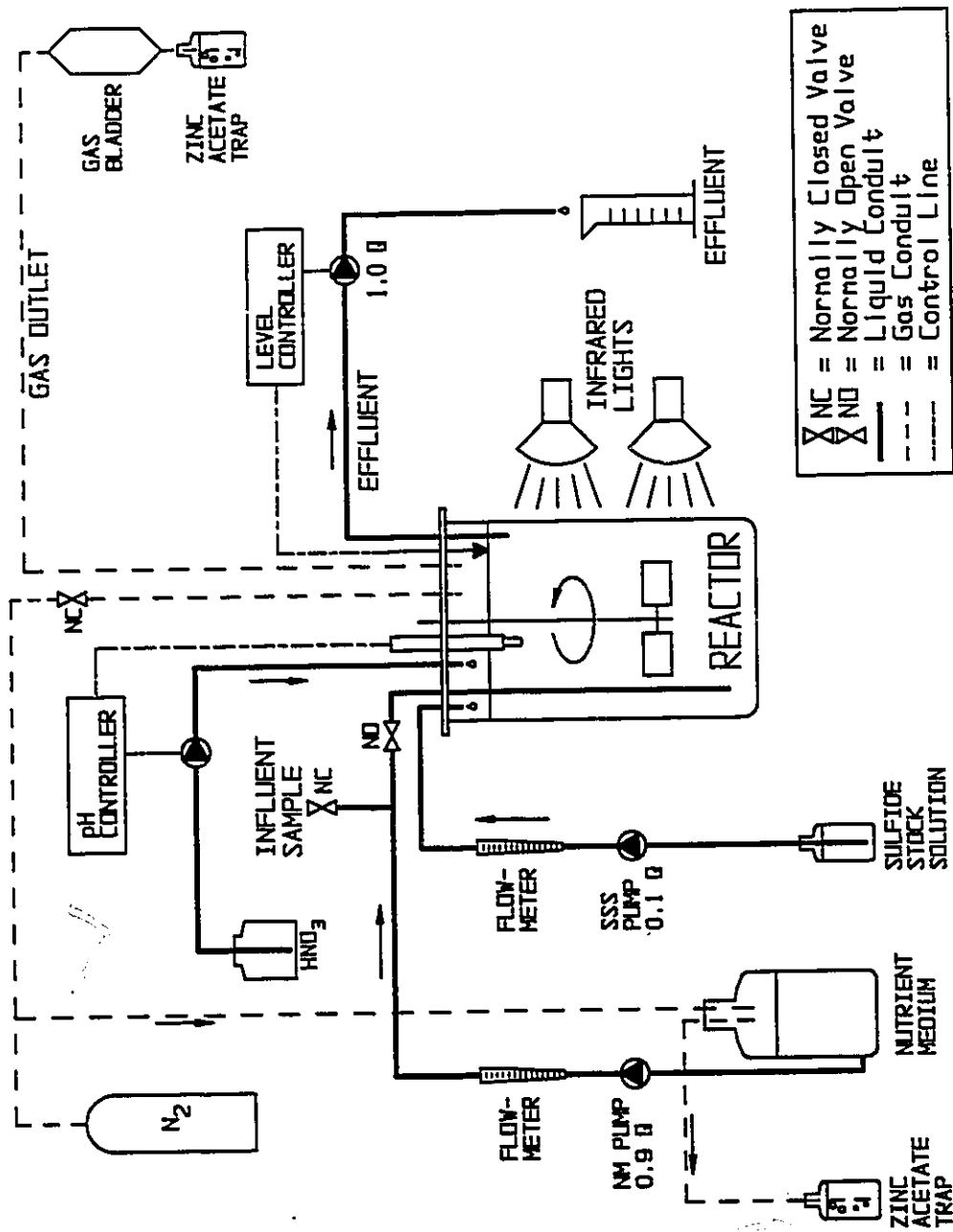FIGURE 3.1 Schematic Diagram for Runs 3, 4, and 5

40

FIGURE 3.2 Schematic Diagram for Trials 9 and 10

41

flow, the effective $S^=$ concentration in the feed was varied.

Trace Element Solution (TES): The TES was made by dissolving 5.757 g

$Na_2EDTA \cdot 2H_2O$ in 800 mL of deH_2O and adding 148 mg $ZnSO_4 \cdot 2H_2O$, 100 mg

$MnCl_2 \cdot 4H_2O$, 6 mg H_3BO_3, 190 mg $CoCl_2 \cdot 6H_2O$, 17 mg $CuCl_2 \cdot 2H_2O$, 28 mg

$NiSO_4 \cdot 6H_2O$, 188 mg $Na_2MoO_4 \cdot 2H_2O$, 30 mg $VOSO_4$, and 2 mg $Na_2WO_4 \cdot 2H_2O$. Then,

ten pellets of NaOH (to neutralize the solution so that salts would not precipitate as

readily) and 1.5 g $FeCl_2 \cdot 4H_2O$ were dissolved in the TES. Finally, it was diluted to 1.0

L with deH_2O. The TES was stored in culture tubes without air space at room

temperature.

Vitamin B_{12} Solution: This solution was made by dissolving 5.0 mg vitamin B_{12}

(cobalamin) in 250 mL deH_2O. The vitamin solution was kept in a brown plastic bottle

in a refrigerator.

Sulfide Stock Solution (SSS): Crystals of $Na_2S \cdot 9H_2O$ (Fisher ACS grade for

Runs 3, 4, and 5 and Trial 9, Sigma ACS grade for Trial 10) were rinsed in deH_2O,

patted dry, weighed, and dissolved in $dadeH_2O$. The solution was stirred during use and

the plastic carboy was covered with Parafilm. The concentration of sulfide was monitored

daily and ranged from 1500 to 4500 mg $S^=$/L.

Concentrated Nutrient Solution (CNS): The CNS is essentially the mineral salts

and bicarbonate portions of Madigan's (1988) growth medium concentrated x5 to give the

proper dilution when mixed with deionized water and SSS. A 20 L carboy containing

10 L deH_2O was filled with 0.975 g $Na_2EDTA \cdot 2H_2O$ (dissolved first before others were

added), 15.0 g $MgSO_4 \cdot 7H_2O$, 3.75 g $CaCl_2 \cdot 2H_2O$, 30.0 g NaCl, 30.0 g NH_4Cl, 37.5 g

KH_2PO_4, 75 mL trace element solution, 75 mL vitamin B_{12} solution, and made up to 15.0 L with deH_2O. After autoclaving, 150.0 g of autoclaved $NaHCO_3$ was added. The concentrated nutrient solution was stirred with a magnetic stir bar and the mixture was bubbled with CO_2 for the duration of the experiment. The biomass growth was not limited by the availability of CO_2, the bacterial substrate (Appendix H). As the solution was bubbled, it became cloudy and when the carboy was nearly empty, it became difficult to see the stirrer to restart it.

Nutrient Medium (NM): The NM is the full medium formulation (Madigan, 1988) but concentrated by a factor of 1.25 or 1.11 for Trials 9 and 10 respectively to compensate for dilution when mixed with the sulfide stock solution. It also contains the minimum amount of sulfide to keep the solution anaerobic in the carboy. For Trial 10, a 10 L carboy containing 4 L deH_2O was filled with 0.125 g $Na_2EDTA \cdot 2H_2O$ (dissolved first before others were added), 2.0 g $MgSO_4 \cdot 7H_2O$, 0.50 g $CaCl_2 \cdot 2H_2O$, 4.0 g NaCl, 4.0 g NH_4Cl, 5.0 g KH_2PO_4, 10 mL trace element solution, 10 mL vitamin B_{12} solution and made up to 4.5 L with deH_2O. A bicarbonate solution was made by dissolving 20.0 g $NaHCO_3$ in 3.6 L of deH_2O and bubbling CO_2 through it for at least ½ hour. A sulfide solution was made by dissolving 7.8 g of rinsed and patted dry $Na_2S \cdot 9H_2O$ crystals in 0.9 L of $dadeH_2O$. The latter two solutions were poured into the mineral salts solution, the carboy was sealed and kept in the dark for 24 hours prior to use. The pH was usually near 7. The solution was stirred while in use, and the headspace of the carboy was pressurized with nitrogen to prevent oxygen contamination. The headspace gas was bubbled through a zinc acetate trap. The concentration of sulfide in the carboy was

43

Zinc Acetate Trap: In a plastic bottle, 19.1 g $Zn(CH_3COO)_2 \cdot 2H_2O$ was dissolved in 800 mL deH_2O.

3.2.3 Reactor

A New Brunswick Scientific Co. model F-14 fermenter was used as a continuous reactor. Valves were added to the air inlet, sparger inlet, and bottom sampling tube. The reactor was wrapped in a metallized mylar film which was held in place by rubber cement (aluminum foil was found to deteriorate in the water bath). Two 105 mm high by 110 mm wide windows were cut one above the other into the film so that the top of the upper window was at the water level of the water bath. A second reactor was used as a submerged light source by removing the stir paddles and clamping two Philips IR 175 Watt R-PAR bulbs inside the vessel.

Both reactors were mounted in a New Brunswick Scientific Co. model FS-314 fermenter drive assembly. The light source was mounted in the centre position with the light bulbs shining directly into the windows of the bioreactor. This resulted in an average irradiance of 258 W/m^2 over both windows. With only the bottom light on, the irradiance was 119 W/m^2 (Appendix C). The waterbath was filled with tapwater. With both lights on, supplemental cooling was required to maintain the temperature below 34°C. This was achieved by pumping the water in the water bath through a heat exchanger immersed in a cold well (New Brunswick Scientific Co.). In addition, cold tap water was continuously trickled into the water bath to cool the system and maintain the water bath at the level of the overflow. These two actions essentially "over-cooled" the water bath, so the water bath thermostat was set at 30°C to accurately maintain the

44

temperature. The fermenter drive assembly's variable speed drive was connected to the bioreactor and the stirring speed adjusted to 200 rpm (Cole-Palmer Digital Tachometer) during Trials 9 and 10. The speed was approximately 200 rpm for Runs 3, 4, and 5. The reactor was considered to be fully mixed (Appendix D).

Masterflex (Cole-Palmer Co.,Chicago) variable speed pumps with Masterflex solid state speed controls and standard pump heads were used for all influent and effluent reactor streams. The liquid level in the reactor was kept constant by a level probe inside the reactor which controlled the effluent pump. When the liquid level reached the probe, there was a 3 minute delay (to avoid short-cycling the pump) then the pump ran until the liquid was below the level of the probe (about 30 seconds).

The pH inside the reactor was kept between 6.8 and 7.2 by an Omega (Omega Engineering Co., Stamford, CT) PHP-166 Chemical Metering Pump controlled by an Omega PHM 55 pH Regulator connected to an Ingold (Ingold Electrodes Inc., Wilmington, MA) 465-35-K9 combined glass electrode inserted into the reactor inside an Infit 761-351B protecting tube. The pump could be configured to deliver either acid or base into the reactor.

3.3 Experimental Protocol

3.3.1 Start-up

The procedure for start-up of the continuous bioreactor took about two weeks. The contents of a 70 mL culture tube containing *C. thio.* were poured into a 1.1 L round bottom flask containing 1.0 L of growth medium. This was incubated under infrared light in a 30°C water bath for about three days while constantly being stirred. On the first day,

in a 30°C water bath for about three days while constantly being stirred. On the first day, the vessel became visibly cloudy and yellow (sulfur). By the third day the yellow colour gave way to a deep green (GSB). The contents of the 1 L reactor were then poured into the fermenter containing 11 to 12 L of growth medium where it was stirred and illuminated for an additional three to four days. The turbidity and colour changes observed in the 1 L reactor were observed in the fermenter also. In some experiments, the bacteria concentration was increased by feeding in *only* sulfide stock solution to provide the bacteria with an electron source without a high liquid turnover through the reactor. Then the other feed pump(s) were turned on and adjusted.

Apart from the culture tubes, the reactors and equipment were not sterile. The recipe for growth medium required that it be kept in the dark for 24 hours so that the sulfide would consume any oxygen in the vessel and prevent algal growth. The combination of anaerobic conditions, lack of organic carbon, and darkness discouraged the growth of other microrganisms, including algae and *Thiobacillus*, but this was not confirmed by micrscopic observations.

3.3.2 Operation

In general, the daily operation of the bioreactor consisted of ensuring adequate quantities of feed solution, checking that the reactor pH, temperature, illumination, level and stirring were constant, measuring in-reactor and feed solution concentrations, and adjusting the feed solution pump rates.

The feed pumps were typically operated at 2 to 10 rpm. The most recent pump calibration was used to adjust the pumping rate during the experiment; however, for

calculations after the completion of an experiment, values of pump capacity (mL/revolution) were interpolated between pump calibrations. Once calibrated, feed pumps were adjusted by turning the variable speed dial and timing the revolutions until the proper rpm was achieved. A piece of foam rubber was jammed under the speed controller dial to ensure that the pump vibrations would not change the setting.

The pH electrode was calibrated every 1 to 12 days by pressurizing the reactor with CO_2 or N_2 (so that oxygen did not enter the reactor), removing the pH electrode, rinsing it, calibrating it in two buffers of pH 7.0 and 4.0 or pH 7.0 and 10.0, and returning it to the reactor.

Occasionally, the reactor windows became obscured with what was presumed to be elemental sulfur. This was remedied by pressurizing the reactor, interrupting reactor stirring, opening the septum port of the reactor, and using a curved wire brush to clean the reactor windows.

The time when a reactor sample was added to the analytical reagents was recorded and considered to be the time of measurement of the parameter. In the case of the sulfate sample, this was the time when Buffer A was added to the diluted sample. For thiosulfate, the time of measurement for all samples taken that day, was approximated as the time of injecting the reactor sample into the IC.

Earlier tests (Run 1) revealed that the bchl concentration in the CNS and SSS was zero. Therefore, this parameter was not measured in subsequent feed solutions. Similarly, three measurements of the S^0 concentration in the CNS of Run 1 were zero so elemental sulfur was not measured in the CNS. The parameters measured in each of the

experiments are summarized in Table 3.1.

TABLE 3.1 Parameters measured during continuous reactor operation

Experiment	Daily	When SSS Changed	When Nutrient Solution (CNS or NM) Changed	Occasionally
Runs 3, 4, and 5	Flow- r(W,N,S) Rtr- S=, SO$_4$=,bchl, c(pH) SSS- S=	(3-4 d) Flow- r(W,N,S), c(W&N,S) Rtr- S=,S^0, SO$_4$=,bchl SSS- S=,S^0, SO$_4$= W&N- SO$_4$=	(10-12 d) Flow- r(W,N,S), c(W&N,S) Rtr- S=,S^0, SO$_4$=,bchl SSS- S=,S^0, SO$_4$= W&N- SO$_4$=	
Trials 9 and 10	Flow- r(N,S) Rtr- S=,bchl SSS- S= NM- S=	(5-9 d) Flow- r(N,S) Rtr- S=,bchl SSS- S= NM- S=	(3-4 d) Flow- r(N,S) Rtr- S=,bchl SSS- S= NM- S= GT- S=	(1-12 d) Rtr- c(pH) (7-16 d) Flow- c(N,S) (at st.st.) Rtr- S=,S^0, SO$_4$=,S$_2$O$_3$=, bchl SSS- S=,S^0, SO$_4$=,S$_2$O$_3$= NM- S=,S^0, SO$_4$=,S$_2$O$_3$=

(# d)= frequency of occurrence in days, r(W,N,S)= rotations of water and nutrient (CNS or NM) and SSS feed pumps, c()= calibration, Rtr= reactor, W&N= combined water and CNS stream, GT= zinc acetate gas trap, (at st.st.)= measured 3 to 4 times when steady state reached.

48

Steady state conditions were deemed to have been reached when the measured concentrations of $S^=$ and bchl in successive daily samples did not change significantly. Buisman *et al.*(1990a) and Sublette and Sylvester (1987a) allowed five HRT's before taking measurements. For full-size anaerobic reactors, Metcalf and Eddy (1991) suggest that steady state is reached in 10 to 20 days in sludge digesters, and 15 days for high rate wastewater treatment.

3.3.2.1 Runs 3, 4, and 5

For these Runs, three feed solutions were used (Figure 3.1). The concentration of the sulfide stock solution was increased in successive Runs while the HRT was held constant (Table 3.2) for all Runs. Throughout each experiment, a constant sulfide loading rate was maintained regardless of the condition in the reactor. Run 2 began with an inoculum from a culture tube (Section 3.3.1) and lasted for 16 days before the pH electrode had to be remediated (Appendix B). However, the biomass remained viable in the reactor and was used for Runs 3, 4, and 5, which were performed subsequent to Run 2 without new inoculations of bacteria.

The desired HRT of Run 3 was determined by calculating the minimum cell retention time and multiplying by a safety factor (Appendix E).

Samples of the combined concentrated nutrients and water were taken by closing the reactor inlet valve and unplugging the inlet sampling tube. A minimum of 30 mL was discarded before the inlet sample was taken. The sulfide stock solution was sampled by placing a syringe directly into the plastic bottle. Reactor samples were taken by pumping out through the bottom sampling tube. A minimum of 100 mL was discarded prior to

49

collecting the reactor sample. The discarded volumes were 1.3 times the calculated volumes of the tubing.

3.3.2.2 Trials 9 and 10

For these experiments, two feed solutions were used (Figure 3.2). In both Trials, HRTs higher than those in Runs 3, 4, and 5 were used. The sulfide loading was adjusted so as to have a low but constant sulfide concentration in the reactor. Both Trials were started from scratch by inoculation from a pure culture (Section 3.3.1). Samples of the nutrient medium were taken by closing the reactor inlet valve and unplugging the inlet sampling tube. A minimum of 30 mL was discarded before the inlet sample was taken. The SSS was sampled by pouring a small portion into a centrifuge tube from which the sample was withdrawn. Reactor samples were taken by pressurizing the reactor with N_2, opening the septum port, inserting a glass pipette directly into the reactor, and withdrawing 25 mL.

TABLE 3.2 Variables in continuous reactor operation

Experiment	Config.	RSL	Vol. (L)	Dur. (h)	$[S^=]_i$ (mg/L)	Load. (mg/h·L)	HRT (h)	pH adj.	$[S^=]_{sss}$ (mg/L)	NI	$[SO_4^=]_i$ (mg/L)
Run 3	3.1	bottom	13.7	316	90	2.1	45	b	1340	1.02	29
Run 4				383	190	4.4	44	b	2760	0.99	30
Run 5				283	260	5.6	46	a	4040	1.05	32
Trial 9	3.2	top	12.0	1680	550	3.2	173	a	2730	1.03	37
Trial 10				1220	260	2.7	99	a	2440	1.01	31

Config.= number indicates Figure number of reactor configuration, RSL= reactor sampling location, Vol.= reactor liquid volume, Dur.= duration of experiment, $[S^=]_i$= effective inlet sulfide concentration, Load.= average reactor sulfide loading (see section 4.1.2), pH adj.= acid (a) or base (b) used to adjust pH in reactor, $[S^=]_{sss}$= sulfide stock solution concentration, NI= nutrient index= the concentration of the nutrient solution times the dilution of this solution as it is mixed with the other influent streams (1.00 is equivalent to the medium perscribed by Madigan,1988), $[SO_4^=]_i$= effective inlet sulfate concentration (another indicator of the influent nutrient concentration).

51

CHAPTER FOUR

RESULTS AND DISCUSSION

The experimenter wound his way through a labyrinth of false starts, misleading side tracks, dead ends, false hopes, disappointments, disasters and delays.

Biedermann (1983)

4.1 Observations

In this Section, each Figure contains data from a single experiment, whereas each Figure in Section 4.2 contains parameters calculated from all of the experiments.

4.1.1 Concentrations

The concentrations of the sulfur species in the reactor, as well as the bchl in the reactor are assumed to be equal to the concentrations leaving the reactor (Appendix D). Concentrations within the reactor are indicated without subscript. Figures 4.1, 4.2, 4.3, 4.4 and 4.5 show these concentrations as functions of time. As well, daily effective sulfide inlet concentrations ($[S^=]_i$) were calculated using linear regressions to smooth the raw feed solution $S^=$ concentrations (Appendix F). Then, 5 day moving averages of these values were calculated and plotted.

As Figure 4.1 shows, the S^0 concentration was reduced to approximately zero after 150 hours as the reactor approached a steady state condition. The plot clearly shows that at least 3 HRTs were required to achieve a steady state. At the steady state condition for Run 3, the inlet sulfide concentration was roughly equal to the outlet sulfate concentration. The $S^=$ concentration in the reactor was essentially zero throughout this experiment. Thus, the bacteria were completely oxidizing the sulfide in the reactor to
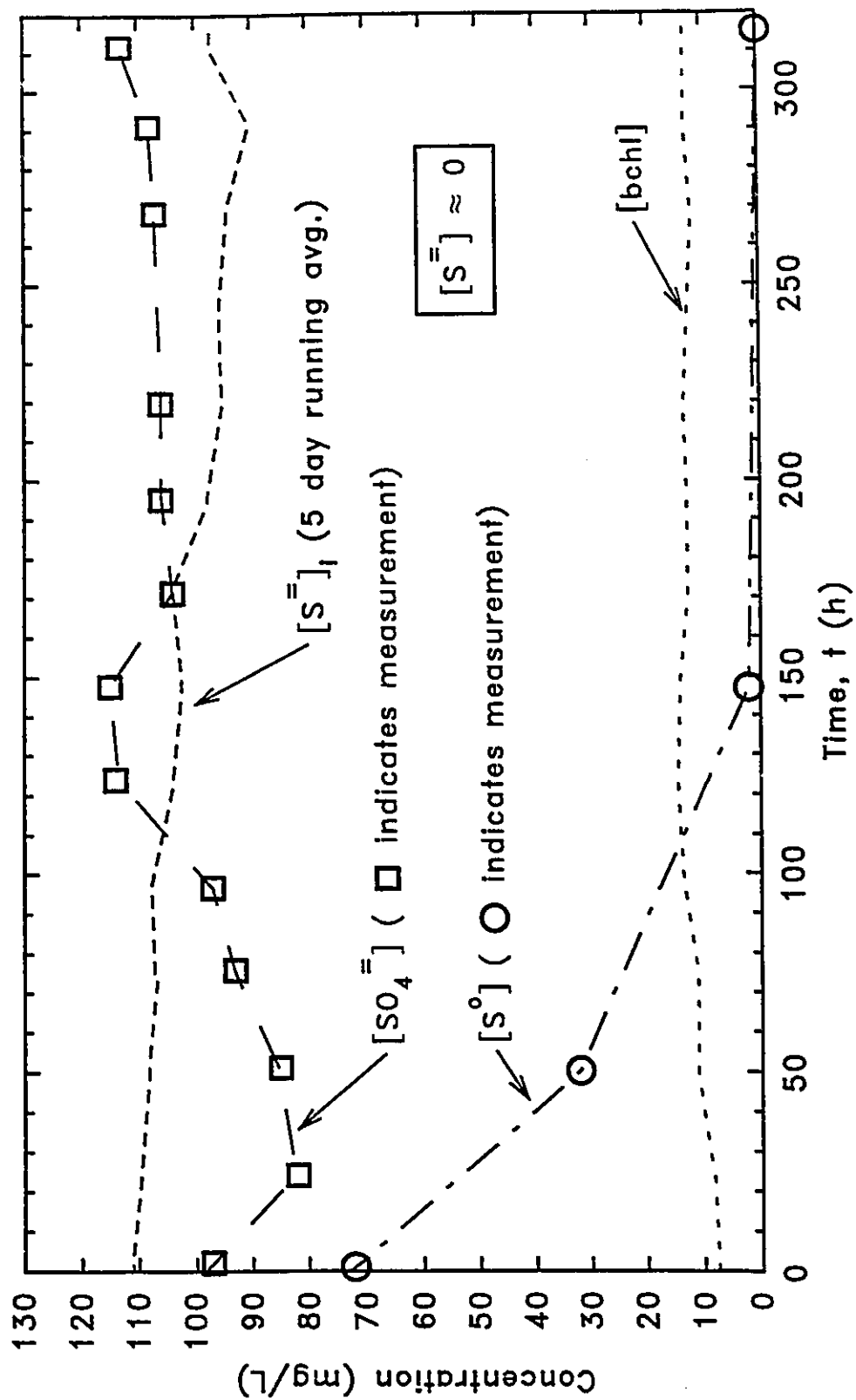
52

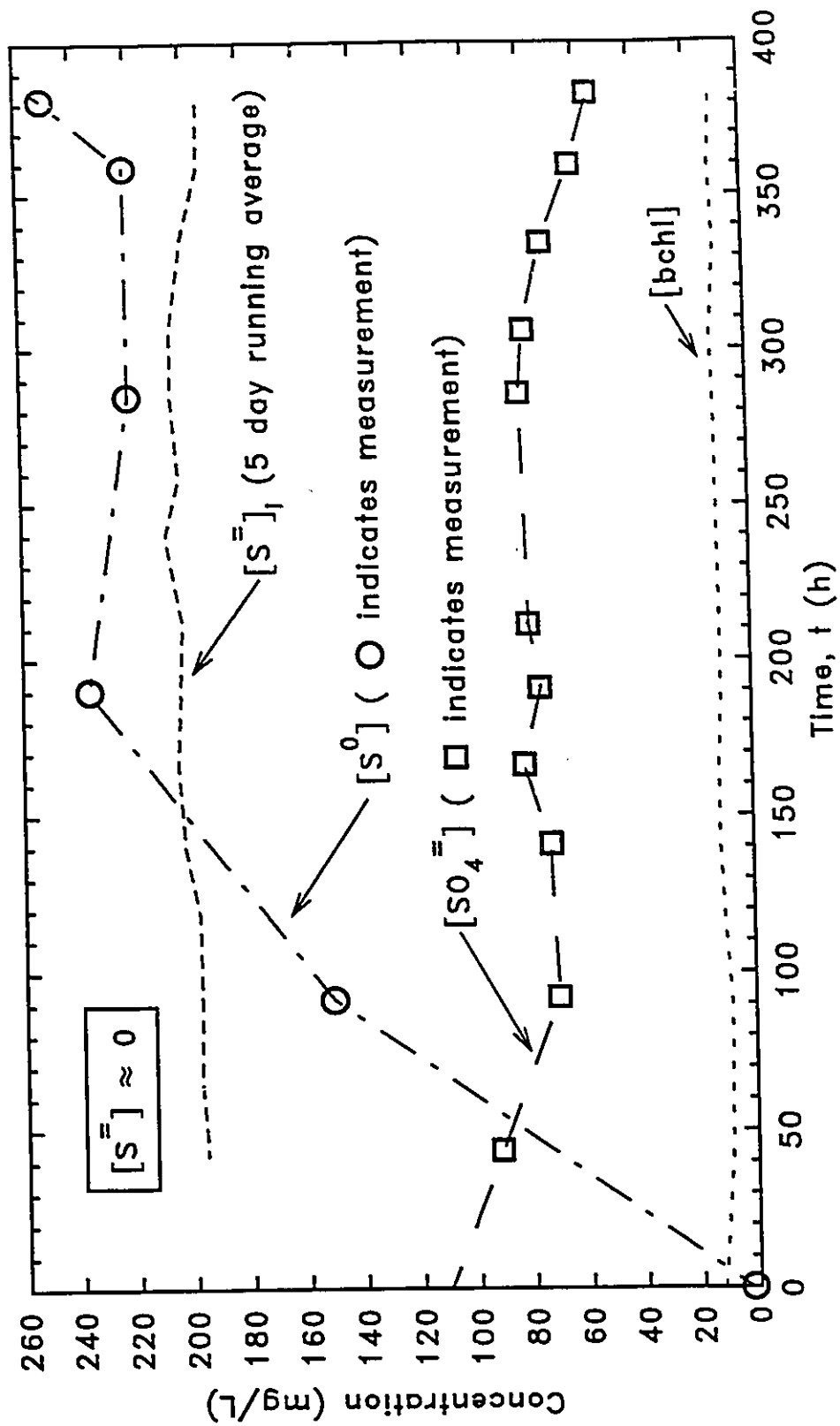FIGURE 4.1 Changes in sulfur and bchl concentrations in Run 3

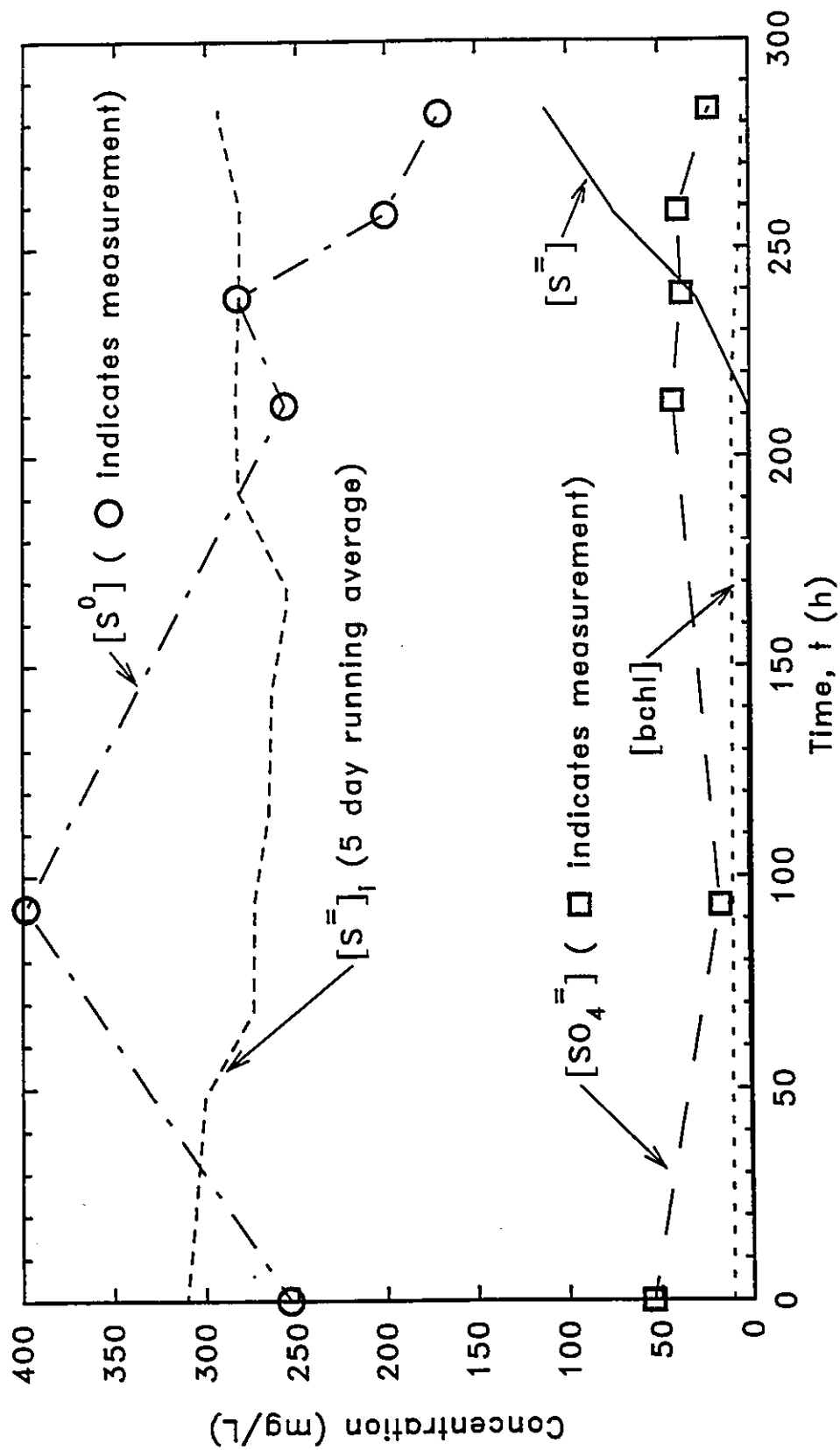FIGURE 4.2 Changes in sulfur and bchl concentrations in Run 4

54

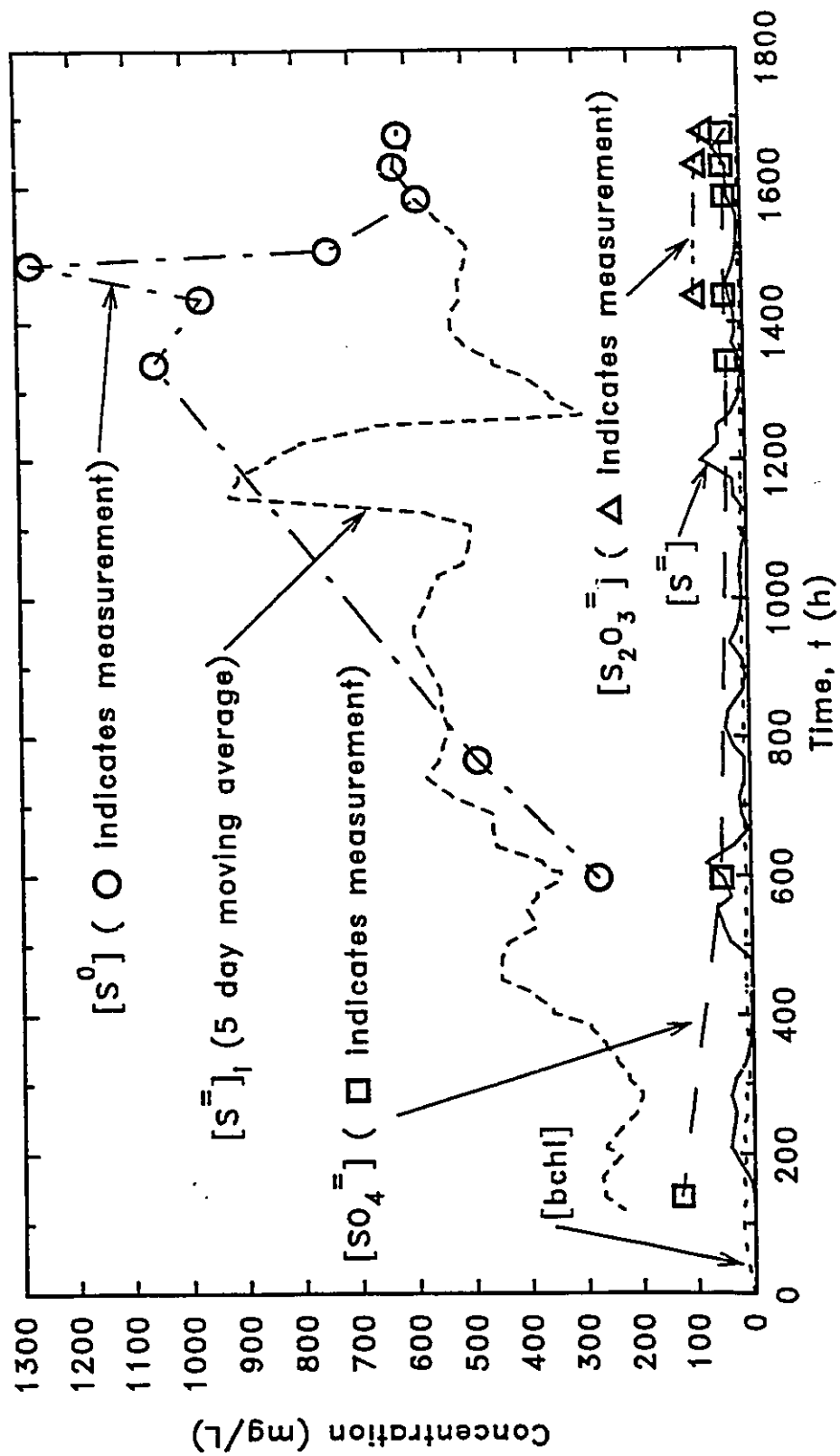FIGURE 4.3 Changes in sulfur and bchl concentrations in Run 5

55

FIGURE 4.4 Changes in sulfur and bchl concentrations in Trial 9
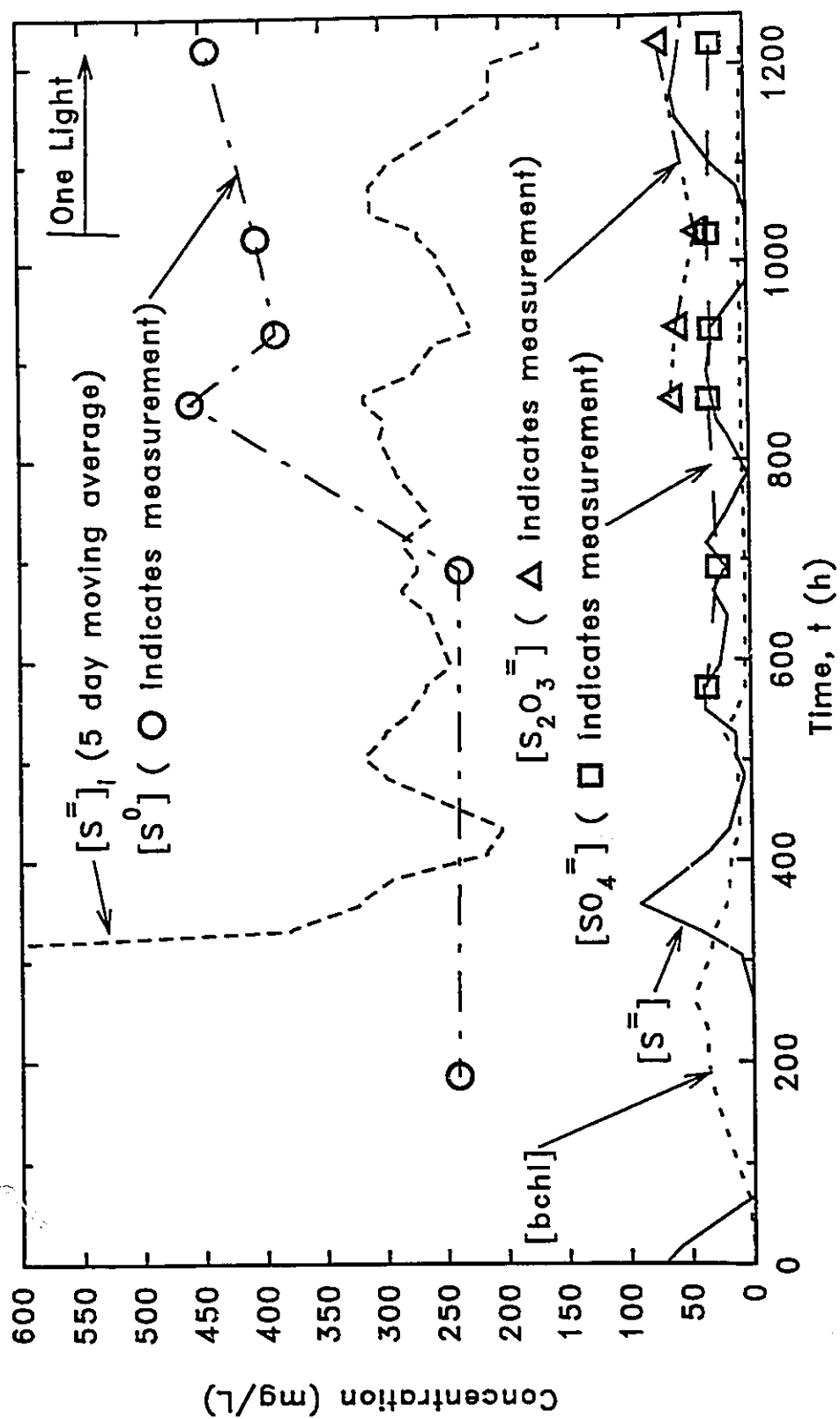
56

FIGURE 4.5 Changes in sulfur and bchl concentrations in Trial 10

57

produce sulfate. Since elemental sulfur is the desired end-product from this process, Run 3 represents an underloaded condition in terms of sulfide. There was not enough sulfide being provided to satisfy the need of the bacteria for electrons and so elemental sulfur was sought as an electron donor. The initially high concentration of elemental sulfur in Figure 4.1 may have been a residual of the elemental sulfur built up in the reactor in Run 2.

In Run 4 (Figure 4.2), the reactor was operated at a nearly optimum sulfide loading. Here, steady state was reached at about 200 hours or 4½ HRTs, as indicated by the levelling off of the S^0 concentration. From this time onward, the effective S^- input concentration was roughly equal to the reactor S^0 concentration, if the uncertainty in the assays are taken into account. Thus, most of the requirement for electrons in the reactor was satisfied by oxidizing $S^=$ to S^0. Again, the reactor S^- concentration was zero. The reactor $SO_4^=$ concentration was about twice that of the inlet SO_4^- concentration (30 mg $SO_4^=$-S/L, Table 3.2) indicating that some of the sulfur was being fully oxidized to SO_4^-.

Run 5 was operated at a high effective inlet sulfide concentration (Table 3.2). As a result, the reactor S^0 concentration slowly decreased and after 210 hours, S^- accumulated in the reactor (Figure 4.3). In this condition, the reactor was overloaded with sulfide since there was insufficient capacity to oxidize all of the inlet sulfide. The experiment did not reach a steady state condition since the concentrations of S^- and S^0 had not reached a plateau. There were two prominent disturbances in this experiment when the sulfide inlet concentration had suddenly decreased. At 115 hours, the SSS pump was accidentally turned off for 22 hours. And at 212 hours, the pump flow rates

58

were adjusted for a 4000 mg $S^=$/L SSS but the next day the SSS concentration had decreased to 2000 mg $S^=$/L. The latter disturbance may have precipitated the failure of the bacteria to consume all of the sulfide resulting in the "breakthrough" of sulfide in the reactor effluent.

Experiments for Trials 9 and 10 were conducted for longer periods than Runs 3, 4, and 5. Therefore, the time scales are bigger and the unsteadiness in inlet $S^=$ concentrations in Figures 4.4 and 4.5 are more pronounced. In addition, these trials were operated so as to have a low but steady sulfide concentration in the reactor of about 10 mg/L. This was done by measuring the $S^=$ concentration in the reactor, considering previous measurements to decide whether the sulfide was increasing or decreasing, and adjusting the sulfide loading by changing the pump speeds. Normally, reactor sulfide concentration should have corrected overnight but sometimes the calculated loading was not achieved because (i) the pump rate changed, or (ii) the sulfide concentration in the feed solution changed more than anticipated, or (iii) the calculated loading was inadequate to bring the sulfide concentration back to 10 mg $S^=$/L. As a result, the magnitude of fluctuations in inlet $S^=$ concentration were greater than in Runs 3, 4, and 5.

Figure 4.4 shows that the reactor was operated at a nearly optimal condition in Trial 9. The elemental sulfur concentration in the outlet equalled or exceeded the effective sulfide inlet concentration. The sulfate concentration in the reactor was steady and nearly equal to the inlet $SO_4^=$ concentration. These two conditions indicate that the reactor was being operated *on* the van Niel curve and complete conversion of $S^=$ to S^0 occurred. At times, sulfide was present in the reactor, which normally indicates overloading, but the

59

sulfide did not accumulate throughout the experiment. The sharp increase in effective sulfide inlet concentration at 1172 hours was due to the shutdown of the NM pump. There was a break in the N_2 gas line leading to the NM reservoir. This appeared to have caused the zinc acetate trap to be sucked into the NM, thereby contaminating it. A new batch of NM was brought on-line within 29 hours.

The reactor was very turbid at the end of Trial 9. At 1459 and 1486 hours the turbidities of the reactor contents were found to be 1600 and >2000 NTU respectively. The turbidity of the 1459 hour sample decreased to about 700 NTU after 15 minutes sitting, indicating the suspended material (probably S^0) was settleable. In the middle portion of the experiment, the S^0 concentration exceeded the effective inlet S^- concentration. This indicates that elemental sulfur had accumulated in the reactor, and then some event, possibly the $[S^-]_i$ spike at 1172 hours precipitated the decline in elemental sulfur concentration.

Trial 10 was also operated at nearly complete S^- to S^0 conversion. However, the steady state reactor elemental sulfur concentration was greater than the effective inlet sulfide concentration (Figure 4.5). As in Trial 9, sulfate concentration was essentially steady and S^- concentration was non-zero but its concentration alternately increased and decreased in the reactor. In this case, S^0 accumulated in the reactor but there was no event which caused the S^0 concentration to return to the value of the inlet sulfide concentration.

4.1.2 Mass Balance on Sulfide

The calculation of the rate of sulfide consumption in the continuous bioreactor was accomplished by use of a mass balance. The general mass balance equation for a control volume is:

$$\begin{pmatrix} Rate\ of \\ Accumulation \end{pmatrix} = \begin{pmatrix} Rate\ of \\ Inflow \end{pmatrix} - \begin{pmatrix} Rate\ of \\ Outflow \end{pmatrix} + \begin{pmatrix} Rate\ of \\ Formation \end{pmatrix} \qquad [4\text{-}1]$$

For chemical A fed into a CSTR, this becomes:

$$V\frac{d[A]}{dt} = Q_i[A]_i - Q_o[A]_o + r_A V \qquad [4\text{-}2]$$

where:
- V is the volume of the reactor (L)
- $d[A]$ is the incremental change in the concentration of A in the reactor (mg/L)
- dt is the incremental change in time (h)
- Q_i is the inlet flow rate (L/h)
- $[A]_i$ is the concentration of A in the influent to the reactor (mg/L)
- Q_o is the outlet flow rate (L/h)
- $[A]_o$ is the concentration of A in the effluent from the reactor (mg/L)
- r_A is the rate of formation of A (mg/h·L), ($r_A < 0$ would mean that A was being consumed)

In a CSTR, the concentration of A leaving the reactor equals that within the reactor, *i.e.* $[A]_o = [A]$. In addition, if the reactor liquid volume is held constant, the influent flow rate equals the effluent flow rate, *i.e.* $Q_i = Q_o = Q$. When these values are substituted and the reactor volume is factored out, Equation 4-2 becomes:

$$\frac{d[A]}{dt} = \frac{Q}{V}[A]_i - \frac{Q}{V}[A] + r_A \qquad [4\text{-}3]$$

The differential value can be approximated by the gross change over a longer time:

$$\frac{\Delta[A]}{\Delta t} = \frac{Q}{V}[A]_i - \frac{Q}{V}[A] + r_A \qquad [4\text{-}4]$$

61

The term $\Delta[A]/\Delta t$ is the rate of change of mass per unit time per unit volume of the reactor, or the rate of change of concentration in the reactor per unit time. The units are mg/h·L.

For all experiments in this dissertation, the rate of sulfide accumulation per unit volume was:

$$\begin{pmatrix} Rate\ of \\ Accumulation \\ of\ S^{=}/Volume \end{pmatrix} = \frac{\Delta[S^{=}]}{\Delta t} = \frac{[S^{=}]_2 - [S^{=}]_1}{t_2 - t_1} \qquad [4\text{-}5]$$

where: $[S^{=}]$ is the reactor sulfide concentration (mg/L)
        1   is a subscript for "at time 1"
        2   is a subscript for "at time 2"

Because of the different reactor configurations, the rates of input were calculated differently in the first three and the last two experiments. For Runs 3, 4, and 5:

$$f_{TOT} = f_{WATER} + f_{CNS} + f_{SSS} \qquad [4\text{-}6]$$

$$[S^{=}]_i = [S^{=}]_{SSS} \frac{f_{SSS}}{f_{TOT}} \qquad [4\text{-}7]$$

where: $[S^{=}]_i$ is the effective inlet sulfide concentration (mg/L)
        f   is a flowrate (mL/min)
        WATER   is a subscript for deH$_2$O
        CNS   is a subscript for concentrated nutrient solution
        SSS   is a subscript for sulfide stock solution
        TOT   is a subscript for the total inlet flow

For Trials 9 and 10:

$$f_{TOT} = f_{NM} + f_{SSS} \qquad [4\text{-}8]$$

$$[S^-]_i = \frac{[S^-]_{NM} f_{NM} + [S^-]_{SSS} f_{SSS}}{f_{TOT}} \qquad [4\text{-}9]$$

where: NM   is a subscript for nutrient medium

In either case:

$$HRT = \frac{V}{Q} = \frac{V}{0.06 \, f_{TOT}} \qquad [4\text{-}10]$$

where: 0.06   is a conversion factor (L·min/mL·h)

$$S^- \; Loading = \frac{Q}{V}[S^-]_i = \frac{[S^-]_i}{HRT} \qquad [4\text{-}11]$$

$$\begin{pmatrix} Rate \; of \\ Input \\ of \; S^-/Volume \end{pmatrix} = \frac{S^- \; Loading_1 + S^- \; Loading_2}{2} \qquad [4\text{-}12]$$

$$\begin{pmatrix} Instantaneous \\ Rate \; of \; Output \\ of \; S^-/Volume \end{pmatrix} = \frac{Q}{V}[S^-] = \frac{[S^-]}{HRT} \qquad [4\text{-}13]$$

$$\begin{pmatrix} Rate \; of \\ Output \\ of \; S^-/Volume \end{pmatrix} = \frac{\dfrac{[S^-]_1}{HRT_1} + \dfrac{[S^-]_2}{HRT_2}}{2} \qquad [4\text{-}14]$$

Applying the mass balance Equation 4-1:

$$-r_{S^-} = \begin{pmatrix} Rate \; of \\ Inflow \\ of \; S^-/Volume \end{pmatrix} - \begin{pmatrix} Rate \; of \\ Outflow \\ of \; S^-/Volume \end{pmatrix} - \begin{pmatrix} Rate \; of \\ Accumulation \\ of \; S^-/Volume \end{pmatrix} \qquad [4\text{-}15]$$

where: $-r_{S^-}$ is the rate of *consumption* of sulfide.

The values of $[S^-]_i$, HRT and loading were calculated at each time step. A time step occurred whenever a measurement was taken or an adjustment to the reactor was made. Thus, the interval between time steps was not uniform. Typically there were several time

steps as measurements were taken and the pumps were adjusted. Then, there was a long overnight time step. As shown in Equations 4-12 and 4-14, in order to compare like quantities, the *average* of input (or output) values at two adjacent time steps was taken to compare with the accumulation which was the *difference* in concentrations between two adjacent time steps. The rates of sulfide accumulation, input, output and consumption are plotted as functions of time in Figures 4.6 to 4.10 for Runs 3, 4, and 5 and Trials 9 and 10 respectively.

In Trials 9 and 10, there was an additional output term due to the $H_2S_{(g)}$ that was collected in the reactor zinc acetate trap (Figure 3.2). The $S^=$ concentration in the trap was multiplied by the trap volume (0.8 L) to get the mass of $S^=$ leaving the reactor as $H_2S_{(g)}$. This mass was divided by the reactor volume and the time that the trap was in service to get the rate of H_2S outflow in mg $S^=$/h·L. As can be seen in Figures 4.9 and 4.10, the rate of loss of $S^=$ through the gas trap was negligible.

In Figures 4.6 and 4.7, the rate of sulfide consumption overlaps the line for the rate of input. This is because the reactor sulfide concentration was zero throughout Runs 3 and 4, and thus the rates of accumulation and output of sulfide were also zero. Therefore, the rate of sulfide consumption equalled the rate of sulfide input. The GSB consumed all of the input sulfide, although, as mentioned in Section 4.1.1, the products of consumption were different in Runs 3 and 4. The dip in inlet sulfur concentration at 240 hours in Run 3 was caused by a dry SSS reservoir which was corrected within 5 hours. In Run 5 (Figure 4.8), the reactor was overloaded and sulfide accumulated at the end of the experiment. The rate of accumulation after 210 hours is a step function because the
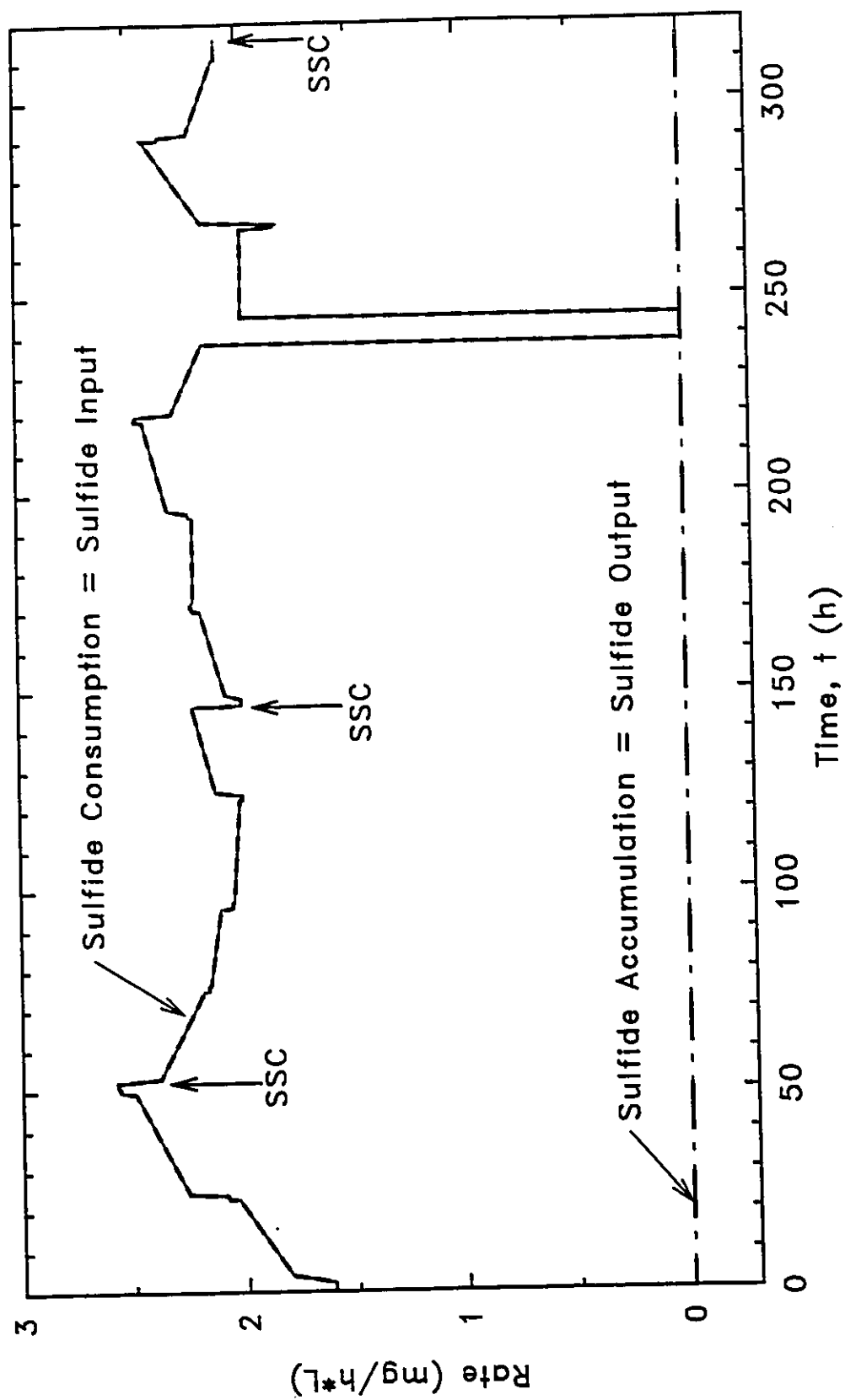
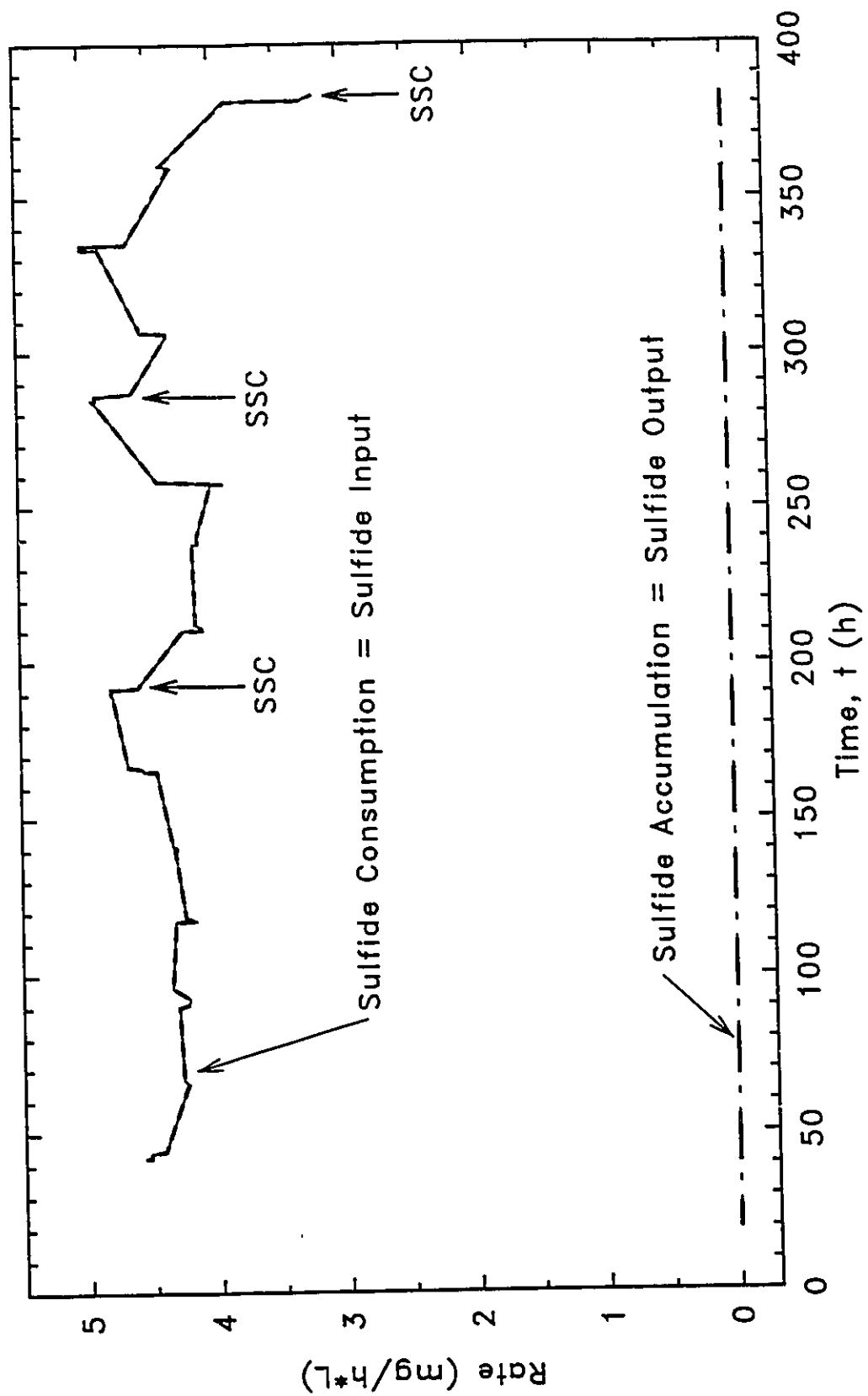FIGURE 4.6 Mass balance of sulfide in the bioreactor in Run 3

65

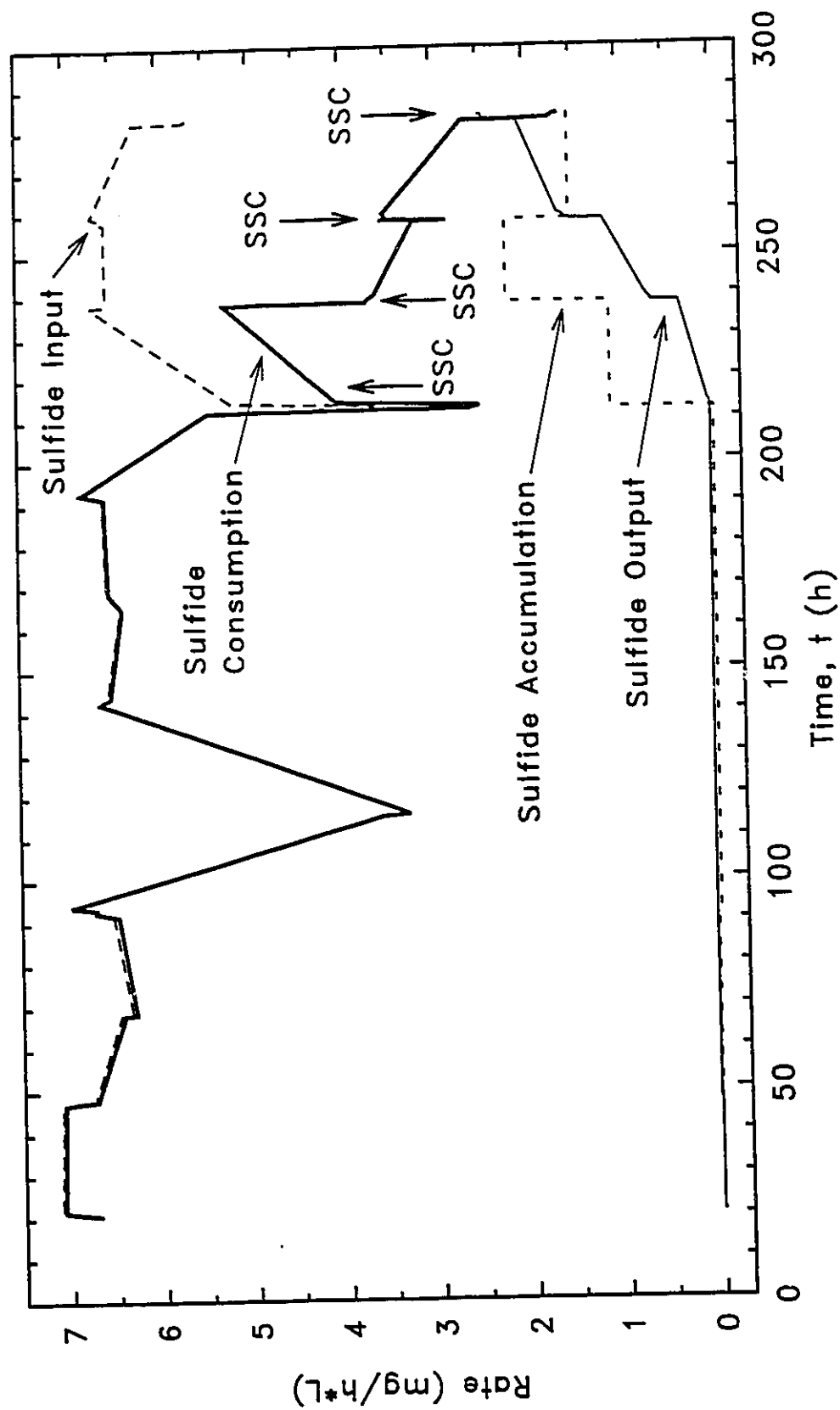FIGURE 4.7 Mass balance of sulfide in the bioreactor in Run 4

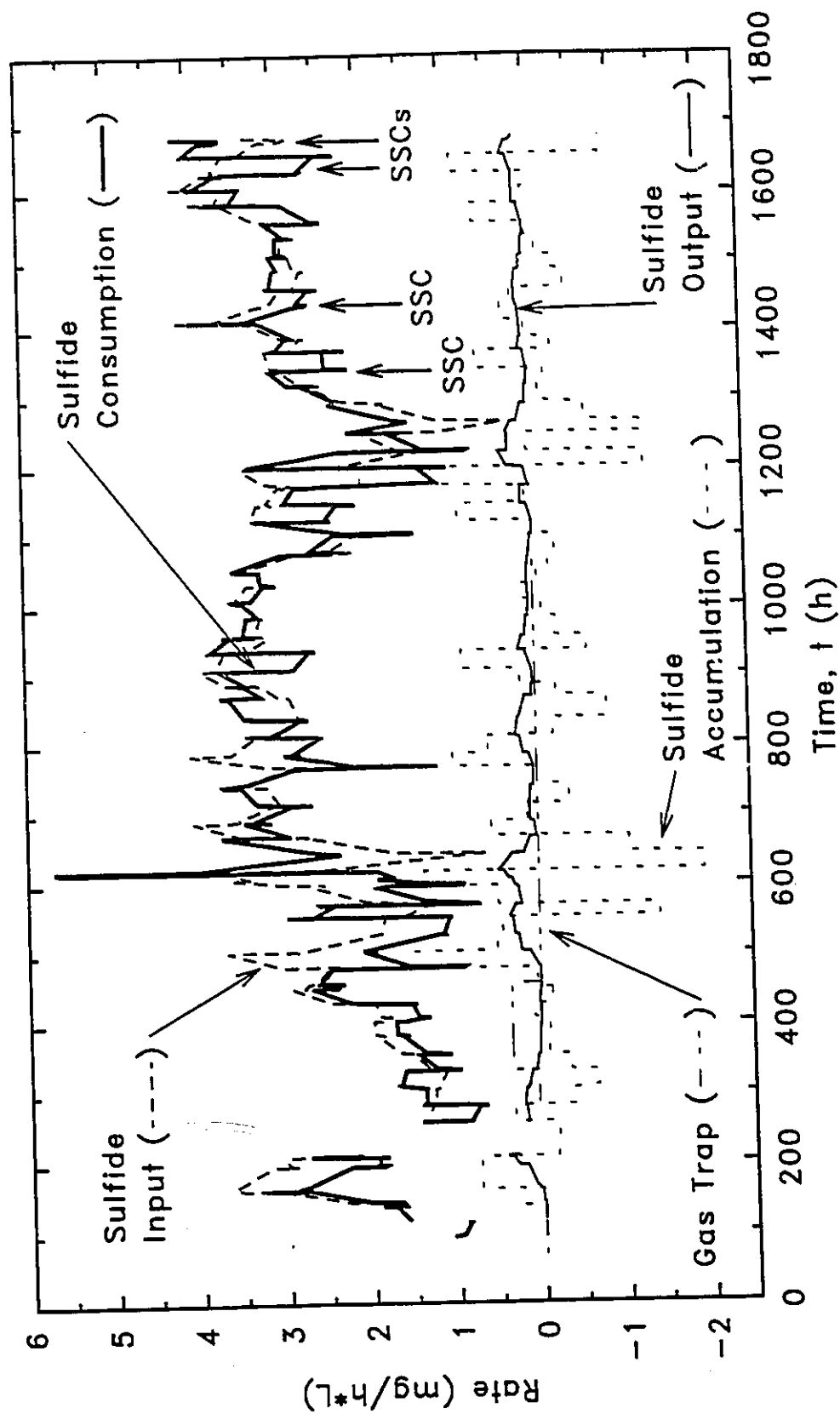FIGURE 4.8 Mass balance of sulfide in the bioreactor in Run 5

FIGURE 4.9 Mass balance of sulfide in the bioreactor in Trial 9
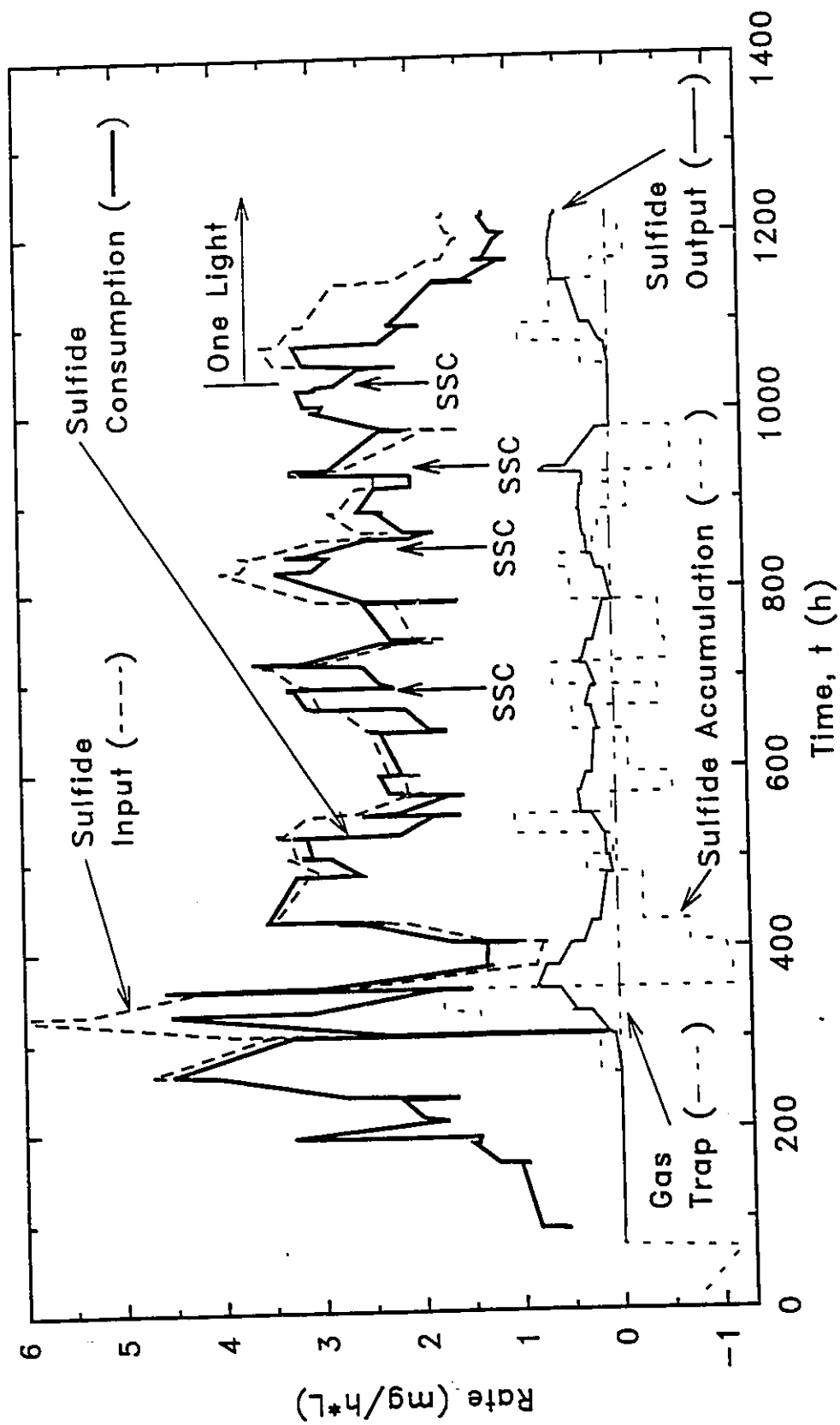
FIGURE 4.10 Mass balance of sulfide in the bioreactor in Trial 10

accumulation was considered constant for the period between daily measurements. Because of the build-up of sulfide in the reactor, the rate of sulfide output became positive. The difference between the rate of $S^=$ input and the rate of $S^=$ consumption is equal to the sum of the rates of $S^=$ accumulation and output. Since this sum was non-zero in Run 5, the rates of $S^=$ input and consumption were not equal, and, unlike Runs 3 and 4, the rate of input and rate of consumption lines are not coincident. Figure 4.8 shows the sudden decrease in sulfide input (and consumption) at 210 hours in Run 5 during pump calibration. This perturbation to the smooth operation of the system may have initiated the build-up of $S^=$ in the reactor. The accidental stoppage of the SSS pump at 115 hours is shown as a "downspike" at 115 hours, but the rate of $S^=$ input did not reach zero because of the averaging effect of calculating the rates *between* measured points.

The sulfide concentration in the reactor was non-zero in Trial 9 as well (Figure 4.9). Therefore, the rate of sulfide consumption line deviates from the rate of input of sulfide line. Sulfide concentration increased and decreased in the reactor. In the latter part of the experiment (1343 to 1677 hours), the rates were fairly steady and it was within this period that several measurements of all sulfur species were taken (sulfur species characterization). The average rate of sulfide consumption in this period was 3.0 mg/h·L whereas the average sulfide input rate was 3.2 mg/h·L. Therefore, on average, 0.2 mg $S^=$/h·L was being discharged from the reactor. Given the HRT of 173 hours, the average outlet sulfide concentration was therefore 35 mg/L, when the discharge of $H_2S_{(g)}$ is neglected.

In Trial 10 (Figure 4.10), the rate of sulfide consumption roughly followed the rate

of input with a steady state being reached from 693 to 1030 hours. During steady state, the rate of sulfide consumption was 2.5 mg/h·L and the average sulfide input rate was 2.7 mg/h·L. Therefore, the average outlet $S^=$ concentration was 20 mg/L. At 1032 hours, the top light was unplugged resulting in a decrease in the sulfide consumption rate. Because the $S^=$ loadings the Trials were controlled so as to maintain a non-zero concentration of $S^=$ in the reactor, the loading in Trial 10 was decreased after the light was unplugged.

4.1.3 Sulfur Species Characterization (SSC)

At various time intervals toward the end of each experiment, the concentrations of all sulfur species were measured in the input and output streams. This provided a "snapshot" of the reactor condition at that moment, and was termed the sulfur species characterization, SSC. A comparison of the sum of concentrations input to the reactor and the sum of those leaving the reactor, indicates how the various species of sulfur were being converted within the reactor. Table 4.1 summarizes the concentrations of all sulfur species. Different sulfur species in each Run/Trial are plotted in Figures 4.11 to 4.15.

Runs 3, 4, and 5 were operated at the same HRT - only the sulfide loading was changed; therefore, Figures 4.11, 4.12 and 4.13 are plotted with the same vertical axes. Similarly, to compare Trials 9 and 10, Figures 4.14 and 4.15 are plotted with the same vertical axes.

In Run 3, the total sulfur input was around 120 mg S/L (Figure 4.11). In the first SSC, at 51.6 hours, the input sulfur was greater than the output. At this point, the reactor was not operating at a steady state. The sulfide input had been increasing until the time

71

TABLE 4.1 Concentrations measured during sulfur species characterizations

Experiment	Time	Influent Concentration (mg/L)					Effluent Concentration (mg/L)					
		$S^=$	S^0	$S_2O_3^=$	$SO_4^=$	Total	$S^=$	S^0	$S_2O_3^=$	$SO_4^=$	Total	bchl
Run 3	51.6	127 ±14	10 ±3	-	30 ±1	167 ±18	0 ±4	32 ±1	-	86 ±14	118 ±19	10.3
	147.8	93 ±10	3 ±2	-	29 ±1	125 ±13	0 ±4	2 ±1	-	115 ±14	117 ±19	13.5
	316.0	89 ±10	8 ±2	-	30 ±4	127 ±17	0 ±4	0 ±1	-	114 ±18	114 ±23	12.5
Run 4	190.8	220 ±15	26 ±3	-	29 ±4	275 ±22	0 ±4	236 ±1	-	76 ±18	312 ±23	11.5
	285.7	220 ±20	27 ±4	-	28 ±4	275 ±28	0 ±4	221 ±1	-	82 ±18	303 ±23	11.5
	382.4	139 ±15	13 ±2	-	30 ±4	182 ±21	0 ±4	251 ±1	-	55 ±18	306 ±23	10.7
Run 5	214.0	305 ±24	0 ±12	-	30 ±5	335 ±40	3 ±4	258 ±2	-	42 ±18	303 ±24	7.2
	238.8	299 ±23	6 ±11	-	29 ±5	334 ±39	31 ±4	279 ±2	-	37 ±14	347 ±20	6.2
	258.8	307 ±24	11 ±12	-	29 ±5	347 ±40	74 ±4	199 ±2	-	39 ±14	312 ±20	6.2
	283.3	254 ±16	17 ±10	-	27 ±5	298 ±31	112 ±7	169 ±1	-	22 ±0	303 ±8	5.0
Trial 9	1343.1	488 ±25	46 ±5	43* ±13	30 ±13	606 ±57	4 ±4	1051 ±1	76* ±13	28 ±0	1159 ±18	5.1
	1438.3	529 ±27	31 ±5	63 ±70	37 ±13	660 ±115	23 ±3	988 ±1	85 ±13	31 ±14	1127 ±32	4.4
	1629.1	627 ±26	0 ±11	27 ±67	31 ±13	635 ±117	26 ±3	622 ±2	78 ±13	31 ±14	757 ±33	3.1
	1676.6	499 ±24	5 ±11	40 ±64	35 ±13	579 ±112	24 ±3	612 ±2	66 ±13	30 ±14	733 ±33	2.8

TABLE 4.1 (continued) Concentrations measured during sulfur species characterizations

Experiment	Time	Influent Concentration (mg/L)					Effluent Concentration (mg/L)					bchl
		$S^=$	S^0	$S_2O_3^=$	$SO_4^=$	Total	$S^=$	S^0	$S_2O_3^=$	$SO_4^=$	Total	
Trial 10	692.6	304 ±12	44 ±3	81[a] ±13	28 ±13	456 ±42	20 ±3	240 ±1	54[a] ±13	26 ±26	339 ±18	3.5
	861.2	239 ±14	72 ±4	107 ±54	29 ±13	446 ±84	30 ±3	457 ±1	62 ±13	32 ±0	581 ±17	5.3
	929.2	245 ±12	11 ±5	37 ±37	32 ±7	326 ±61	30 ±3	388 ±1	58 ±13	29 ±0	505 ±18	5.4
	1027.9	297 ±15	38 ±7	100 ±48	27 ±6	462 ±76	0 ±3	402 ±2	41 ±13	31 ±0	474 ±18	5.4

[a] = not measured, used the average of the three later measurements in this experiment.
bchl = 5 day running average.
± = shows the uncertainty in the measurement of the value. The uncertainty in the Total value is the sum of uncertainties of the individual measurements.
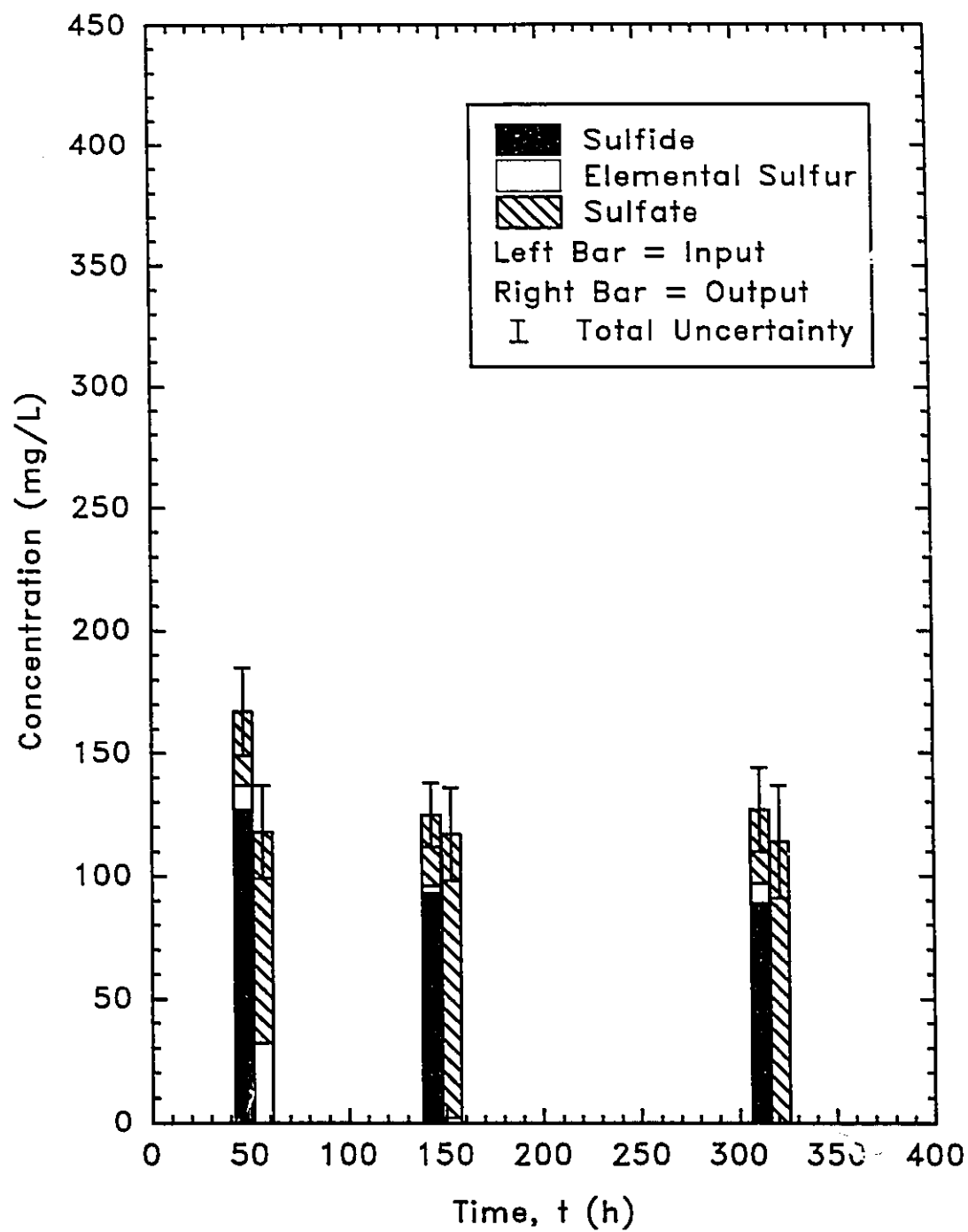
FIGURE 4.11 Sulfur species characterization in Run 3
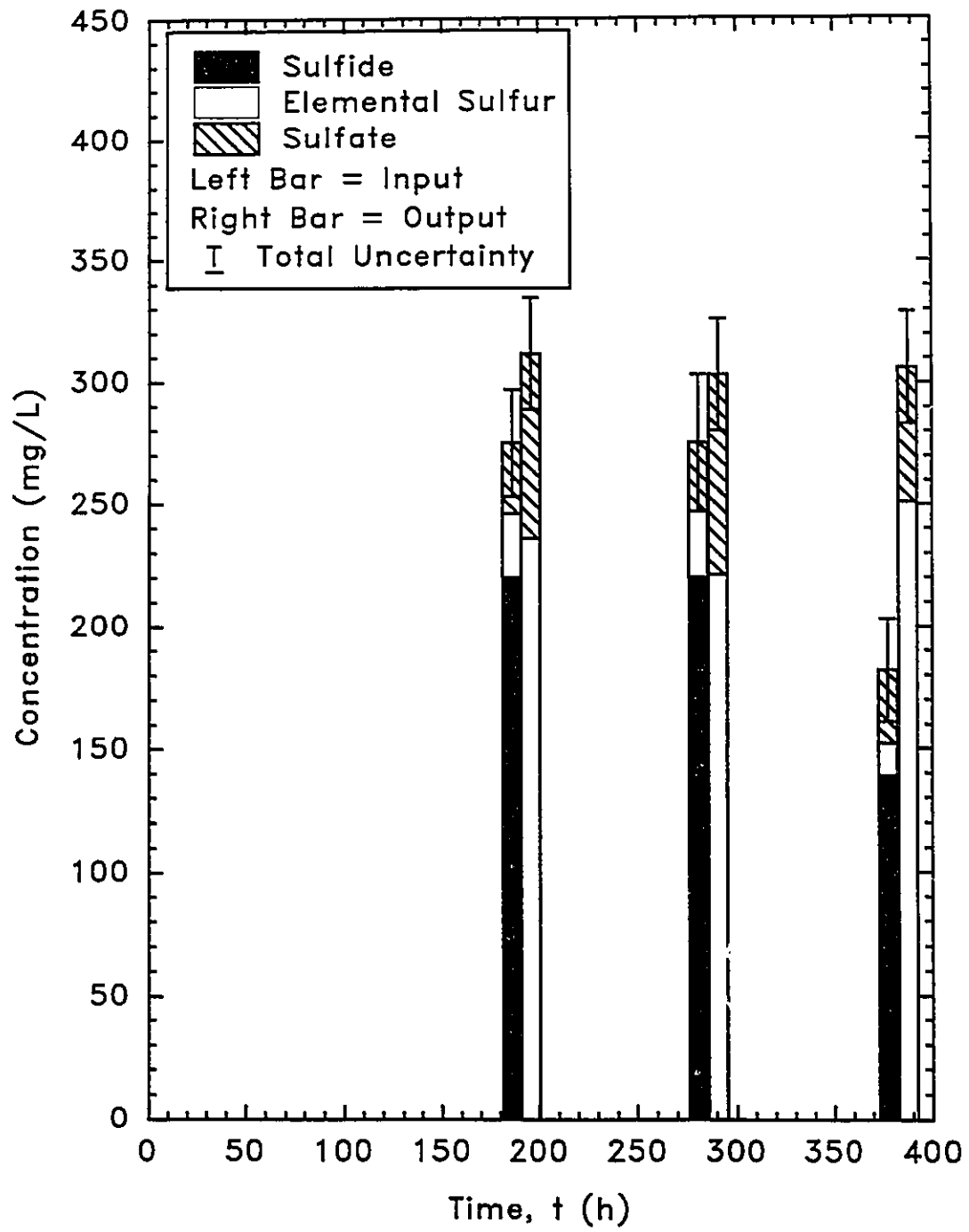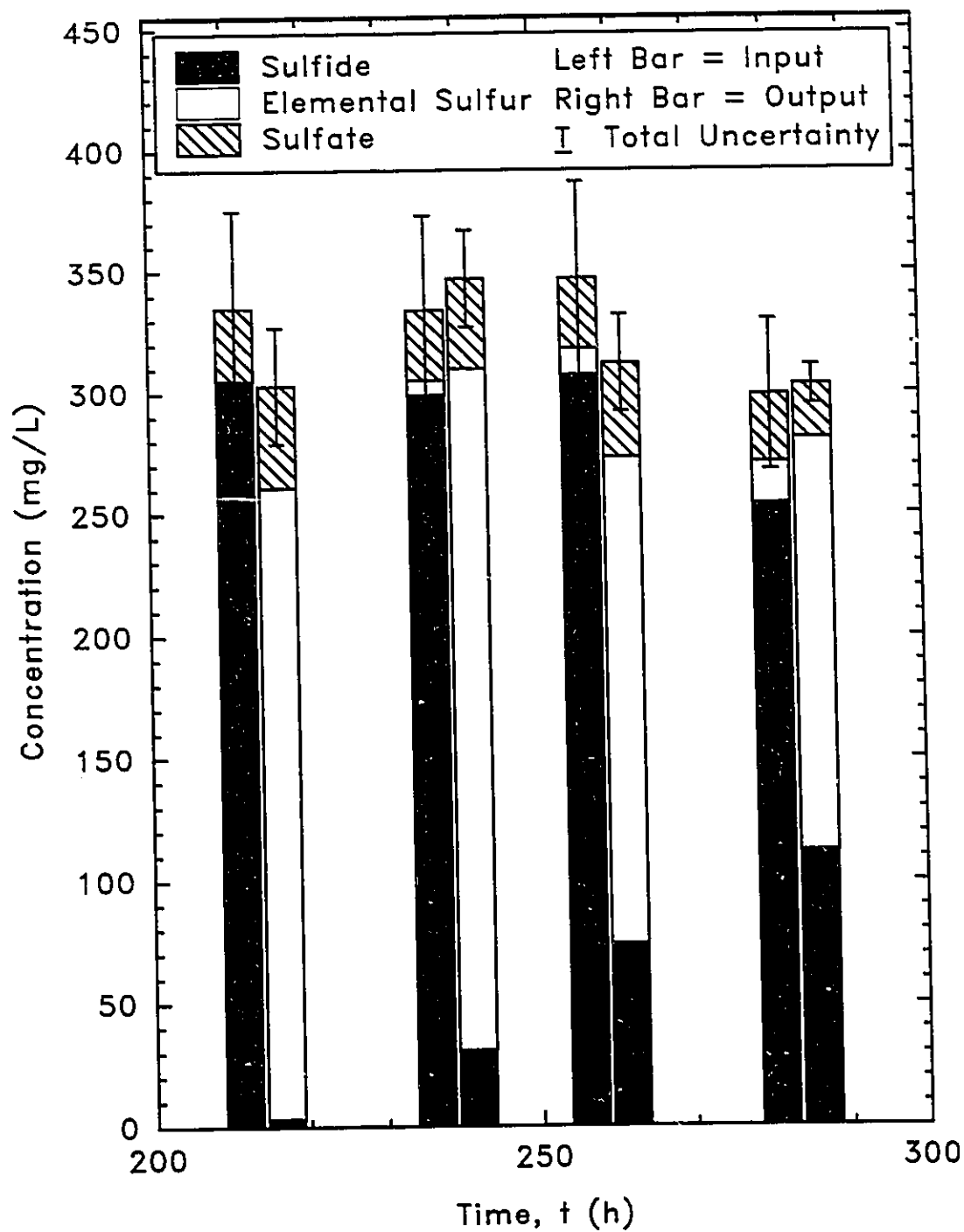
74

FIGURE 4.12 Sulfur species characterization in Run 4
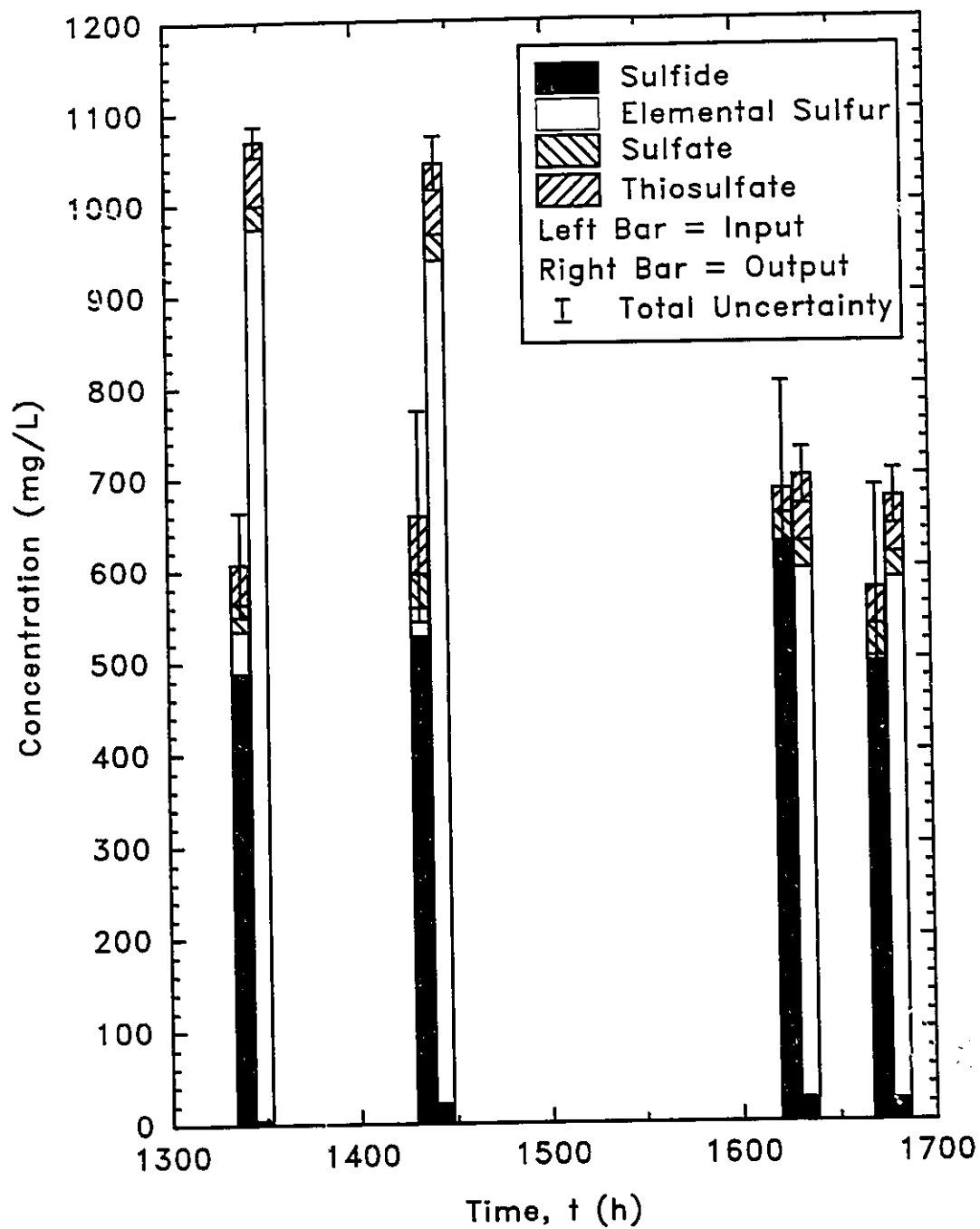
75

FIGURE 4.13 Sulfur species characterization in Run 5

76

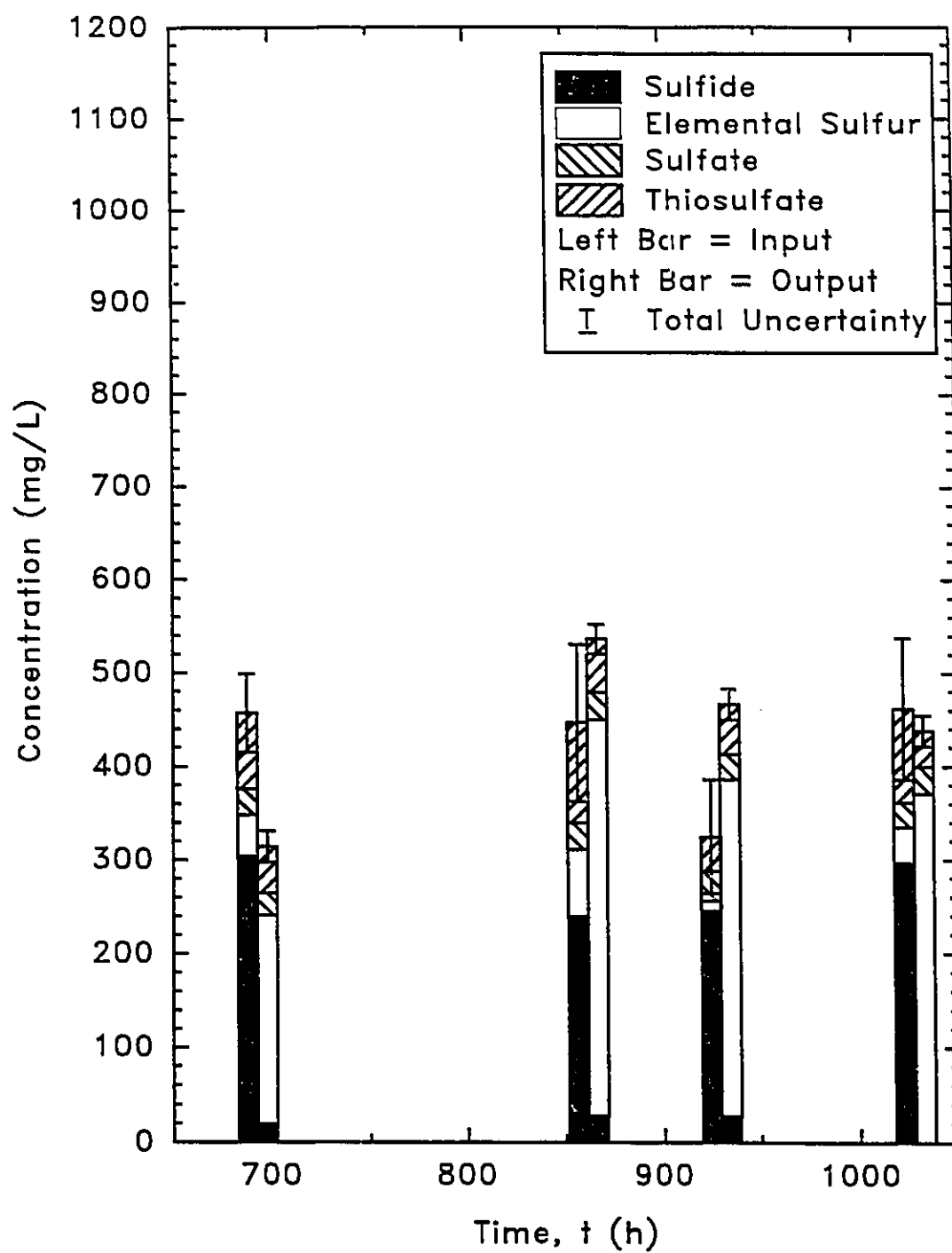FIGURE 4.14 Sulfur species characterization in Trial 9

77

FIGURE 4.15 Sulfur species characterization in Trial 10

78

of these measurements (Figures 4.1 and 4.6) and at the SSC, the $S^=$ input was high. However, not enough sulfur had yet accumulated in the reactor so that its total concentration equalled the input. To understand this concept, consider the extreme case where a CSTR containing no sulfur of any form is suddenly fed a solution of constant $[S^=]$ at a constant flow rate (step feed). The sulfur concentration in the reactor would increase until it equalled that of the input. There would be a time delay between the initial pumping of $S^=$ feed solution and the achievement of steady state in the reactor. If measurements of the sulfur input and output are made during the delay period, a discrepancy would result since not enough sulfur had accumulated in the reactor. A similar phenomenon occurred at the beginning of Run 3.

For the second and third SSCs in Run 3 at 147.8 and 316.0 hours respectively, sulfur input and output were equal within the accumulated error of the measurement (error bars). The stacked bars in Figure 4.11 also illustrate the underloaded condition where all input sulfide and elemental sulfur are converted to sulfate.

Figure 4.12 illustrates the sulfur species characterization in Run 4. For the first two characterizations at 190.8 and 285.7 hours respectively, total sulfur input balanced total sulfur output within experimental error. Note that the SSS contained S^0 which contributed to the mass of sulfur input to the reactor. The error bars overlap at a value of 295 mg S/L. The output at the third sampling time, 382.4 hours, was equivalent to the first two, but the input was down. As in Run 3, the imbalance was caused by a short term fluctuation in the input stream. For a short time, the concentration of sulfur in the input stream was less than that required to maintain the steady state concentration of sulfur in

the reactor. Had the low inlet concentration persisted, the sulfur concentration *in the reactor* would have decreased to that of the inlet. During this period of unsteady state, the reactor sulfur concentration would have been greater than the inlet sulfur concentration. In Run 4 the input decreased due to an unexpected overnight drop in the sulfide stock solution concentration (Figure 4.7). Generally for Run 4, the input S^- was converted entirely to S^0 with some coincident production of SO_4^- from either S^- or S^0.

Run 5 was operated in an overloaded sulfide condition. Total input and output sulfur concentrations were equal within experimental error, but the concentration, where the input and output error bars overlap, fluctuated with time (Figure 4.13). Since the input fluctuations were small (< 30 mg S/L), the reactor concentration was able to keep pace. Sulfide accumulated in the reactor in this loading condition as shown by the increasing height of the solid bar in the output stack in Figure 4.13.

In Trial 9 (Figure 4.14), only the third SSC achieved a true mass balance. At this time (1629.1 hours), sulfide was converted quantitatively to elemental sulfur. Some sulfide remained in the reactor and also there was an increase in SO_4^- from input to output. These latter two observations seem at odds - one indicating overloading and the other underloading. The fourth SSC was probably affected by a momentarily low input causing an inequality between total input and output (Figure 4.9).

The mass balances in the first two SSCs of Trial 9 are skewed by an unusually high S^0 value. These values were out of the calibration range for standards extracted-from-water so standards at a greater concentration were run on the day of the HPLC test. The analytical response was linear for the unextracted standards. Therefore it was assumed

that the range of the extracted standards could also be extended.

It appears that S^0 had accumulated in the reactor sometime in the first 1300 hours of operation and was subsequently flushed out. There are many possible explanations of this phenomenon, assuming the assays were not subject to error. Five are listed here:

1) There was a spike in $S^=$ inlet *concentration* at 1172.1 hours due to zinc acetate contamination of the nutrient medium requiring its pump to be shut down for 29 hours (Figure 4.4). During pump shut-down, the $S^=$ *loading* remained within normal fluctuations (Figure 4.9) and the HRT increased to 790 hours. Due to the slower flushing rate of the reactor, the S^0 produced remained in the reactor, and increased the reactor $[S^0]$. With time, however, the high $[S^0]$ was flushed out of the reactor.

In order to refute this scenario, one must examine the mass balance of S^0 in the reactor. Applying the mass balance Equation 4-4 to elemental sulfur:

$$\frac{\Delta [S^0]}{\Delta t} = \frac{Q}{V}[S^0]_i - \frac{Q}{V}[S^0] + r_{S^0} \qquad [4\text{-}16]$$

The S^0 inlet concentration is essentially zero:

$$\frac{\Delta [S^0]}{\Delta t} = - \frac{Q}{V}[S^0] + r_{S^0} \qquad [4\text{-}17]$$

Sulfide oxidation to elemental sulfur, or the rate of formation of S^0, is controlled by the relationship between light and loading (van Niel curve). Since these remained essentially unchanged in Trial 9, the rate of S^0 production was constant and presumably equal to the $S^=$ consumption rate, 3.0 mg/h·L. As mentioned above, V/Q = 790 hours and Δt = 29 hours. The only measured value of $[S^0]$ prior to the spike was 490 mg/L at 766 hours. Substituting these numbers into Equation 4-17 results in $\Delta [S^0]$ = 69 mg/L, which is a

much lower value than the observed concentration increase of around 500 mg/L between 800 and 1300 hours as shown in Figure 4.4.

2) The mixing in the reactor was inadequate, and sulfur settled to the bottom.

In this case, the elemental sulfur mass balance Equation 4-17 has an extra term:

$$\frac{\Delta [S^0]}{\Delta t} = -\frac{Q}{V}[S^0] + r_{S^0} - r_{Sed} \qquad [4\text{-}18]$$

where: r_{Sed} is the rate of sedimentation (mg/h·L).

If all other parameters are considered to be equal, the presence of settling decreases the value of $\Delta[S^0]$. Therefore settling may have caused the decrease in elemental sulfur concentration after 1486 hours in Trial 9, but it does not explain the increase prior to this time or the reason for the change in $\Delta[S^0]/\Delta t$.

3) Elemental sulfur stuck to the sides and appurtenances of the reactor when the reactor concentration of S^0 was high, causing a drop in the S^0 concentration.

The rate of adherence of S^0 would probably be proportional to its concentration in the reactor. Thus:

$$\frac{\Delta [S^0]}{\Delta t} = -\frac{Q}{V}[S^0] + r_{S^0} - k_{adh}[S^0] \qquad [4\text{-}19]$$

where: k_{adh} is a rate constant for the adherence of S^0 to the sides of the reactor (min^{-1}).

Again, if the values of the other parameters are the same as in the base case, the reactor S^0 concentration would decrease due to the phenomenon of sticking. Evidence for adherence to the sides of the reactor is clear from the need to clean the reactor windows on a daily basis. However, based on qualitative observations, there appears to be no correlation between the need for window cleaning and the S^0 concentration.

82

4) The reactor was homogeneous but the liquid in the effluent tube leading upward from the reactor remained stagnant in the time interval between effluent pump runs. During this time, some S^0 settled out of the effluent tube, so that when the pump started, the initial draw from the reactor was lower in S^0 than the reactor bulk concentration. Over time, the net effect of pumping liquid with lower-than-reactor $[S^0]$ was an increase in the reactor S^0 concentration. The increased $[S^0]$ may be higher than the level of sulfide input, as seen in the initial part of Trial 9. Trial 10 also exhibits a gradual increase in $[S^0]$. Runs 3 to 5 did not exhibit this phenomenon even though the effluent tube extended vertically downward to the bottom of the reactor. This may have been due to the different effluent pump speed used in these experiments.

5) Finally, it is possible that the increase and subsequent decrease in $[S^0]$ was due to a combination of phenomena. The reactor concentration may have increased due to settling from the effluent tube (explanation 4), but once a critical reactor S^0 concentration was reached, adherence (explanation 3) or settling (explanation 2) in the reactor dominated, decreasing the reactor $[S^0]$ back to its expected levels. Alternatively, the concentration spike at 1172 hours may have caused an upset in the bacteria population which affected the rate of S^0 production, or the settling or adhesion characteristics of the S^0 granules.

Figure 4.15 shows that Trial 10 operated at lower levels of sulfide input and output than Trial 9. Mass balance, or overlap of the error bars was only achieved at the last sulfur species characterization (1027.9 hours). At this time, all of the input S^- and some of the input $S_2O_3^-$ was converted to S^0. The reactor in this condition was neither overloaded nor underloaded. The SSCs at other times in this experiment reflect the same

condition, with some sulfide observed in the reactor. The average total sulfur input for the four sulfur species characterizations was 423 ± 60 mg S/L and the output was 475 ± 18 mg S/L. The ranges overlap by 26 mg S/L indicating an overall balance.

The results of the SSCs were used to quantify the conversion of $S^=$ to S^0. Table 4.2 shows the percentage of conversion for only those SSCs where a sulfur balance was achieved. Realistically, Run 3 showed essentially zero conversion of $S^=$ to S^0. Run 4 averaged about 91% and Run 5 was 94%. The Trials achieved essentially 100% conversions. The high conversion value at 1027.9 hours in Trial 10 (123%), was due to the oxidation of some thiosulfate in the influent to elemental sulfur (Figure 4.15). In

TABLE 4.2 Conversion of sulfide to elemental sulfur for those SSCs where inlet sulfur equals outlet sulfur

Experiment	Time (h)	$[S^=]_i-[S^=]$ (mg/L)	$[S^0]-[S^0]_i$ (mg/L)	$\Delta[S^0]/\Delta[S^=]$ (%)
Run 3	147.8	93 ±14	-1 ±3	-1 ±2
	316.0	89 ±14	-8 ±3	-9 ±2
Run 4	190.8	220 ±19	210 ±3	95 ±9
	285.7	220 ±24	194 ±5	88 ±11
Run 5	214.0	302 ±28	258 ±13	85 ±36
	238.8	268 ±27	273 ±13	102 ±15
	258.8	233 ±28	188 ±13	81 ±16
	283.3	142 ±22	152 ±11	107 ±24
Trial 9	1629.1	601 ±29	622 ±13	103 ±8
Trial 10	1027.9	297 ±18	364 ±9	123 ±10

± = shows the uncertainty of the measurement of the value.

84

terms of the calculation of conversion, this decrease in thiosulfate concentration would increase $\Delta[S^0]$ but not $\Delta[S^=]$, contributing to a conversions greater than 100%. The highest conversions of *removed* $S^=$ to S^0 were achieved only when $S^=$ was found in the effluent (Run 5, Trials 9 and 10). This was similar to the findings of Buisman *et al.* (1990b).

4.2 Relationships

In this section, the data from all experiments were used to find relationships between the consumption of $S^=$, the production of S^0, and the growth of the biomass in terms of various reactor parameters.

Sulfide loading rates and the effective sulfide inlet concentrations were calculated at every time step, as described in Section 4.1.2, but only the values which corresponded to the times of the SSCs were selected for use in this section. Rates of $S^=$ consumption, S^0 production and $SO_4^=$ production were calculated between each pair of successive SSCs, analogous to the treatment of sulfide concentrations (Equations 4-5 to 4-15). Thus the rate of reaction in each case, was determined by subtracting the rates of accumulation and output from the rate of input.

Although [bchl] was measured daily, for the calculations in this section, a five day moving average of the bchl concentration was used, the middle value of which was the value on the day of the SSC. Again a mass balance was performed using Equations 4-5 to 4-15 wherein [bchl] was substituted for [S$^=$].

An effort has been made to show only those graphs where a definite relationship was found. When the relationship was poor, it is simply described as such. The rate and

concentration data upon which these relationships are based are summarized in Table 4.3.

4.2.1 Sulfide Consumption

Simple chemical kinetics suggest that the rate of removal of chemical A should be some function of the concentration of A, it follows that:

$$-r_A = f([A])$$ [4-20]

However, the correlation between the rate of sulfide consumption and the sulfide concentration was poor. In Runs 3 and 4, the reactor $S^=$ concentration was zero but the rate of sulfide consumption was equal to the loading, which was different in these two experiments. Trial 9 had similar rates of $S^=$ consumption to Trial 10 but the concentration of sulfide in the reactor fluctuated throughout both experiments. Maka and Cork (1990) also reported varying rates of $S^=$ consumption (32 and 64 mg $S^=/h \cdot L$) even though the reactor $S^=$ concentration was zero.

Figure 4.16 shows that up to a sulfide loading of 5 mg/h·L, the rate of sulfide consumption was equal to the rate of sulfide loading. In other words, all of the sulfide input to the reactor was consumed. The product of the consumption was S^0 in all cases except Run 3, where the underloaded reactor produced $SO_4^=$. The loading rates in Run 5 were all above 6 mg/h·L. This Run was described previously (Section 4.11, 4.12) as an overloaded condition. One would have expected the consumption/loading curve to level off when the maximum loading had been reached. In fact, the reactor was "failing" in Run 5 and $S^=$ consumption decreased in each successive period between sulfur species characterizations. Had the experiment been allowed to continue, the sulfide concentration would have reached the point of toxicity to the bacteria (if it had not already) and the rate

TABLE 4.3 Parameters calculated between sulfur species characterizations in continuous reactor experiments

| Experiment | Independant Variables | | Average Concentrations | | | Rates of Formation | | | Specific Growth Rate |
	Average $S^=$ Loading (mg/h·L)	Average HRT (h)	$[S^=]$ (mg/L)	$[S^0]$ (mg/L)	[bchl] (mg/L)	$S^=$ (mg/h·L)	S^0 (mg/h·L)	$SO_4^=$ (mg/h·L)	μ (h⁻¹)
Run 3	2.3*	48	0	17	11.9	-2.3	-0.10	1.8	0.024
	2.1	45	0	1	13.0	-2.0	-0.11	1.9	0.022
Run 4	4.9*	45	0	229	11.5	-4.9	4.3	1.2	0.022
	4.1	44	0	236	11.1	-4.0	5.2	0.61	0.022
Run 5	6.7	45	17	269	6.7	-5.2	6.7	0.021	0.016
	6.6*	46	53	239	6.2	-3.3	1.0	0.30	0.022
	6.1	46	93	184	5.6	-2.5	2.5	-0.64	0.013
Trial 9	2.9	175	14	1020	4.8	-2.6	4.9	0.013	0.0042
	3.4*	172	24	805	3.8	-3.2	2.7	-0.019	0.0040
	3.3	172	25	617	3.0	-3.2	3.4	-0.036	0.0037
Trial 10	2.7	99	25	348	4.4	-2.4	4.2	0.040	0.013
	2.4	100	30	422	5.4	-2.1	2.8	-0.035	0.010
	2.7*	100	15	395	5.4	-2.9	3.8	0.022	0.010

* = values chosen for Section 4.2.4
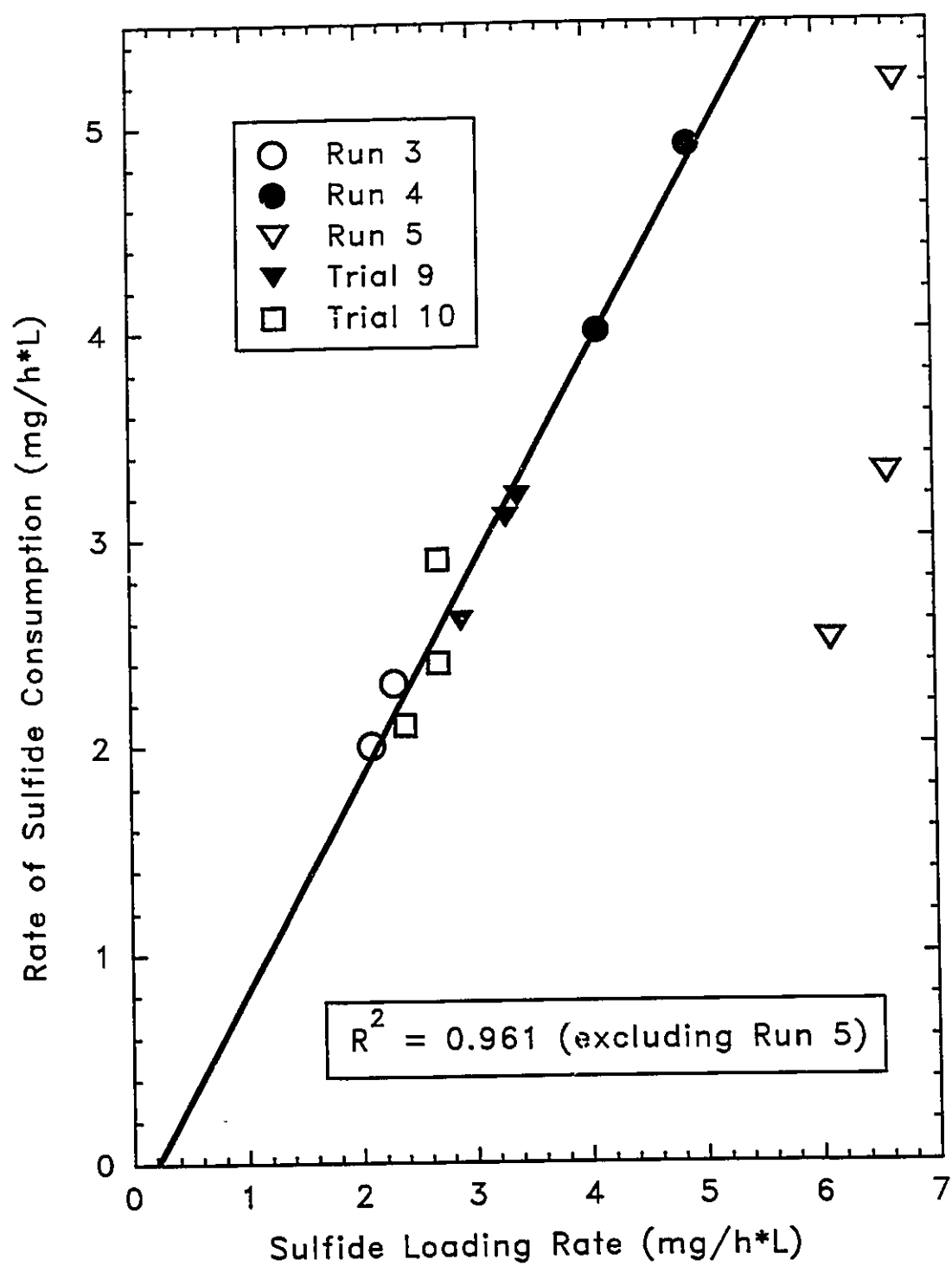
FIGURE 4.16 Sulfide consumption and loading

of sulfide utilization would have equalled zero.

Maka and Cork (1990) found that sulfide consumption equalled $S^=$ loading up to and including a loading of 64 mg/h·L.

The rate of $S^=$ consumption was not found to be related to the elemental sulfur concentration in the experiments in this study.

4.2.2 Elemental Sulfur Production

The correlation between the rate of elemental sulfur production and the reactor elemental sulfur concentration was poor ($R^2 = 0.18$). Since S^0 is presumed to be the initial product of $S^=$ oxidation, one might think that the rates of sulfide consumption and S^0 production were related. Even after excluding the data from Run 3 (where SO_4^- was the end-product) and the latter part of Run 5 (overloaded condition), the coefficient of determination (R^2) was only 0.34. There are two reasons for this low value. First, the rate data selected for this statistical test are all fairly close in value (1 to 6 mg/h·L), so normal experimental variations overshadow any trend in the data. Secondly, problems of total sulfur mass imbalance (where the elemental sulfur concentrations in the reactor were found to be greater than the total sulfur inlet concentrations) distorted the value of the rate of S^0 production. Unfortunately, due to the sparsity of SSC data, these values had to be used.

Neither the rate of S^0 production nor the concentration of S^0 were found to be related to the $S^=$ loading rate.

A strong relationship ($R^2 = 0.92$) was found between the elemental sulfur concentration and the HRT (Figure 4.17). Considering the mass balance equation
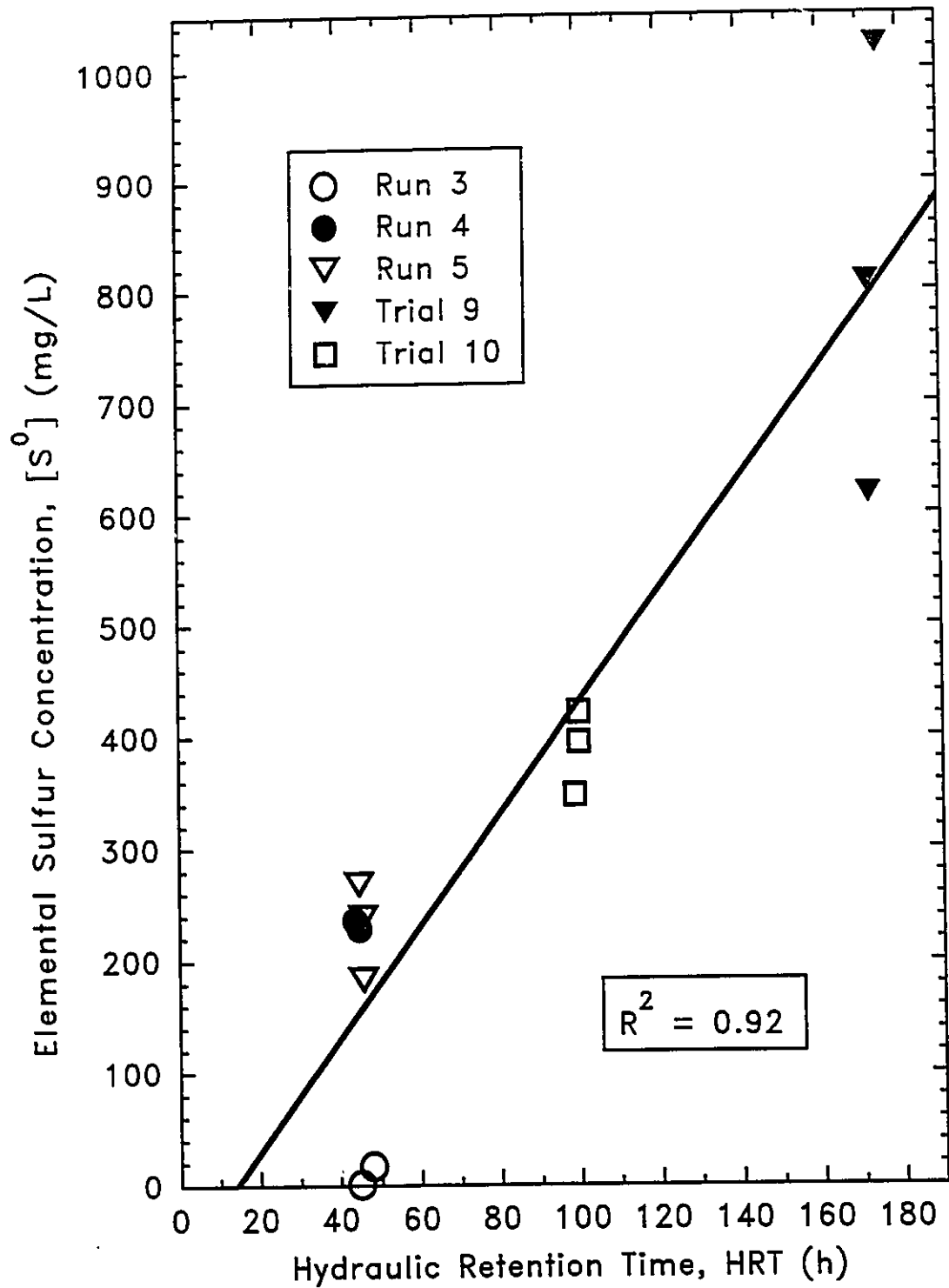
89

FIGURE 4.17 The relation between elemental sulfur concentration and the hydraulic retention time

(Equation 4-4) and noting that $[S^0]_i \approx 0$ mg/L, and the accumulation term is small because the reactor was in a steady state, the equation simplifies to:

$$r_{S^0} = \frac{[S^0]}{HRT} \qquad [4-21]$$

Assuming the rates of S^0 production were approximately constant in the latter parts of each experiment where the SSCs were made, the S^0 concentration becomes proportional to the HRT. The constant of proportionality is r_{S_0}, which as mentioned before, was roughly the same for all experiments.

4.2.3 Bacterial Growth

The concentration of bacteria was found to be related neither to the S^z concentration nor to the rate of S^z consumption.

The rate of production of bacteria is normally expressed in terms of the specific growth rate, μ:

$$r_x = \mu X \qquad [4-22]$$

where: r_x is the rate of production (growth) of bacteria (mg/h·L)
           X is the concentration of bacteria (mg VSS/L, mg dry mass/L, or mg bchl/L as used in this dissertation)

Rearranging the mass balance Equation 4-4 and noting that the concentration of biomass entering the reactor was zero:

$$r_x = \frac{Q}{V}X + \frac{\Delta X}{\Delta t} = \frac{X}{HRT} + \frac{\Delta X}{\Delta t} \qquad [4-23]$$

Substituting in values for the time step:

$$r_x = \left(\frac{\dfrac{X_1}{HRT_1} + \dfrac{X_2}{HRT_2}}{2} \right) + \left(\frac{X_2 - X_1}{t_2 - t_1} \right) \qquad [4\text{-}24]$$

And:

$$\mu = \frac{r_x}{\overline{X}} = \frac{2r_x}{X_1 + X_2} \qquad [4\text{-}25]$$

This provides a way of calculating the value for μ between each pair of SSCs from observed bchl concentrations without assuming the reactor was operating at steady state.

The correlation between specific growth rate and reactor [$S^=$] was poor. Likewise there was no relation between μ and the rate of consumption of $S^=$. However, there was a hyperbolic relationship between μ and the HRT (Figure 4.18). If the reactor is operating at steady state, the accumulation term, $\Delta X/\Delta t$, in Equation 4-23 is zero, and the equation becomes:

$$r_x = \frac{X}{HRT} \qquad [4\text{-}26]$$

Substituting in the expression for r_x (Equation 4-19) and cancelling yields:

$$\mu = \frac{1}{HRT} \qquad [4\text{-}27]$$

This is the standard equation for a chemostat (Gaudy & Gaudy, 1980). For the data in Figure 4.18, the coefficient of determination for the linear relationship between μ and 1/HRT is 0.91. The experimental results fit the relationship derived from the mass balance at steady state, and therefore the steady state assumption is verified.

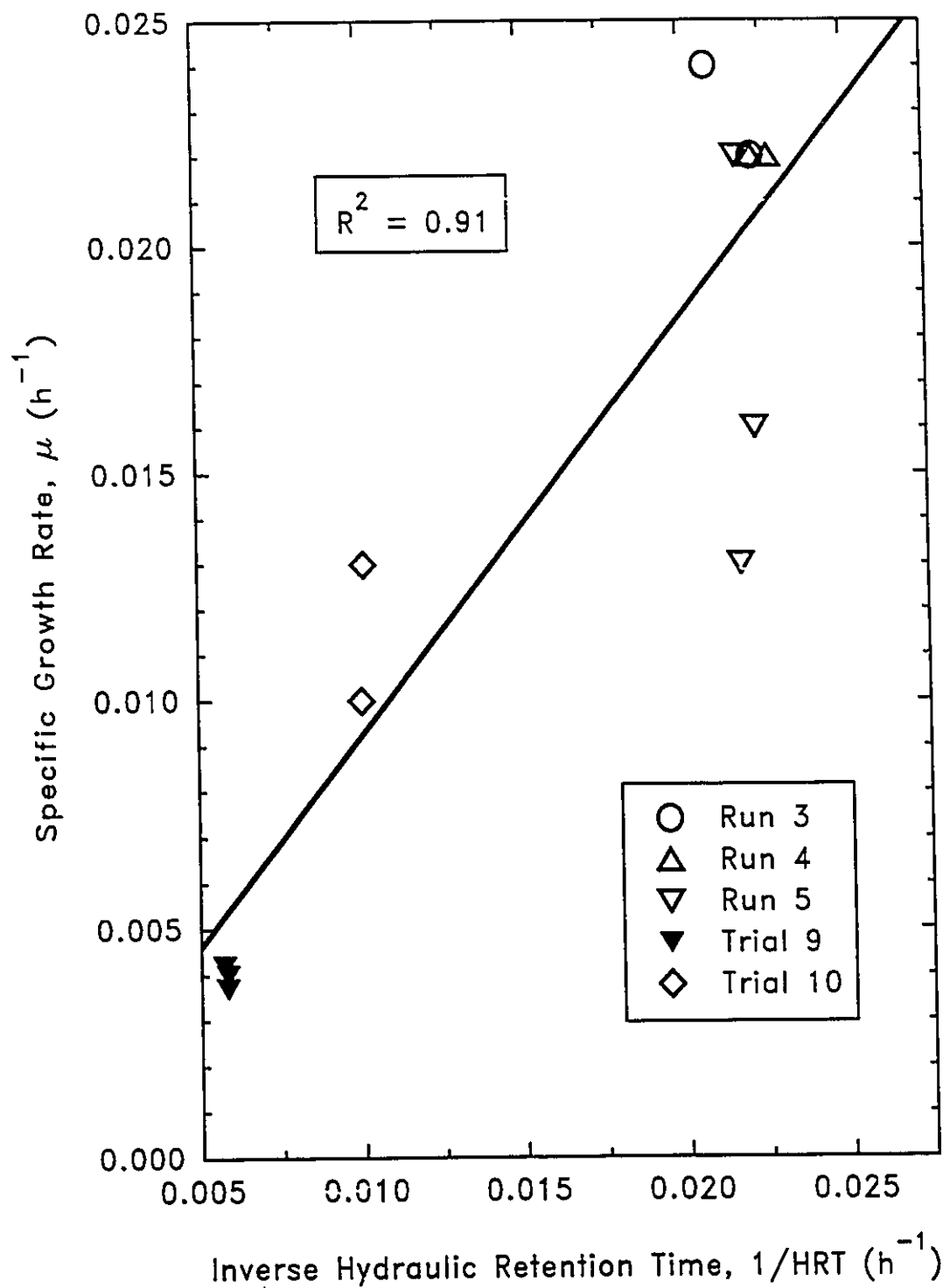There was a low specific growth rate in Trial 9 (Table 4.3) which is one of the

FIGURE 4.18 The relationship between the specific growth rate and the inverse of the hydraulic retention time

reasons that 1300 hours were allowed to lapsed before the SSCs. There was a strong inverse relationship between μ and the S^0 concentration (Figure 4.19). This phenomenon may have been due the scattering of light by S^0 in the reactor, making it unavailable for the bacteria. However, the relationship between incident light and μ resulted in a weaker correlation ($R^2=0.64$) than that between $[S^0]$ and μ ($R^2=0.75$). The calculation of incident light took into account the effects of light scattering by S^0 and absorbance by bacteria (Kim *et al.*, 1992), although even at the highest $[S^0]$, the incident light was attenuated by only 0.9%. A better explanation is that since μ is a function of 1/HRT (Figure 4.18) and $[S^0]$ is a function of HRT (Figure 4.17), $[S^0]$ is a linear function of $1/\mu$. Indeed, $[S^0]$ is more related to $1/\mu$ ($R^2=0.79$) than μ ($R^2=0.75$).

Although Figure 4.17 appears to be the inverse of Figure 4.19, and should be according to Equation 4-27, the ordinate values for Figure 4.19 were calculated from bchl and HRT data, whereas those in Figure 4-17 were calculated from only HRT data.

4.2.4 Re-examination of the van Niel Curve

If the radiant flux and $S^=$ loading data for all of the experiments in this dissertation were plotted onto the van Niel curve of Maka and Cork (1990) (Figure 2.3), their position would indicate that *all* of the experiments in this study were operated in an extremely underloaded condition. However, only Run 3 was underloaded. Maka and Cork's experiments were performed using a 0.8 L reactor whereas those in this dissertation employed a reactor volume of 12.0 or 13.7 L (Table 3.2). The radiant flux *per unit reactor volume* was calculated and plotted against the $S^=$ loading, and there was a better match between the experiments in this study and those of Maka and Cork (Figure 4.20).
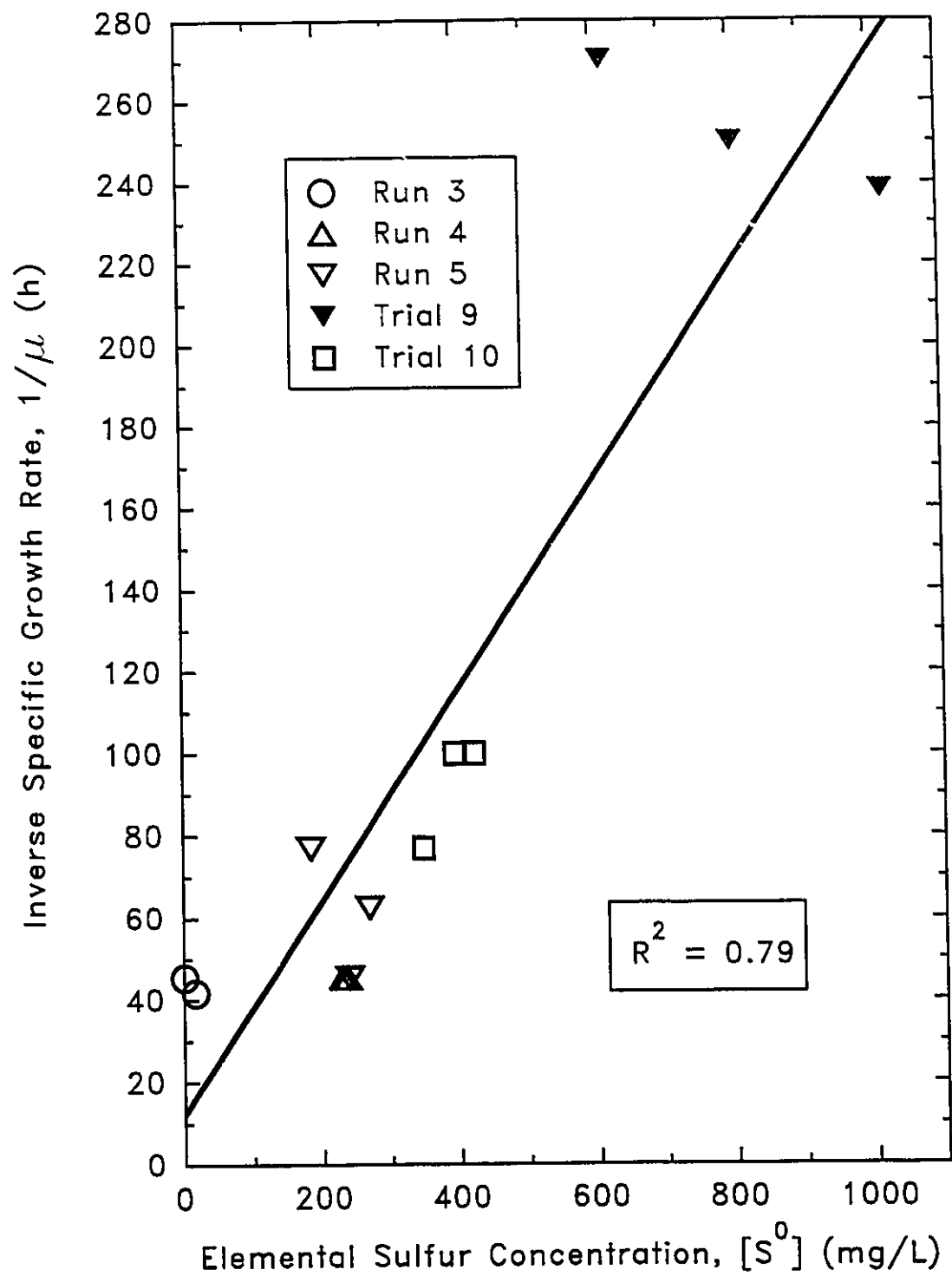
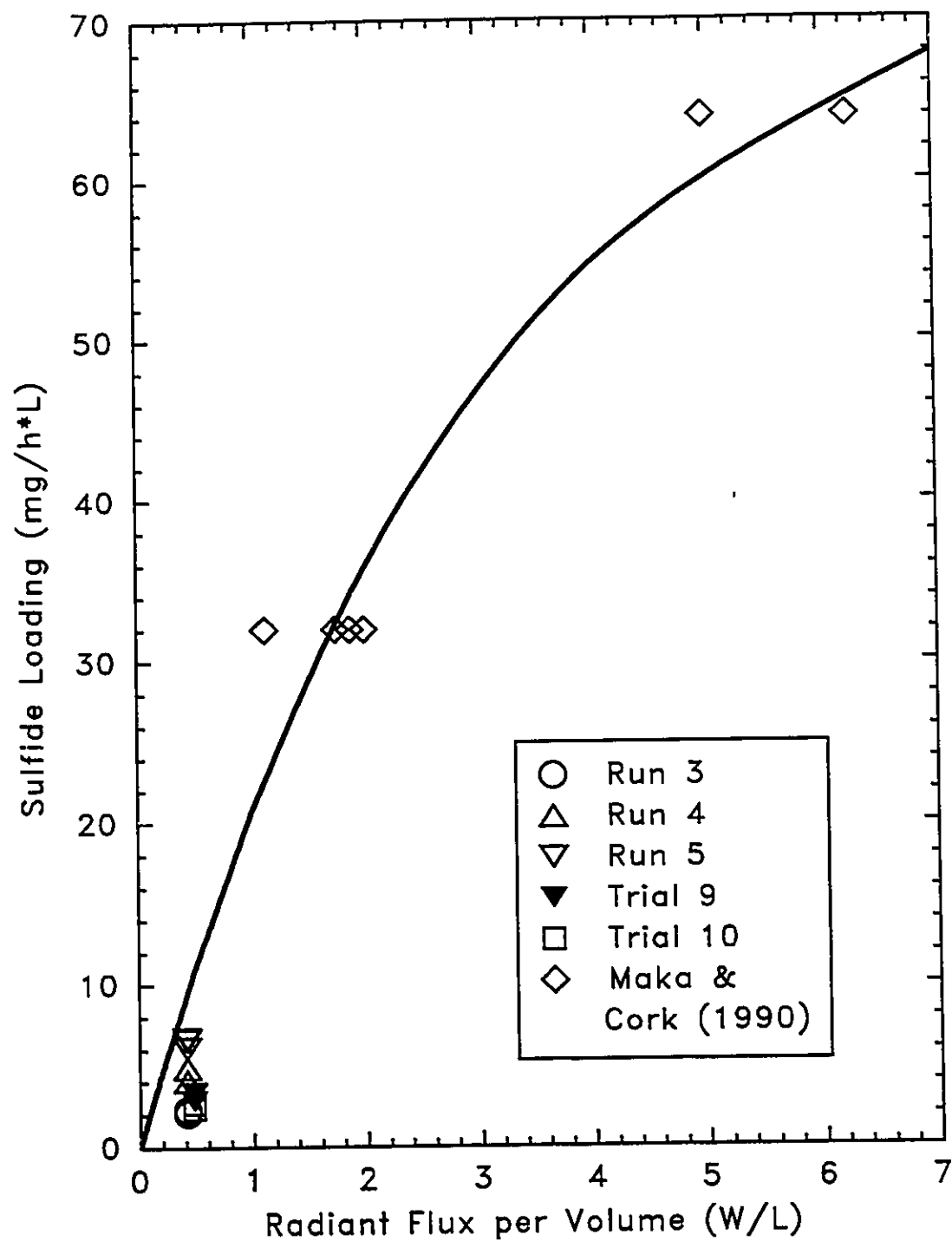FIGURE 4.19 The inverse relationship between specific growth rate and elemental sulfur concentration

FIGURE 4.20 Sulfide loading rate as a function of radiant flux per volume. The solid line was obtained by fitting the data of Maka & Cork (1990) to an equation of the form $y=c(1-e^{kx})$ where $c = 76.12$ and $k = -0.317$.

The light per volume is clearly an important parameter in the consumption of sulfide. Also relevant to the consumption of sulfide is the concentration of bacteria in the reactor. The parameter radiant flux per volume times the bchl concentration represents the capacity of the reactor to consume sulfide. Using this parameter as the abscissa and $S^=$ loading as the ordinate results in better coherence between the data from this study and those of Maka and Cork (Figure 4.21). The extraction of bchl concentrations from Maka and Cork's experiments is described in Appendix G.

The region of Figure 4.21 near the origin has been expanded in Figure 4.22 to show how the van Niel curve (from Maka & Cork's data) neatly divides the overloaded and underloaded experiments. The solid line was based on Maka and Cork's data and does not take into account Runs 3, 4 and 5, or Trials 9 and 10.

The specific loading rate was calculated for each experiment by dividing the $S^=$ loading rate by the concentration of biomass. Plotting the specific loading rate as a function of the capacity parameter for those experiments in this study as well as those of Maka and Cork resulted in the loss of the distinction between the over and underloaded regions. There was a similarly poor relationship between the specific loading rate as and the radiant flux/volume.

The van Niel curve shows that the light input determines the number of electrons transferred. For a sulfide loading "on the curve", the electron requirement is met by the removal of two electrons from $S^=$ to form S^0. If the electron requirement increases, further oxidation from S^0 to $SO_4^=$ can yield six *more* electrons. The number of moles of electrons transferred in an experiment was calculated from the rates of formation of the
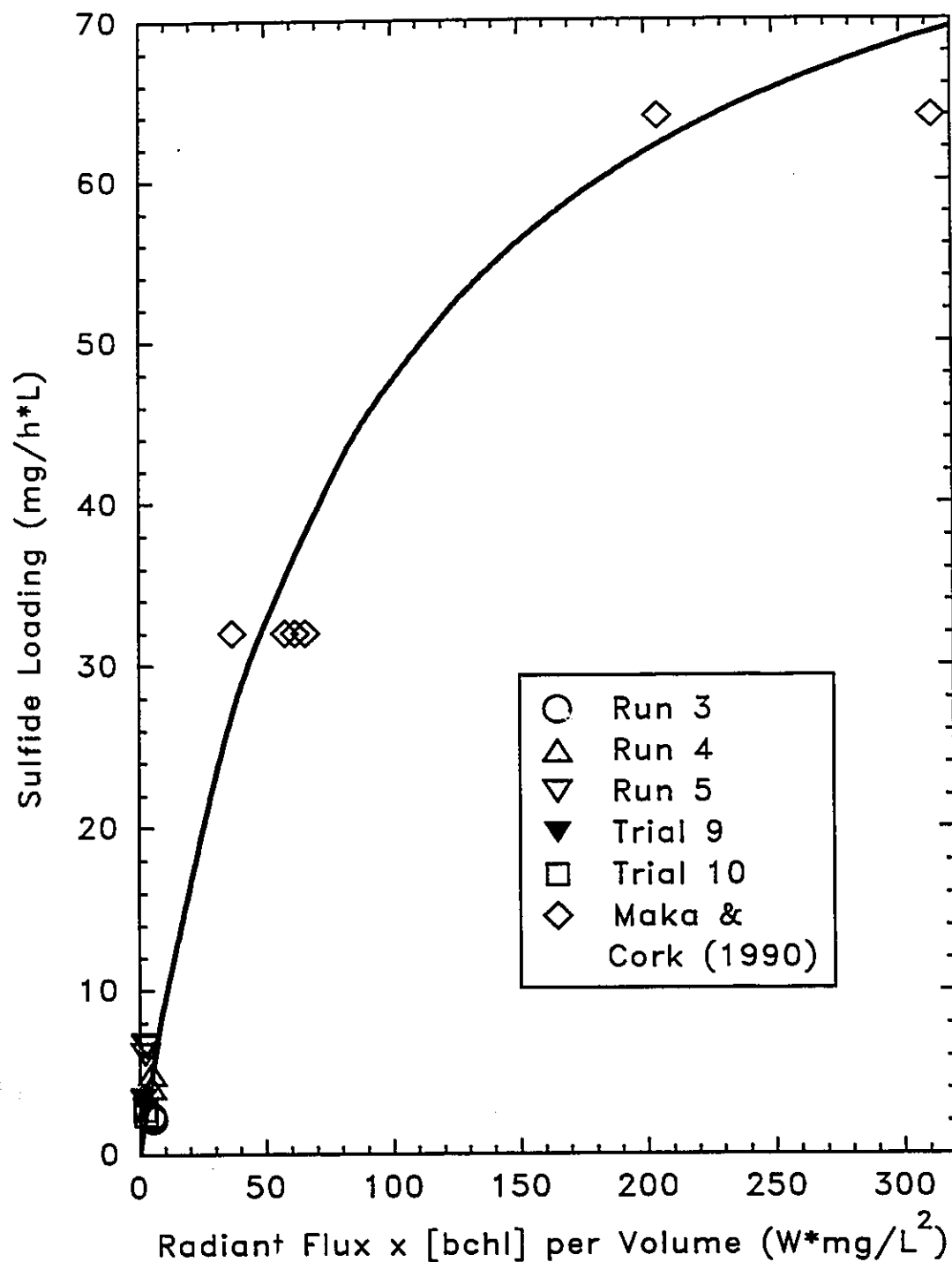
97

FIGURE 4.21 Sulfide loading as a function of radiant flux per unit volume times bacteriochlorophyll. The solid line was obtained by fitting the data of Maka & Cork (1990) to an equation of the form $y=c(1-e^{kx})$ where $c = 69.3$ and $k = -0.0119$.
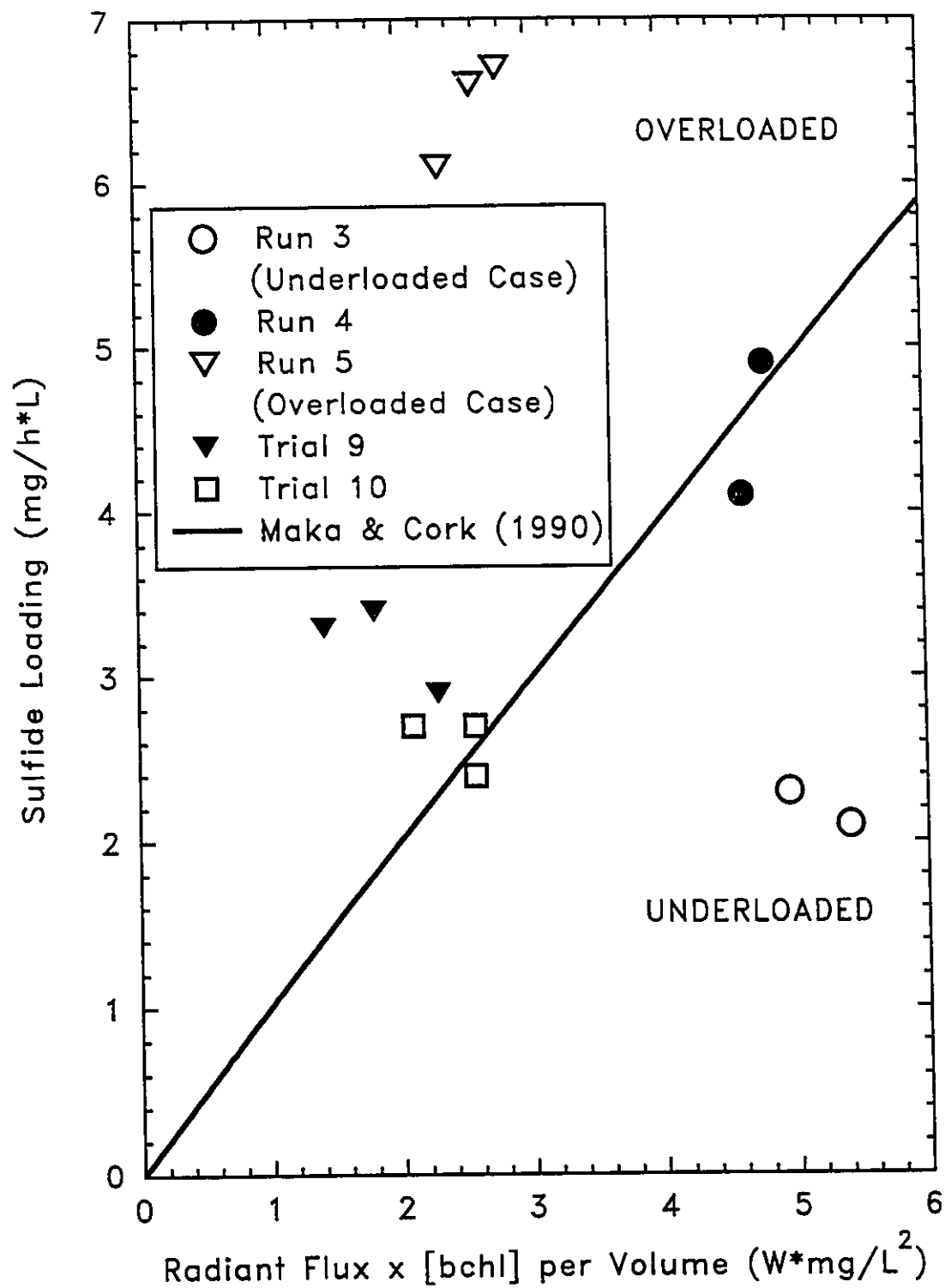
FIGURE 4.22 Sulfide loading as a function of radiant flux per unit volume times bacteriochlorophyll (Figure 4.21 enlarged)

oxidized compounds (this dissertation) or the percentages of the total sulfur equivalents of each compound after oxidation (Maka & Cork's data). For the data from this dissertation, the rate values were calculated between SSCs, thus there were 2 or 3 rate values determined in each experiment. Only one of these values was chosen from each experiment, as indicated in Table 4.3, typically that with the best mass balance or rate data. The rates of formation in mg $S/h \cdot L$ (as different species) were divided by 32 to give mmole $S/h \cdot L$. Then the molar rates of formation of S^0, $S_2O_3^=$ and $SO_4^=$ were multiplied by 2, 4 and 8 respectively to give the rates of electron release (mmole $e^-/h \cdot L$) for each mmole of $S^=$ oxidized to each of the compounds. From Maka and Cork's data, the total sulfide loadings in mmole/h·L were multiplied by the fraction of each species remaining at the end of the experiment and by 2, 4 and 8 for S^0, $S_2O_3^=$ and $SO_4^=$ respectively (sulfide remaining at the end of the experiment contributed no electrons to the bacteria). In either case, the rates of electron transfer were summed and plotted against light/volume (Figure 4.23). This relation describes the PRC. For each unit of light input, there is a certain number of electrons transferred. The number of electrons per unit of light energy (slope of solid line in Figure 4.23) decreases as the light energy increases. This may be attributed to the fact that the PRC becomes light saturated (already in the excited state) at high light levels. This figure also shows that the experiments in this dissertation are at the lower end of the radiant flux/volume scale. Unfortunately, the use of a conventional fermentor with lights shining from only one direction limited the light energy/volume that could be made available to the bacteria.

All electrons are not created equal; or at least the energy released oxidizing an
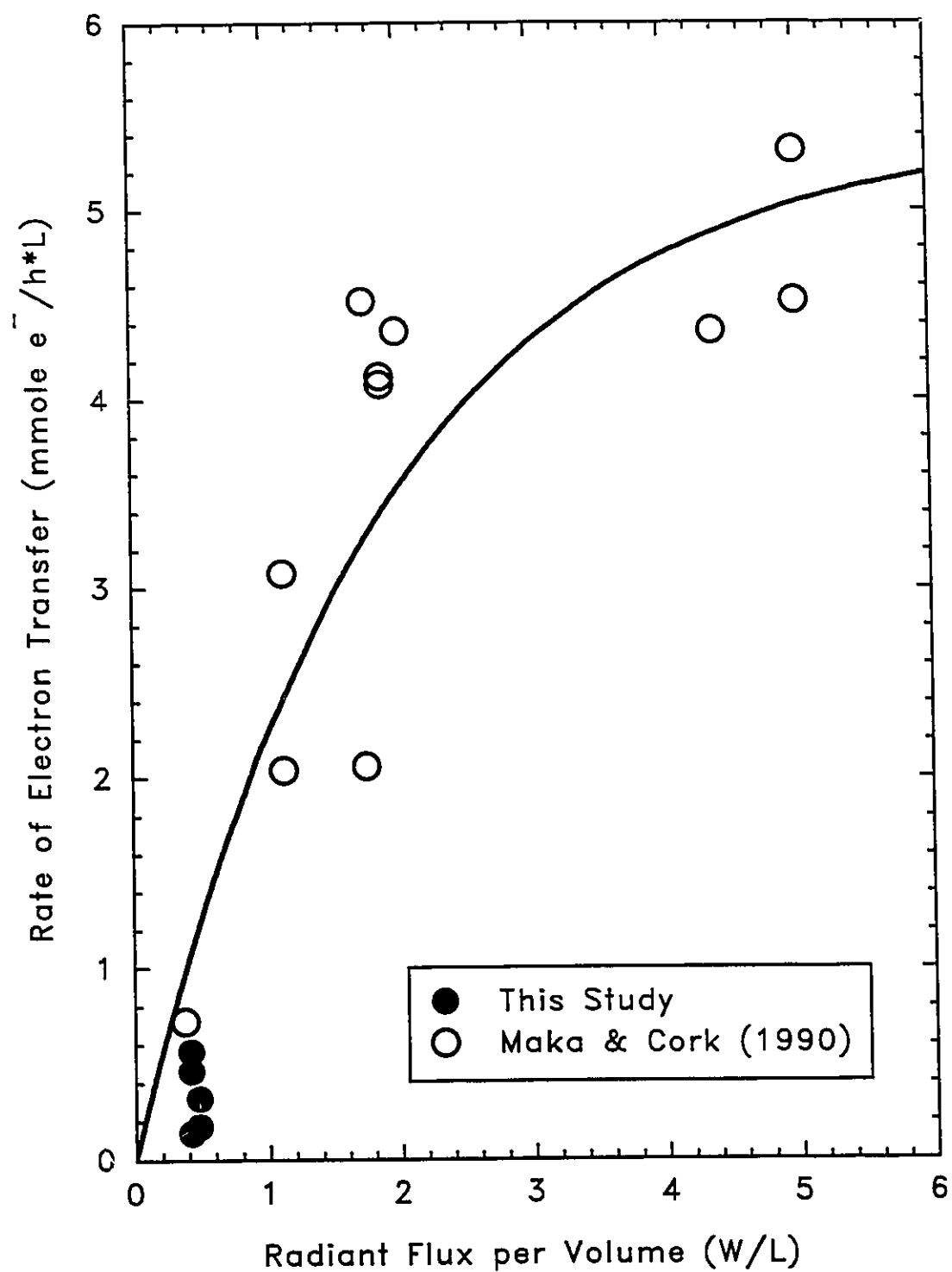
FIGURE 4.23 Rate of electron transfer as a function of radiant flux per unit volume

101

electron from $S^=$ to S^0 is not the same as the energy released by an electron resulting from

oxidizing S^0 to $SO_4^=$. Table 4.4 lists the energies per electron released from the oxidation

half reactions involving sulfur. These values were calculated by subtracting the energies

of formation of the reactant molecules from those of the product molecules (Brock and

Madigan & Brock, 1988). This table also illustrates the thermodynamic advantage of

using electrons from $S^=$ as opposed to those from S^0 or $S_2O_3^=$. When these energies are

incorporated into the calculations for electron transfer by multiplying the electron yield

for each sulfur conversion by the appropriate energy, the correlation with light/volume is

very good (Figure 4.24).

TABLE 4.4 Energy released from sulfur oxidation

Half Reaction	Number of Electrons Transferred	Free Energy Change at pH 7 $\Delta G^{0'}$ (kJ/mole)	Energy per Mole Electrons (kJ)
$S^= \rightarrow S^0$	2	-52	26
$S^0 \qquad \rightarrow SO_4^=$	6	-115	19
$S^= \rightarrow \quad \frac{1}{2}S_2O_3^=$	4	-71	18
$\frac{1}{2}S_2O_3^= \rightarrow SO_4^=$	4	-96	24
$S^= \qquad \rightarrow \qquad SO_4^=$	8	-167	21

Figure 4.24 also gives a loose indication of the efficiency of the bacterial

photosystem for the infrared light source. An input of energy of 4 W/L yields a chemical

energy release equivalent to 93 J/h·L. This equals 0.026 J/s·L or 0.026 W/L. Therefore,

the photosystem efficiency could be calculated as 100x(0.026/4) or 0.6%. However, this
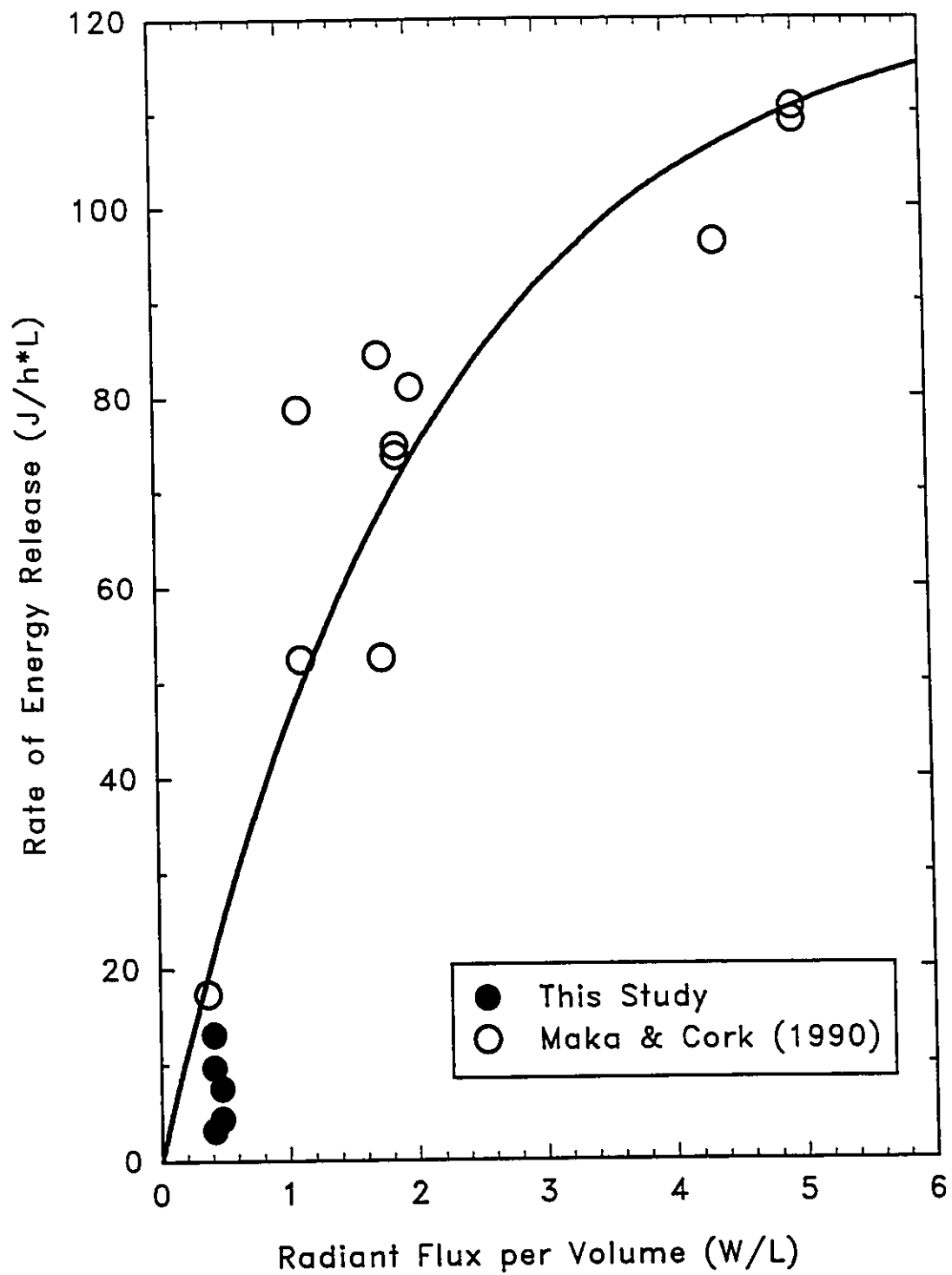
FIGURE 4.24 Energy released by sulfur oxidation as a function of the radiant flux per volume entering the reactor.

calculation is flawed, in that the light that is absorbed by the photochemical reaction centre supplies energy for *both* cyclic and non-cyclic photophosphorylation. It may be possible though, to estimate the relative energies devoted to cyclic and non-cyclic photophosphorylation from the heats of formation of ATP and NADPH, and the 7 to 10 molar ratio of the two that are required to manufacture glucose.

The quantum requirement for *C. thio.* was defined as the number of photons of light required to produce one molecule of elemental sulfur from one molecule of sulfide (Maka & Cork, 1990). The lowest quantum requirement in this study occurred in Run 4. For this experiment, an average of 4.8 mg S^0/h·L were produced. This equals 9.03×10^{19} molecules/h·L converted. The radiant flux per volume received by the reactor in Run 4 was 0.415 W/L = 0.415 J/s·L = 1494 J/h·L. One photon of infrared light (assuming an average wavelength of 900 nm) has 2.21×10^{-19} J of energy. Therefore the number of photons received by the reactor was 676×10^{19}/h·L. Dividing the number of photons by the number of molecules of S^0 formed yields a quantum requirement of 75 photons/molecule of S^0. This requirement compares favourably with those reported by Maka and Cork for broad-band infrared radiation and 760 nm radiation of 59 and 47 photons/molecule of S^0 respectively. The other experiments in this study had higher quantum requirements because the average rate of S^0 production was less than Run 3 (Table 4.3). Again, it is noted that the calculation of quantum requirement ignores the facts that: not all of the light entering the bioreactor is absorbed by the bacteria, and the light that is absorbed is directed to cyclic *and* non-cyclic photophosphorylation.

CHAPTER FIVE

MODEL DEVELOPMENT

Everything should be made as simple as possible, but not simpler.
Albert Einstein (Cohen & Cohen, 1980)

5.1 Purpose of Model

Three models have been developed to simulate the concentrations of inorganic sulfur

species and biomass in bioreactors employing the green sulfur bacterium *C. thio*. These

are: the yield-based model, the pathway-based model and the empirical model.

5.2 Yield-based Model

This model is analogous to that used in designing biological wastewater treatment

plants. In designing a biological treatment reactor, mass balance equations are written for

the substrate and the biomass. These two equations are then linked by the yield

coefficient, which relates the rate of substrate utilisation to the rate of biomass growth.

Once the yield coefficient is measured from experimental studies, one of the rates can be

eliminated and the two equations solved. In the experiments described in this dissertation,

the substrate, carbon dioxide, was not limiting the bacterial growth (Appendix H).

Instead, the electron donor $S^=$ (or S^0) was measured and a mass balance was applied to

determine its rate of consumption (or formation). Also, the rate of bacterial growth was

calculated (Section 4.2.3). The ratio of the two gave the yield coefficient.

The rate of sulfide utilisation was calculated as outlined in Section 4.1.2, and the first

yield coefficient was calculated as:

$$Y^{\cdot}_1 = \frac{r_x}{-r_{S^-}} \qquad\qquad [5\text{-}1]$$

Similarly the second yield coefficient for S^0 was calculated:

$$Y^{\cdot}_2 = \frac{r_x}{r_{S^0}} \qquad\qquad [5\text{-}2]$$

The yield coefficients, $Y^{\cdot}_3$ and $Y^{\cdot}_4$ were calculated in a similar manner, based on $S_2O_3^=$ and $SO_4^=$ respectively. The superscript asterisk ($^{\cdot}$) indicates that these yield coefficient values are in units of mg bchl/mg S as opposed to the more typical units of mg VSS/mg BOD.

The values for yield coefficients in the continuous reactor experiments performed in this study as well as some batch reactor experiments (Henshaw, 1990) are summarized in Table 5.1. It can be seen that neither the first nor the second yield coefficient values are constant. The yields also do not seem to be functions of the $S^=$ or bchl concentrations. The yield values from Run 3, where the bioreactor was underloaded and was converting $S^=$ to $SO_4^=$, were higher than from the other experiments. This behaviour was confirmed by observations during previous batch studies (Henshaw, 1990) and in the inoculation of the continuous reactor during start-up, where the increase in green colour occurred *after* the elemental sulfur was formed in the reactor. If the yield coefficient values from Run 3 are ignored, two observations can be made. First, the yield coefficient values show wide variations, $Y^{\cdot}_1$ ranging from 0.003 to 0.06 and $Y^{\cdot}_2$ from 0.003 to 0.13. Secondly, there is an inverse relationship between the yield coefficient and the elemental sulfur concentration (Figure 5.1). This relationship may be hyperbolic as evidenced by

TABLE 5.1 Calculation of yield coefficient values

Experiment	Rate of Bacteria Growth[a] (mg/h·L)	Rate of S$^=$ Consump. (mg/h·L)	Y'$_1$ (mg/mg)	Rate of S^0 Formation (mg/h·L)	Y'$_2$ (mg/mg)	Rate of S$_2$O$_3^=$ Formation (mg/h·L)	Y'$_3$ (mg/mg)	Rate of SO$_4^=$ Formation (mg/h·L)	Y'$_4$ (mg/mg)
Run 3	0.28	2.3	0.12	-0.10	-2.8	-	-	1.8	0.16
	0.28	2.0	0.14	-0.11	-2.5	-	-	1.9	0.15
Run 4	0.25	4.9	0.052	4.3	0.059	-	-	1.2	0.22
	0.24	4.0	0.060	5.2	0.047	-	-	0.61	0.40
Run 5	0.11	5.2	0.021	6.7	0.016	-	-	0.021	5.3
	0.13	3.3	0.041	1.0	0.13	-	-	0.30	0.46
	0.073	2.5	0.029	2.5	0.029	-	-	-0.64	-0.11
Trial 9	0.020	2.6	0.0075	4.9	0.0040	0.26	0.077	0.013	1.5
	0.015	3.2	0.0047	2.7	0.0056	0.18	0.084	-0.019	-0.80
	0.011	3.2	0.0034	3.4	0.0032	-0.029	-0.37	-0.036	-0.30
Trial 10	0.055	2.4	0.023	4.2	0.013	-0.31	-0.18	0.040	1.4
	0.055	2.1	0.026	2.8	0.020	-0.20	-0.28	-0.035	-1.6
	0.054	2.9	0.019	3.8	0.014	-0.36	-0.15	0.022	2.4

TABLE 5.1 (continued) Calculation of yield coefficient values

Experi-ment	Rate of Bacteria Growth[a] (mg/h·L)	Rate of S= Consump. (mg/h·L)	Y'_1 (mg/mg)	Rate of S° Formation (mg/h·L)	Y'_2 (mg/mg)	Rate of $S_2O_3^=$ Formation (mg/h·L)	Y'_3 (mg/mg)	Rate of $SO_4^=$ Formation (mg/h·L)	Y'_4 (mg/mg)
Batch Reactor	0.15	1.6	0.094	1.4	0.11	-	-	-	-
	0.30	2.1	0.14	1.8	0.16	-	-	-	-
	0.22	8.2	0.028	5	0.045	-	-	-	-
	0.16	4.3	0.036	2.2	0.070	-	-	-	-
	0.94	7.5	0.13	2.3	0.41	-	-	-	-
		average[b]= std.dev.[b]=	0.026 0.019	average[b]= std.dev.[b]=	0.031 0.037	average= std.dev.=	-0.14 0.19	average= std.dev.=	0.71 1.72

[a] = based on bacteriochlorophyll: mg bchl/h·L
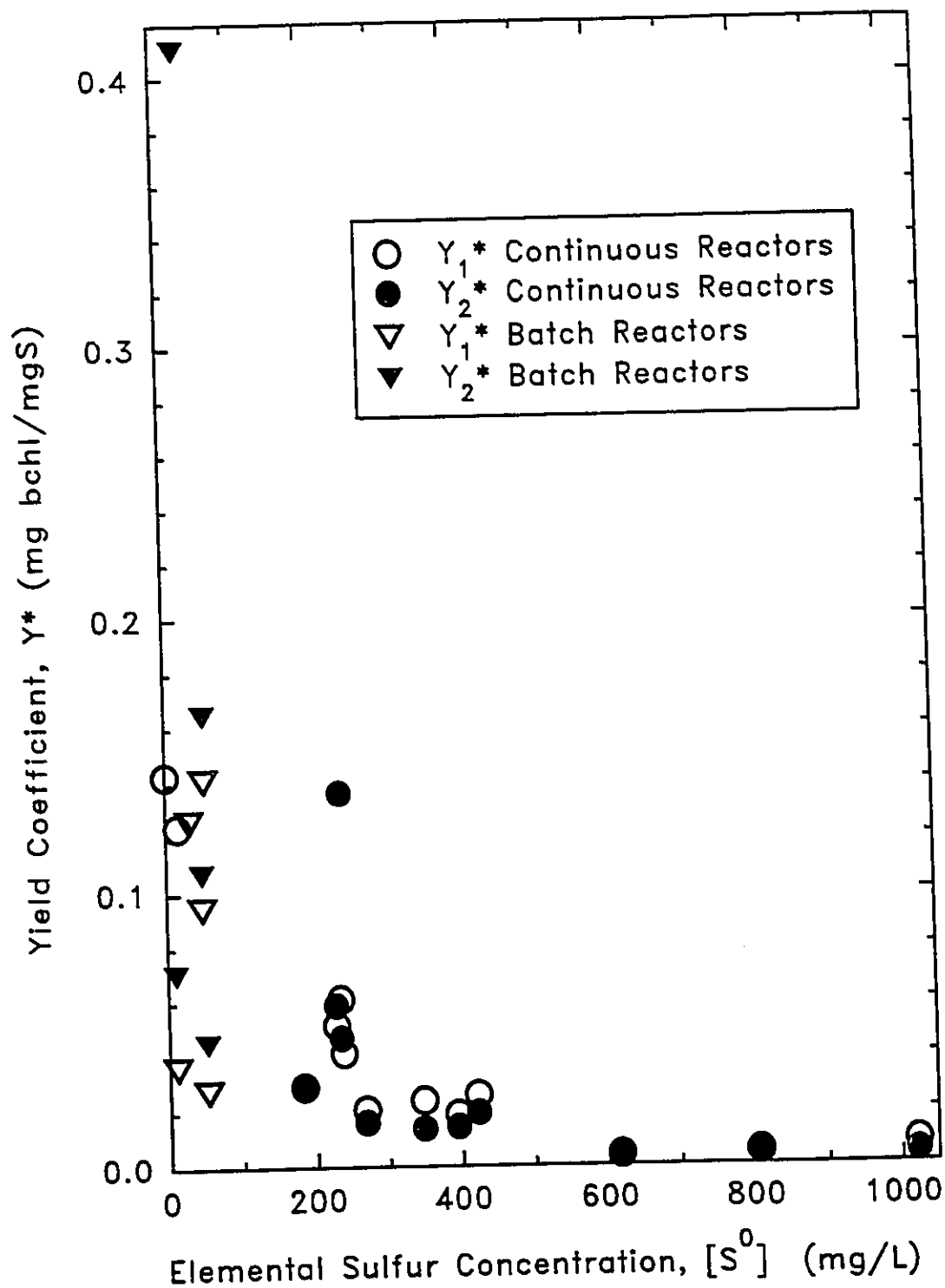
[b] = excluding Run 3 and Batch Reactor data.

108

FIGURE 5.1 The relationship between the yield coefficient and the elemental sulfur concentration

109

the moderate (R^2=0.67) correlation between $1/Y^*$ and [S^0] (Figure 5.2). The existence of a relationship between Y^* and [S^0] is not surprising since there is a relation between [S^0] and μ (Figure 4.19), and μ is a component of r_X (Equation 4-22) which in turn is the numerator of the yield coefficient definition. As for the denominator, r_{So} is proportional to [S^0] once steady state has been reached (Equation 4-21). In addition, one would expect $Y^*_1 = Y^*_2$ for a given time in a given experiment, because $S^=$ consumption and S^0 formation are linked and occurred at similar rates in all experiments except Run 3. In fact, there is a moderate relationship between Y^*_1 and Y^*_2, the coefficient of determination between the two being 0.67.

These values compare favourably to those derived from Maka and Cork (1990) which range from 0.02 to 0.04 mg bchl/mg $S^=$, providing partial verification of this model. If the yield coefficient values presented in this dissertation were converted to units of mg VSS/mg $S^=$ (assuming bchl is 5% of VSS; Section A.6), the range of Y^*_1 values would be 0.06 to 0.12. Yield values of 0.02 to 0.1 mg VSS/mg BOD_5 reported for anaerobic wastewater treatment using various substrates (Metcalf and Eddy, 1991).

5.3 Pathway-based Model

A scheme was developed which accommodated the sulfur conversions in GSB as reported in the literature. If kinetic parameters could be derived from experimental data for each these reactions, then the fate of all species in the reactor could be simulated.

5.3.1 Conversion of Sulfur Species

Table 5.2 summarizes the qualitative evidence that led to the development of a scheme of reaction pathways for sulfide oxidation by *C. thio.*
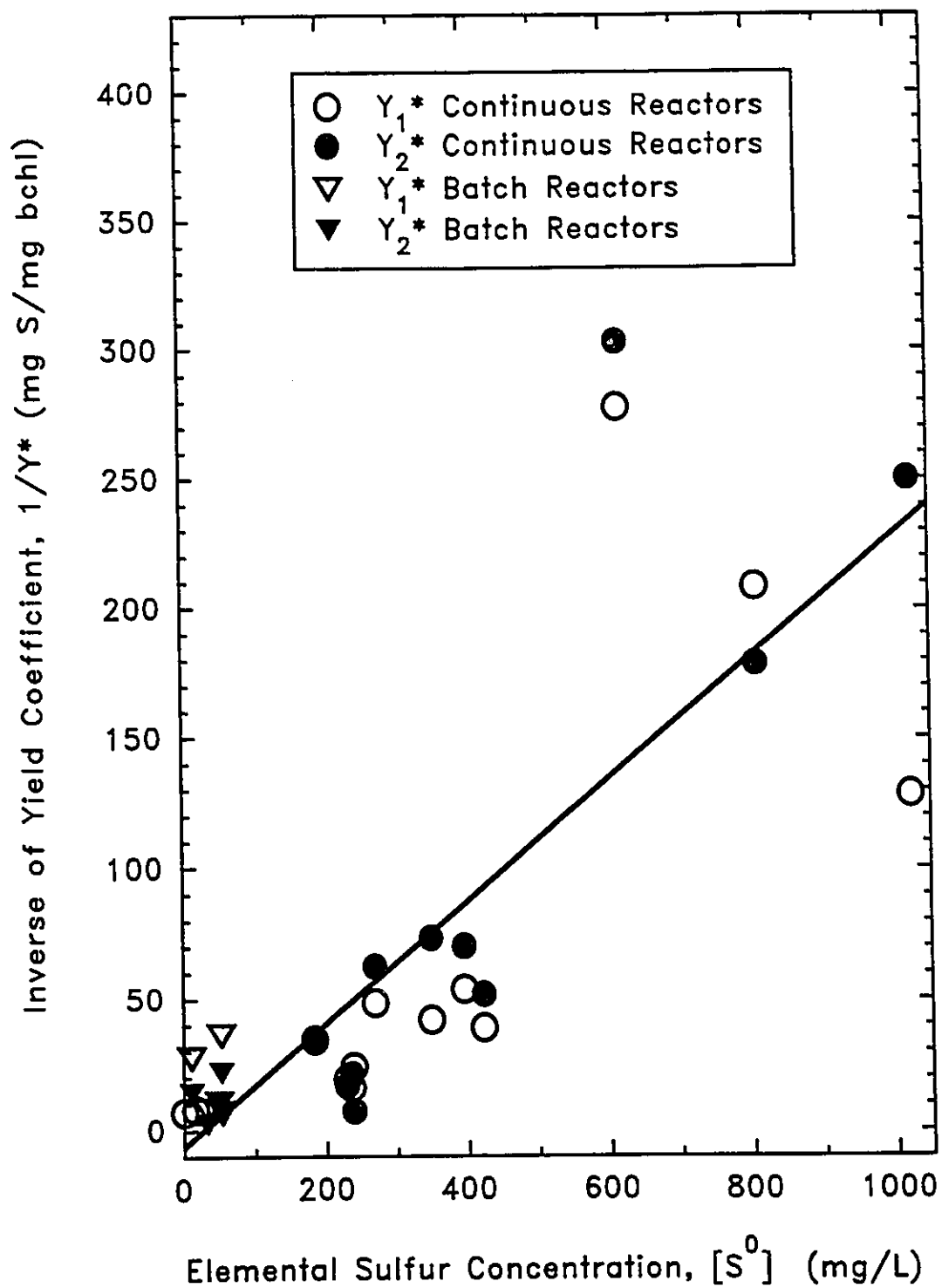
FIGURE 5.2 The relationship between the inverse of the yield coefficient and the elemental sulfur concentration

TABLE 5.2 Sulfur reactions observed in phototrophic bacteria

No.	Reaction	Comment	Ref.
I	$H_2S \rightarrow S_0, S_2O_3^= \rightarrow SO_4^=$	$S_2O_3^=$ formed before S^0 in batch culture; $S_2O_3^=$ not formed in continuous culture	T,B
II	$S^0 \rightarrow SO_4^=$	No H_2S or $S_2O_3^=$ formed	T
III	$S_2O_3^= \rightarrow SO_4^=$	No extracellular S^0 formed	T,B
IV	$S^0 \rightarrow H_2S + SO_3^=$	CO_2 and H_2S removed	T,B
V	$H_2S \leftarrow S^0$	In dark environment	B

Ref.= references: T= Truper and Fischer (1982), B= Brune(1989)

The following sequence of reactions

$$H_2S \rightarrow S^0 \rightarrow S_2O_3^= \rightarrow SO_4^= \qquad [5\text{-}3]$$
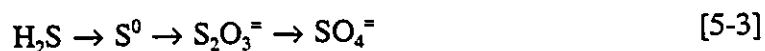
satisfies the observed reactions in Table 5.2 except Number II. Changing the order to allow thiosulfate to be the second intermediate, the alternate sequence of reactions

$$H_2S \rightarrow S_2O_3^= \rightarrow S^0 \rightarrow SO_4^= \qquad [5\text{-}4]$$
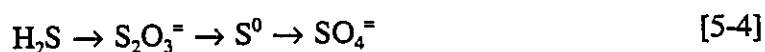
is not possible if reaction Number III occurs without extracellular S^0 formation. If the sulfur formed in reaction Number III is intracellular, as suggested by Brune (1989) then sequence 5-4 would not result in the observed extracellular sulfur formation.

The oxidation of H_2S with *parallel* formation of S^0 and $S_2O_3^=$ can be seen in Figure 5.3 (Brune, 1989). Both elemental sulfur and thiosulfate were formed starting at time zero in a batch *C. thio.* culture and the concentrations of both compounds began to decrease when the sulfide concentration dropped to zero.
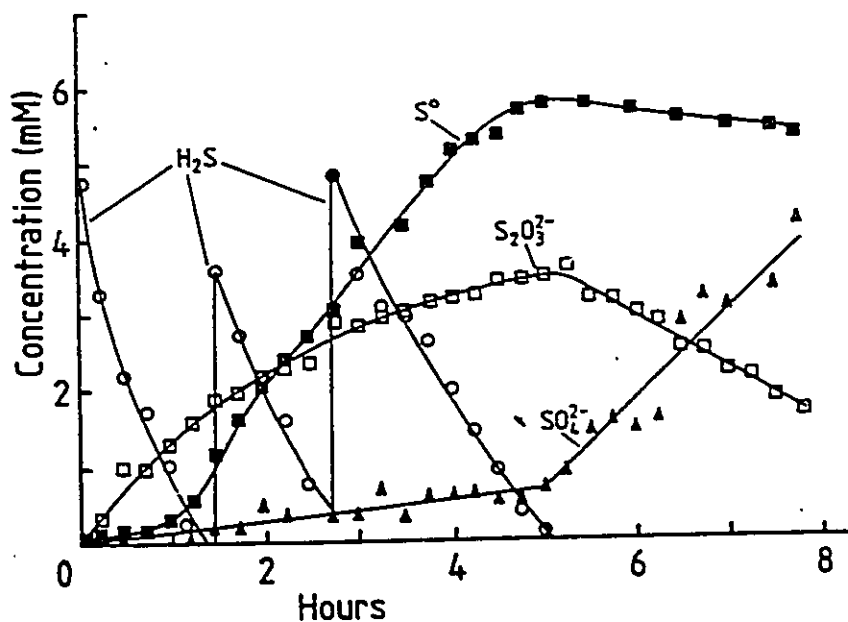
FIGURE 5.3 Concentrations of H_2S (O), $S_2O_3^-$ (□), S^0 (■), and SO_4^- (▲) as functions of time in a batch culture (Brune, 1989)

5.3.1.1 Enzymes in Pathways

The pathway-based model assumes the parallel formation of $S_2O_3^-$ and S^0 with separate oxidation pathways to SO_4^- (Figure 5.4).
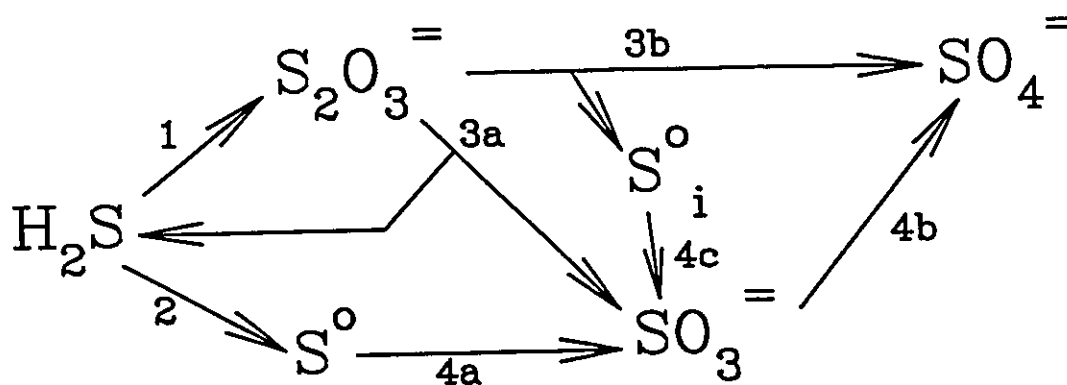

FIGURE 5.4 Proposed reaction pathways

The enzyme for Reaction 1 was originally believed to be flavocytochrome c (Truper & Fischer, 1982), but this hypothesis has been questioned (Brune, 1989). More likely, flavocytochrome c is the sulfide dehydrogenase in Reaction 2 (Brune, 1989). Reaction 2 can also be catalysed by a quinone (Brune, 1989). The enzyme catalysing Reaction 3a could be either a rhodanese or thiosulfate reductase, both of which are found in *C. thio.* It has been proposed that Reaction 4a is catalysed by a sulfite reductase operating in reverse, but this enzyme has not yet been isolated from green sulfur bacteria. Experiments with *Chlorobium vibrioforme* forma *thiosulfatophilum* demonstrated the splitting of $S_2O_3^=$ into S^0 and another product, which was quickly released into the medium as $SO_4^=$ as depicted by Reaction 3b (Brune, 1989). The S^0 was trapped on a membrane filter with the cell material, indicating that it may have been intracellular elemental sulfur, S^0_i. This intracellular sulfur is assumed to be oxidized to $SO_3^=$ as in Reaction 4c since S^0 does not appear extracellularly on oxidizing $S_2O_3^=$. Enzymes have been isolated from *C. thio.* to perform Reaction 4b (Brune, 1989).

5.3.1.3 Simplified Reaction Pathways

Although an enzyme for Reaction 3a has been isolated, Reaction 3b is the preferred route for the oxidation of $S_2O_3^=$ for two reasons. First, as noted in Number III of Table 5.2, the addition of $S_2O_3^=$ to *C. thio.* did not result in the production of extracellular S^0, as would be the case if the product H_2S from Reaction 3a had been further converted to S^0 by Reaction 2. Secondly, Reaction 3a is the only pathway in this model which is not energetically favoured. Thus, Reaction 3a ($\Delta G = 7.8 \times 10^7$ J·mole^{-1}) is eliminated in favour of Reaction 3b ($\Delta G = -7.4 \times 10^7$ J·mole^{-1}). A further simplification can be made

by combining Reactions 4a and 4b to eliminate the intermediate $SO_3^=$. Presumably, one of these reactions is slower and dominates the conversion of S^0 to $SO_4^=$. The concentration of the intermediate $SO_3^=$ need not be calculated since it was not measured in the experiments in this study.

Reactions 3b and 4c would not have been simplified if the intermediate intracellular elemental sulfur (S_i^0) had been measured separately. Both the present (Section 3.1.2) and previous (Henshaw, 1990) analytical methods for elemental sulfur involved a vigorous extraction with an organic solvent. It is assumed that this extraction broke the bacteria cell membrane and extracted any intracellular sulfur. Therefore, the measurement of S^0 includes S_i^0. Thus, Reaction 4c can be eliminated entirely and S_i^0 grouped with S^0. Based on these considerations, the pathway-based model is simplified as in Figure 5.5.
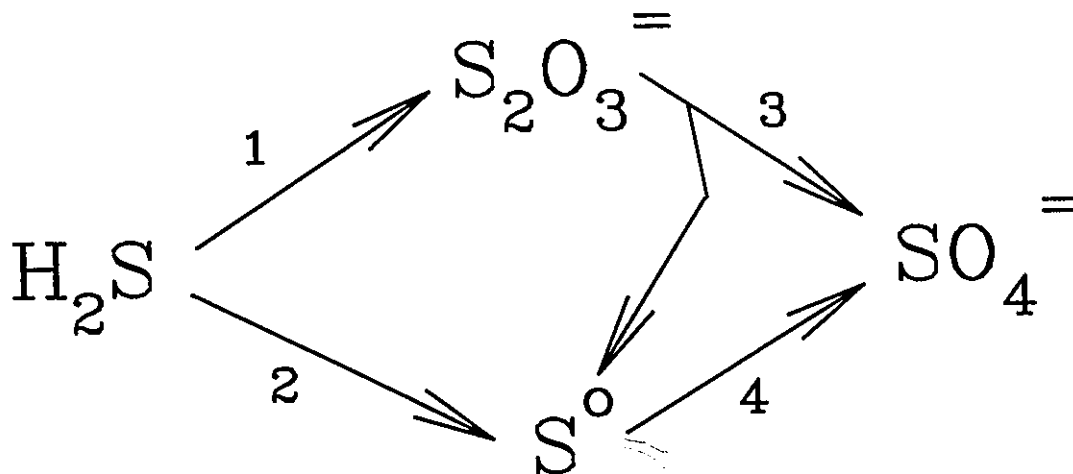
FIGURE 5.5 Simplified reaction pathways

The reactions for the model in Figure 5.5 are summarized in the following four equations, in which both dissolved hydrogen sulfide ($H_2S_{(aq)}$) and bisulfide (HS^-) are shown because they are present in roughly equal amounts at neutral pH:

Reaction 1 $H_2S_{(aq)} + HS^- + 3H_2O \rightarrow S_2O_3^= + 9H^+ + 8e^-$

Reaction 2 $H_2S_{(aq)} + HS^- \rightarrow 2S^0 + 3H^+ + 4e^-$

Reaction 3 $S_2O_3^= + H_2O \rightarrow S^0 + SO_4^= + 2H^+ + 2e^-$

Reaction 4 $S^0 + 4H_2O \rightarrow SO_4^= + 8H^+ + 6e^-$
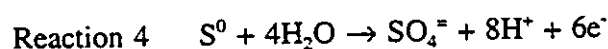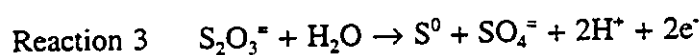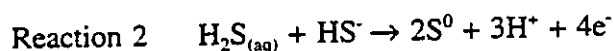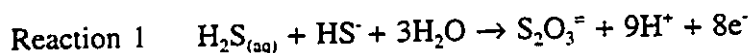
5.3.2 Simulation

Once the reaction pathways have been established, it remains to translate these into a workable computational model. Two strategies can be used. The first strategy is to employ enzyme kinetics to calculate the rate of changes of each of the species measured. To do this, the maximum reaction velocity, V_{max}, and the half-maximum velocity concentration, K_m, values for each of the enzymes must be known. Unfortunately, for the four pathways of the model, only two of the enzymes have been isolated. Also, the V_{max} varies with the enzyme concentration (Gaudy & Gaudy, 1980). In addition, the determination of the enzyme concentrations would be difficult, because they change with time and not necessarily in proportion to the change in biomass concentration.

The second approach is to apply the mass balance equation (4-1) to each electron donor species of sulfur. Then, the rate of total electron transfer is related to biomass. This approach was used in the pathway-based model.

Fundamentally, only two types of the many reactions that occur in phototrophic anoxygenic bacteria are considered. The "light reactions" use photon energy to remove electrons from an electron donor (noncyclic photophosphorylation) and the "dark reactions" utilize those electrons to assimilate carbon dioxide (the substrate) to form carbohydrates (reversed citric acid cycle). Both of these reactions are catalysed by

116

bacteria (Figure 5.6). In the case of *C. thio.*, the electron donors can be H_2S, S^0, or $S_2O_3^=$.

Different electron donors yield different numbers of electrons (see Reactions 1 to 4 discussed earlier). Also, more than one electron donor may be consumed simultaneously, eg. S^0 and $S_2O_3^=$. The number of available electrons is the common currency that links the light (electron producing) reactions and the dark (electron consuming) reactions.
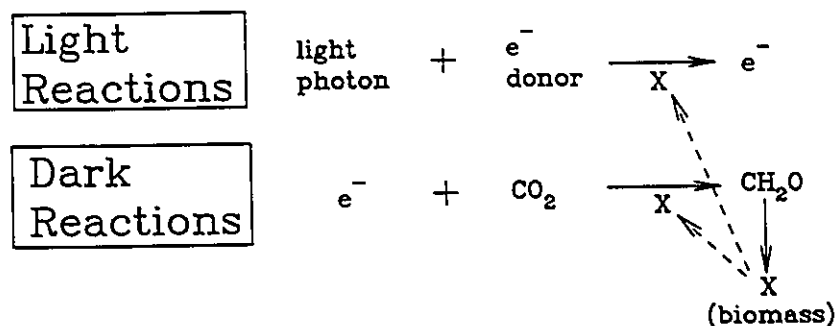
FIGURE 5.6 Light and dark reactions in green sulfur bacteria

Note that this approach assumes that the contribution of cyclic photophosphorylation to produce ATP does not limit the ability of the GSB to assimilate CO_2.

A certain amount of the light from the light source does not reach a given bacterium due to scattering by suspended sulfur particles, the distance the light must travel, and absorption by other bacterial cells (Kim *et al.*, 1992). The effect of these factors is small (Section 4.2.3) and was not taken into consideration in calculating the light power incident on the reactor (radiant flux) in this chapter.

5.3.2.1 Kinetics of Sulfur Oxidation

In this section, the mass balance Equation 4-1 is applied to each reactant sulfur species. The term "reactants" is used here instead of "substrate" to avoid confusion with

CO_2 which is the substrate for the *overall* metabolism of *C. thio*. The equation for rate

of consumption of a reactant, r_A, is normally dependant on the reactant concentration, [A].

The dependency of the rate on [A] determines the order of the reaction. In this thesis,

only the first order relationship in terms of the reactant was tested:

$$-r_A = k \cdot [A] \qquad [5\text{-}5]$$

In addition, the dependency of the rate equation on the radiant flux, L, and biomass

concentration, X, was also considered:

$$-r_A = k' \cdot X \cdot L \cdot [A] \qquad [5\text{-}6]$$

In addition to the experiments in this dissertation, rate and concentration data from

batch reactor studies (Henshaw, 1990) were also considered. Five of the seven batch

reactor runs were used. Data from batch reactor Run 4 were not used because a high

sulfide concentration resulted in negative bacterial growth. Data from batch reactor Run

5 were not used because the elemental sulfur data were not complete in the region of

logarithmic bacteria growth. In batch Run 3, the complete oxidation of H_2S was

monitored; S^0 increased as H_2S was consumed, then S^0 began to decrease after H_2S was

depleted. Therefore, this experiment is represented by three points: one while S^0 was

being formed and two while S^0 was being consumed (Table 5.3). For each batch reactor

experiment, data were interpolated to achieve the concentrations of all sulfur species at

the beginning and end of the log-growth phase of the bacteria. Thiosulfate was not

measured in the batch reactor studies, so its concentration was calculated by subtracting

the total concentrations of all sulfur species from the initial total. The rates of reaction

for the batch reactor experiments were calculated from the accumulation term of the mass

TABLE 5.3 Rate and concentration data for the pathway-based model

Experiment		Average Concentration (mg/L)					Rate of Formation (mg/h·L)			
		[S=]	[S0]	[S2O3=]	[SO4=]	[bchl]	S=	S0	S2O3=	SO4=
Cont.	Run 3	0	1	-	115	13.0	-2.0	-0.11	-	1.9
	Run 4	0	229	-	80	11.5	-4.9	4.3	-	1.2
	Run 5	53	239	-	38	6.2	-3.3	1.0	-	0.3
	Trial 9	24	807	82	31	3.8	-3.2	2.7	0.18	-0.02
	Trial 10	15	395	50	30	5.4	-2.9	3.8	-0.36	0.02
Batch	Run 1	21	49	22	28	1.8	-1.6	1.4	0.15	0.03
	Run 2	15	54	28	49	5.6	-2.1	1.8	-0.24	0.54
	Run 3	54	53	20	53	4.6	-8.2	5.0	2.33	0.82
		1	62	50	67	7.8	0	-5.7	4.09	1.66
		1	21	55	104	10.7	0	-1.3	-1.11	2.44
	Run 6	12	12	6	56	1.9	-4.3	2.2	1.79	0.15
	Run 7	29	33	27	59	4.5	-7.5	2.3	4.88	0.24

Cont. = continous reactor experiments.

balance as follows:

$$r_A = \frac{\Delta [A]}{\Delta t} = \frac{[A]_2 - [A]_1}{t_2 - t_1} \qquad [5\text{-}7]$$

For the continuous reactor data presented in this dissertation, rates were calculated as described in Section 4.2. The rate and concentration data are presented in Table 5.3.

Each pathway in Figure 5.5 affects more than one sulfur species. According to the simplified pathway-based model, sulfide consumption is the resultant of Reactions 1 and 2. Thus, the rate of sulfide consumption is the sum of these two rates:

$$-r_{S^=} = r_{S^=-S^0} + r_{S^=-S_2O_3^-} \qquad [5\text{-}8]$$

In terms of kinetic constants and concentrations:

$$-r_{S^=} = k_2[S^-] + k_1[S^-] = (k_1+k_2)[S^-] \qquad [5\text{-}9]$$

For the batch reactor data alone, the correlation between the rate of $S^=$ consumption and the $S^=$ concentration is moderate since R^2, the coefficient of determination, is 0.76 (Table 5.4). For the batch and continuous data pooled together the R^2 is 0.35. As mentioned in Section 4.2.1, the rate of $S^=$ consumption for the continuous reactor varied for each experiment, but the $S^=$ concentration was low in all cases. When light and biomass are factored in, the rate equation becomes:

$$-r_{S^=} = (k_1'+k_2')X \cdot L \cdot [S^-] \qquad [5\text{-}10]$$

The correlation between the rate of $S^=$ consumption and the term $X \cdot L \cdot [S^-]$ is 0.46, which is an improvement over the previous relation, but still weak.

For elemental sulfur, the rate of formation has three components, because Reactions 2, 3 and 4 are involved:

120

TABLE 5.4 Relationship between rates and concentrations for the pathway-based model

Independant Variable	Dependant Variable	Coefficient of Determination (R^2)
$[S^=]$	$-r(S^=)$	0.35
$X \cdot L \cdot [S^=]$	$-r(S^=)$	0.46
$[S^0]$	$r(S^0)$	0.09
$X \cdot L \cdot [S^0]$	$r(S^0)$	0.09
$[S^=]$	$r(S^0)$	0.19
$X \cdot L \cdot [S^=]$	$r(S^0)$	0.18
$[S_2O_3^=]$	$r(S^0)$	0.06
$X \cdot L \cdot [S_2O_3^=]$	$r(S^0)$	0.46
$[S^=]$	$r(S_2O_3^=)$	0.06
$X \cdot L \cdot [S^=]$	$r(S_2O_3^=)$	0.10
$[S_2O_3^=]$	$r(S_2O_3^=)$	0.09
$X \cdot L \cdot [S_2O_3^=]$	$r(S_2O_3^=)$	0.10
$[S_2O_3^=]$	$r(SO_4^=)$	0.05
$X \cdot L \cdot [S_2O_3^=]$	$r(SO_4^=)$	0.80
$[S^0]$	$r(SO_4^=)$	0.18
$X \cdot L \cdot [S^0]$	$r(SO_4^=)$	0.08
$[SO_4^=]$	$r(SO_4^=)$	0.81
$X \cdot L \cdot [SO_4^=]$	$r(SO_4^=)$	0.93

$$r_{S^0} = r_{S^- - S^0} - r_{S^0 - SO_4^-} + \frac{1}{2} r_{S_2O_3^- - SO_4^-, S^0} \qquad [5\text{-}11]$$

In terms of rate constants and concentrations:

$$r_{S^0} = k_2[S^-] - k_4[S^0] + \frac{1}{2} k_3[S_2O_3^-] \qquad [5\text{-}12]$$

Presumably, one of these rates is faster and dominates the rate equation. If Reaction 2 dominates:

$$r_{S^0} = r_{S^- - S^0} = k_2[S^-] \qquad [5\text{-}13]$$

If Reaction 3 were to dominate:

$$r_{S^0} = \frac{1}{2} r_{S_2O_3^- - SO_4^-, S^0} = \frac{1}{2} k_3[S_2O_3^-] \qquad [5\text{-}14]$$

And if Reaction 4 dominates:

$$r_{S^0} = -r_{S^0 - SO_4^-} = -k_4[S^0] \qquad [5\text{-}15]$$

To that end, the correlation between the rate of S^0 formation and the concentrations of $S^=$, S^0 and $S_2O_3^-$ were determined, and R^2 was found to be 0.09, 0.19 and 0.06 respectively (Table 5.4). The inclusion of light and biomass in the rate equations as in Equation 5-5 did not significantly improve the correlation, the values of R^2 being 0.09, 0.18 and 0.46. These correlations are weak ($R^2 < 0.5$), so the rate of S^0 production does not depend upon any of the variables examined.

For thiosulfate, the rate is composed of two components:

$$r_{S_2O_3^-} = r_{S^- - S_2O_3^-} - r_{S_2O_3 - SO_4^-, S^0} \qquad [5\text{-}16]$$

If Reaction 1 dominates:

$$r_{S_2O_3^-} = r_{S^--S_2O_3^-} = k_1[S^-] \qquad\qquad [5\text{-}17]$$

And if Reaction 3 dominates:

$$r_{S_2O_3^-} = -r_{S_2O_3^--SO_4^-,S^0} = -k_3[S_2O_3^-] \qquad\qquad [5\text{-}18]$$

The correlations between the rate of $S_2O_3^-$ formation and the concentrations of S^- and $S_2O_3^-$ are weak with R^2 of 0.06 and 0.09 respectively. Even after adding the factors of light and biomass concentration, the correlations are still weak, R^2 for both being 0.10.

The rate of sulfate formation is influenced by Reactions 3 and 4, such that:

$$r_{SO_4^-} = \frac{1}{2}r_{S_2O_3^--SO_4^-,S^0} + r_{S^0-SO_4^-} \qquad\qquad [5\text{-}19]$$

Again, one would expect one of the two components to dominate. If Reaction 3 is faster, the rate becomes:

$$r_{SO_4^-} = \frac{1}{2}r_{S_2O_3^--SO_4^-,S^0} = \frac{1}{2}k_3[S_2O_3^-] \qquad\qquad [5\text{-}20]$$

If reaction 4 is faster, the rate of SO_4^- formation becomes:

$$r_{SO_4^-} = r_{S^0-SO_4^-} = k_4[S^0] \qquad\qquad [5\text{-}21]$$

But neither the $S_2O_3^-$ concentration nor the S^0 concentration is well correlated to the rate of SO_4^- formation, the values of R^2 being 0.05 and 0.18 respectively. The additional factors of biomass and light change the R^2 to 0.80 and 0.08. The seemingly high relationship between $X \cdot L \cdot [S_2O_3^-]$ and the rate of SO_4^- formation is due to two points in the latter part of Run 3 in the batch reactor data, which have a high biomass concentration and moderately high light levels resulting in two extreme points which skew the linear correlation and reduce the R^2.

Surprisingly, the rate of $SO_4^=$ *formation* is strongly related to the $SO_4^=$ concentration, the R^2 being 0.81. With the light and biomass factors the correlation between the rate of $SO_4^=$ production and $X \cdot L \cdot [SO_4^=]$ gives $R^2 = 0.93$. This high correlation is not an artifact of a few points that skew the statistical analysis as in the case of $S_2O_3^=$ (Figure 5.7).

5.3.2.2 Utilisation of Carbon Dioxide

Sulfur species are the electron donors for the reduction of carbon dioxide to cellular material (dark reaction, Figure 5.6). Therefore, it would seem reasonable that the growth rate of bacteria (r_X) is related to the rate of release of electrons in the light reactions (r_e). The production of electrons was calculated as described in Section 4.2.4. Accordingly, the $S^=$ to S^0 conversion liberates two electrons, $S^=$ to $SO_4^=$ liberates 8 and so forth.

A regression between the specific growth rate, μ, and the electron movement per unit time, resulted in a weak correlation ($R^2=0.46$). Including the data from Maka and Cork did not improve the relationship ($R^2=0.42$). The strong relation between light input and electron movement (Figure 4.24) may have been due to the fact that only one area of the GSB metabolism, the PRC, was being examined. Whereas, the weak relation between electron movement and growth may have occurred because growth involves the *whole* metabolism of the bacteria. For example, considering only the electron transfer from sulfide ignores the metabolic contribution of cyclic photophosphorylation.

5.4 Empirical Model

This model is based on the relationships described in Section 4.2 and provides a way to determine the volume and light requirements of a once-through bioreactor, given the flowrate and [$S^=$] in the wastewater stream. For purposes of illustration, the design of a
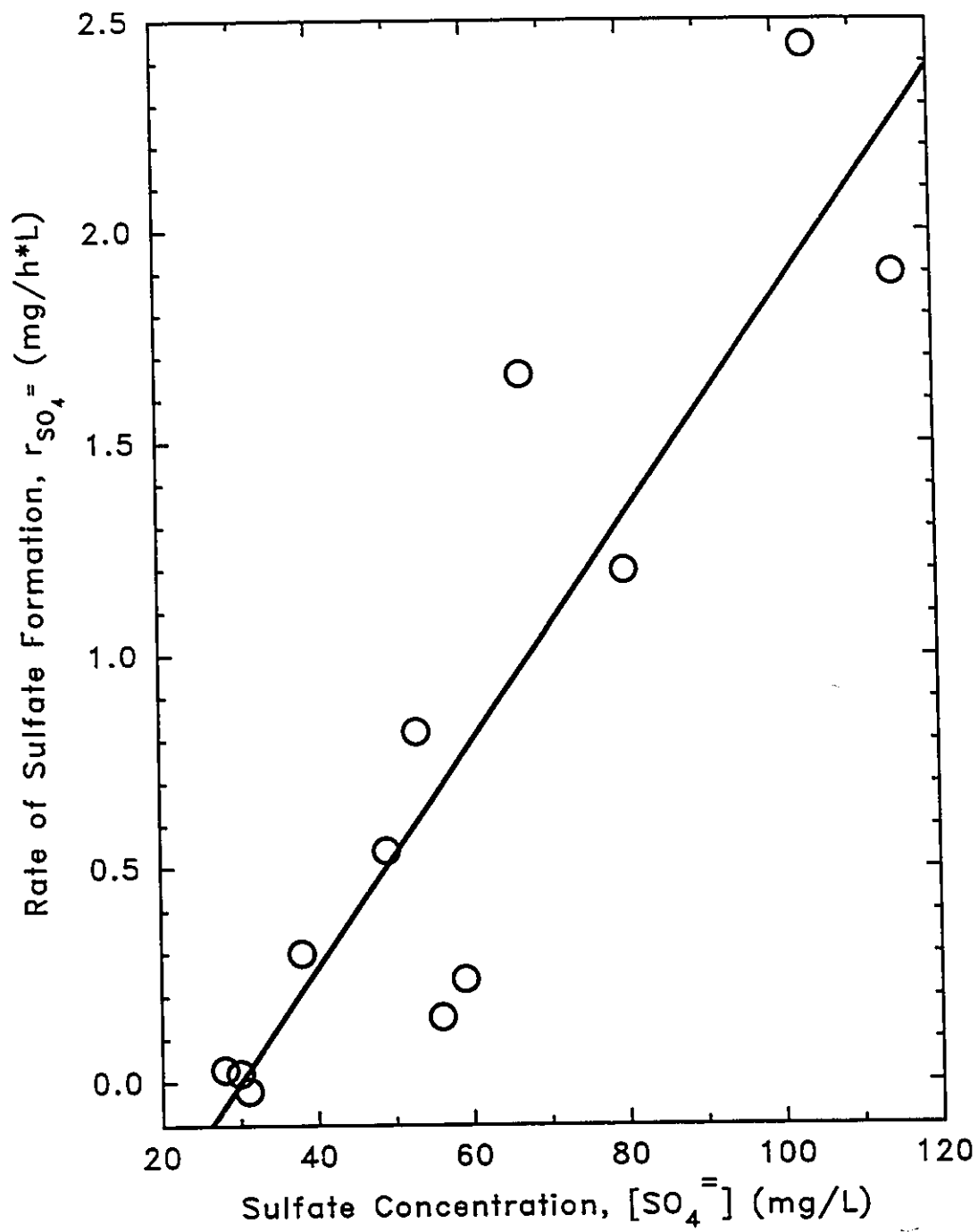
FIGURE 5.7 The rate of sulfate formation as a function of sulfate concentration

125

pilot bioreactor to treat 10 L/s of wastewater containing 80 mg $S^=$/L is worked through, with sample calculations in parentheses { }.

The steps are as follows:

1) An initial assumption of the reactor volume, V_1, is made. $\{V_1 = 1200 \text{ m}^3\}$

2) The HRT_1 is calculated (Equation 4-10).

   $\{HRT_1 = V_1/Q = (1200 \text{ m}^3)/(10 \text{ L/s}) = (1200 \text{ m}^3)/(36 \text{ m}^3/h) = 33.3 \text{ h}\}$

3) The reactor sulfide loading is calculated (Equation 4-11).

   $\{S^= \text{ loading} = [S^=]_i/HRT_1 = (80 \text{ mg/L})/(33.3 \text{ h}) = 2.4 \text{ mg/h·L}\}$

4) The rate of sulfide consumption is assumed to be equal to the sulfide loading. This assumption is valid when the $S^=$ loading rate is less than 5.0 mg/h·L (Figure 4.16).

   $\{r_{S^=} = 2.4 \text{ mg/h·L}\}$

5) Further, it is assumed that the desired end-product is elemental sulfur and that the rate of S^0 formation is equal to the rate of $S^=$ consumption. $\{r_{S_0} = 2.4 \text{ mg/h·L}\}$

6) The relation between the rate of S^0 formation and the concentration of S^0 at steady state (Equation 4-21) is used to calculate the latter concentration.

   $\{[S^0] = r_{S_0}(HRT_1) = (2.4 \text{ mg/h·L})(33.3 \text{ h}) = 80 \text{ mg } S^0/L\}$

7) The specific growth rate, μ, is determined from the S^0 concentration as in Figure 4.19. $\{[S^0] = 80 \text{ mg } S^0/L \rightarrow 1/\mu = 32 \text{ h}\}$

8) The HRT_2 is calculated as the inverse of μ (Equation 4-27). $\{HRT_2 = 32 \text{ h}\}$

9) The reactor volume, V_2, is calculated from the HRT_2.

   $\{V_2 = HRT_2 \cdot Q = (32 \text{ h})(36 \text{ m}^3/h) = 1152 \text{ m}^3\}$

10) The V_2 is compared to V_1. An adjustment is made to the volume and steps 2 to 10

are repeated until $V_1 \approx V_2$. $\{1152 \text{ m}^3 \approx 1200 \text{ m}^3\}$

11) Once the reactor volume is established, the most recent calculation of the $S^=$ loading is used to find the (radiant flux x bchl)/volume parameter via Figure 4.21 or Figure 4.22. $\{S^= \text{ loading} = 2.4 \text{ mg/l} \cdot \text{h} \rightarrow \text{radiant flux} \cdot [\text{bchl}]/\text{volume} = 2.4 \text{ W} \cdot \text{mg/L}^2\}$

12) Similarly, the radiant flux/volume is determined graphically from the rate of electron transfer and Figure 4.23. The rate of electron transfer is calculated by dividing the rate of $S^=$ consumption (mg/h·L) by 32 mg/mmole and by 2 electrons per $S^= \rightarrow S^0$ conversion. $\{$rate of e^- transfer $= 2(r_{s=}/32) = 2(2.4 \text{ mg } S^=/\text{h} \cdot \text{L})/32 = 0.15 \text{ mmole } e^-$ /h·L $\rightarrow$ radiant flux/volume $= 0.3 \text{ W/L}\}$

13) The bchl concentration is calculated by dividing the result of step 11 by the result of step 12. $\{[\text{bchl}] = (2.4 \text{ W} \cdot \text{mg/L}^2)/(0.3 \text{ W/L}) = 8.0 \text{ mg/L}\}$

14) The radiant flux is calculated by multiplying the result of step 12 by the volume determined in step 10. $\{$radiant flux $= (0.3 \text{ W/L})(1200 \text{ m}^3) = 3.6 \times 10^5 \text{ W}\}$

As with all empirical models, this model is limited to applications where the parameters are within the bounds of experience. In other words, its ability to predict values outside those determined in this dissertation is questionable. However, it may be used in conjunction with other models to design an experiment to increase the envelope of understanding of this bioreactor.

127

CHAPTER SIX

CONCLUSIONS AND RECOMMENDATIONS

For the mystical alchemists, the art involved both a chemical process and a spiritual process, both the turning of lead into gold and the transmutation of the alchemist from a state of 'leaden' earthly impurity to one of 'golden' spiritual perfection.

Biedermann (1983)

6.1 Conclusions

The production of elemental sulfur from dissolved sulfide in the liquid input to a continuous-flow once-through reactor has been demonstrated. Under proper conditions, 100% of the $S^=$ removed was converted to S^0. However, this conversion rate occurred in Trials 9 and 10 where there was $S^=$ in the reactor effluent. Typically, 90% of the sulfide can be converted to elemental sulfur if zero sulfide in the effluent is desired (Run 4).

The maximum sustainable sulfide loading rate in this study was 5 mg/h·L as compared to reported values of 100 to 1000 mg/h·L (Buisman *et al.*) and 30 to 100 mg/h·L (Cork *et al.*). The loading rates in this dissertation were lower due to limitations on the light intensity (light/volume) that could be achieved by this apparatus. The loading rate is a function of the concentration and flowrate of the reactor influent. For example, sour water stripper effluent with a sulfide concentration of 80 $mgS^=/L$ would require an HRT of 16 hours if the reactor were operated at the maximum loading of 5 mg/h·L. The size of the reactor(s) to treat this effluent would be proportional to the flowrate of the wastewater. In addition, the radiant flux incident upon the reactor windows would have to be increased to maintain the required light intensity. It may be necessary to provide several units in series/parallel to satisfy the requirement for volume and light.

Generally, the values of the yield coefficient, in terms of biomass produced per unit of sulfide consumed, compared favourably with other photosynthetic reactors and anaerobic bioreactors. In this study, poor correlation was found between reaction rates and sulfur species concentrations. However, strong relationships were found between the light entering the reactor and the rate of electron transfer by the bacteria. The fundamental concept of the van Niel curve, wherein there is a relationship between the capacity of the bioreactor to consume sulfide and the sulfide loading rate, was verified. This study has shown that the capacity of the reactor to consume sulfide is a function of the radiant flux incident upon the reactor surface, the bacteria concentration, and the volume of the reactor.

6.2 Recommendations

1. The analytical methods used in this dissertation were found to be adequate. However, the uncertainties associated with the assays could be reduced.

2. The light/volume ratio for the reactor used in this dissertation is extremely low. Further research should be conducted with a more light intensive reactor design.

3. The lack of a simple method of separating elemental sulfur from the reactor effluent will limit the use of this bioreactor system. To this end, tests have been conducted using the contents of batch bioreactors. These results should be verified using the effluent of the continuous-flow reactor.

4. Experiments should be conducted to determine the best method of concentrating the biomass in the bioreactor effluent in order to recirculate it back into the reactor.

5. The possibility of using a fixed-film photobioreactor should be re-examined.

REFERENCES

APHA, AWWA, & WEF (1992). Standard Methods for the Examination of Water and Wastewater (18th ed.). Washington: American Public Health Assoc.

Anderson, J.W. (1978). Sulfur in Biology. London: Edward Arnold (Publishers) Limited.

Ass, G.Y., Shpiner, B.S., Pen, E.Z., Fed'kushov, Y.I., & Shablevich, S.I. (1983). Removing hydrogen sulfide from wastewater from mineral water baths by biochemical methods. Sov. J. Water Chem. Technol., 5, 102-107.

Biedermann, H. (1983). Alchemy. In Richard Cavendish (Ed.), Man, Myth and Magic: the Illustrated Encyclopedia of Mythology, Religion, and the Unknown (pp. 93-99). New York: Marshall Cavendish.

Brune, D.C. (1989). Sulfur oxidation by phototrophic bacteria. Biochem. Biophys. Acta, 975, 189-221.

Buisman, C.J.N., Geraats, B.G., Ijspeert, P., & Lettinga, G. (1990a). Optimization of sulphur production in a biotechnological sulphide-removing reactor. Biotechnol. Bioeng., 35, 50-56.

Buisman, C.J., Wit, B., & Lettinga, G. (1990b). Biotechnological sulphide removal in three polyurethane carrier reactors: stirred reactor, biorotor reactor and upflow reactor. Wat. Res., 24 (2), 245-251.

Cadena, F., & Peters, R.W. (1988). Evaluation of chemical oxidizers for hydrogen sulfide control. J. WPCF, 60 (7), 1259-1263.

Chen, K.Y. (1974). Chemistry of sulfur species and their removal from water supply. In A.J. Rubin (Ed.), Chemistry of Water Supply, Treatment, and Distribution (pp. 109-135). Ann Arbor, Mich.: Ann Arbor Science Publishers, Inc.

Cohen, J.M., & Cohen, M.J. (1980). The Penguin Book of Modern Quotations. New York: Penguin Books.

Cork, D.J. (1978). Kinetics of sulfate conversion to elemental sulfur by a bacterial mutualism: a hydrometallurgical application. Ph.D. Dissertation, Univ. Arizona, 127 p.

Cork, D.J. (1984a). microbial conversion of gypsum to sulfur. Belgian Patent BE 897,493.

Cork, D.J. (1984b). Computerized control of photoautotrophic biocatalysis: industrial implications. In R.L. Crawford, & R.S. Hanson (Eds.), Microb. Growth C1 Compd., Proc. Int. Symp. (pp. 306-311). Washington: Amer. Soc. for Microbiology.

Cork, D.J. (1987). Photosynthetic bioconversion sulfur removal. U.S. Patent 4,666,852.

Cork, D., Mathers, J., Maka, A., & Smak, A. (1985). Control of oxidative sulfur metabolism of Chlorobium limicola forma thiosulfatophilum. Appl. Environ. Microbiol, 49, 269-272.

Cork, D.J., Jerger, D.E., & Maka, A. (1986). Biocatalytic production of sulfur from process waste streams. Biotechnol. Bioeng., 16, 149-162.

CRC (1979). In R.C. Weast (Ed.), CRC Handbook of Chemistry and Physics (pp. F90-F132). Boca Raton, Fla.: CRC Press, Inc.

Dantas, B.J. (1992). Elemental sulfur and biomass separation by centrifugation and filtration. Report Submitted to the Dept. of Civil & Environmental Engineering, Univ. Windsor, 45 p.

Diemer, D. (1991). Separation of elemental sulfur from biomass by settling. Report Submitted to the Dept. of Civil & Environmental Engineering, Univ. Windsor, 62 p.

Fogler, H.S. (1986). Elements of Chemical Reactor Engineering. Englewood Cliffs, N.J.: Prentice Hall.

Gulens, J., Herrington, H.D., Thorpe, J.W., Mainprize, G., Cooke, M.G., Dal Bello, P., & MacDougall, S. (1982). Comparison of sulfide-selective electrode and gas-stripping monitors for hydrogen sulfide in effluents. Anal. Chim. Acta, 138, 55-63.

Gaudy, F. A., & Gaudy, E. T. (1980). Microbiology for Environmental Scientists and Engineers. Toronto: McGraw-Hill Book Company.

Hamilton (1992). Hamilton HPLC Application Catalogue. Reno, Nevada: Hamilton Co.

Henshaw, P.F. (1990). Biological removal of hydrogen sulfide from refinery wastewater and conversion to elemental sulfur. M.A.Sc. Thesis, Univ. Windsor, 142 p.

Henshaw, P.F., Bewtra, J.K., Biswas, N., & Franklin, M. (1991). Biological removal of hydrogen sulfide from refinery wastewater and conversion to elemental sulfur. Proc. Can. Soc. Civil Eng. Conf.,May 29-31, 1991, Vancouver, B.C., IV, 287-296.

Kakidas, L.B. (1982). Bioconversion of hydrogen sulfide and carbon dioxide to starch by Chlorobium limicola forma thiosulfatophilum. M.Sc. Thesis, Illinois Inst. Tech., 87 p.

131

Kim, B.W., & Chang, H.N. (1991). Removal of hydrogen sulfide by chorobium thiosulfatophilum in immobilized-cell and sulfur-settling free-cell recycle reactors. Biotechnol. Prog., **7**, 495-500.

Kim, B.W., Kim, E.H., & Chang, H.N. (1991). Application of light emitting diodes as a light source to a photosynthetic culture of Chlorobium thiosulfatophilum. Biotechnol. Tech., **5** (5), 343-348.

Kim, B.W., Chang, H.N., Kim, I.K., & Lee, K.S. (1992). Growth kinetics of the photosynthetic bacterium Chlorobium thiosulfatophilum in a fed-batch reactor. Biotechnol. Bioeng., **40**, 583-592.

Kim, B.W., Kim, E.H., Lee, S.C., & Chang, H.N. (1993). Model-based control of feed rate and illuminance in a photosynthetic fed-batch reactor for H2S removal. Bioproc. Eng., **8**, 263-269.

Kobayashi, H.A., Stenstrom, M., & Mah, R.A. (1983). Use of photosynthetic bacteria for hydrogen sulfide removal from anaerobic waste treatment effluent. Wat. Res., **17**, 579-587.

Lauren, D.R., & Watkinson, J.H. (1985). Elemental sulfur analysis using HPLC om 10um rigid polymer particles. J. Chrom., **348**, 317.

Lizama, H.M., & Sankey, B.M. (1993). Conversion of hydrogen sulfide by acidophilic bacteria. Appl. Microb. Biotech., **39**, 276.

Losier, L. (1990). Environmental Status Report of the Canadian Petroleum Refinery Industry. Ottawa: Supply and Services Canada.

Ly, Y.P. (1990). Separation of elemental sulfur from biomass. Report Submitted to the Dept. of Civil & Environmental Engineering, Univ. Windsor, 88 p.

Madigan, M.T. (1988). Microbiology, physiology and ecology of phototrophic bacteria. In A.J.B. Zehnder (Ed.), Biology of Anaerobic Microorganisms (pp. 39-111). Toronto: John Wiley & Sons.

Madigan, M.T., & Brock, T.D. (1988). Biology of Microorganisms (5th ed.). Englewood Cliffs, N.J.: Prentice-Hall.

Maka, A. (1986). Control of oxidative sulfur metabolism in Chlorobium. Ph.D. Dissertation, Illinois Inst. Tech., 155 p.

Maka, A., & Cork, D. (1990). Quantum efficiency requirements for an anaerobic photobioreactor. J. Ind. Micro., **5**, 337-354.

Maree, J.P., & Strydom, W.F. (1985). Biological sulphate removal in an upflow packed bed reactor. Wat. Res., 19, 1101-1106.

Maree, J.P., & Strydom, W.F. (1987). Biological sulphate removal from industrial effluent in an upflow packed bed reactor. Wat. Res., 21, 141-146.

Maree, J.P., Gerber, A., & Strydom, W.F. (1986). A biological process for sulfate removal from industrial effluents. Water SA, 12, 139-144.

Maree, J.P., & Hill, E. (1989). Biological removal of sulfate from industrial effluents and concommitent production of sulfur. Wat. Sci. Tech., 21, 265.

Mathers, J.J., & Cork, D.J. (1985). Microcomputer-based gas control schemes for investigating sulfur oxidation of Chlorobium limicola forma thiosulfatophilum. Dev. Ind. Microbiol., 26, 581-585.

Metcalf and Eddy, Inc. (1991). Wastewater Engineering. Toronto: McGraw-Hill Publ. Co.

MOE (1987). Environmental Contaminants in Petroleum Refinery Wastewaters: An Assessment of Current Information and a Monitoring Approach. Toronto: Ontario Ministry of the Environment.

MOE, Water Resources Branch (1992). Background Document on the Development of the Draft Petroleum Refining Sector Effluent Limits Regulation. Toronto: Ontario Ministry of the Environment.

MOEE (1994). Ontario Drinking Water Objectives. Toronto: Ontario Ministry of the Environment and Energy.

MSDS (1988). Material Safety Data Sheet for Sodium Sulfide (ACS 852). Toronto: BDH Inc.

Neave, B., & LaRiviere, D. (1993). Dissolved gas floatation to separate sulfur from biomass. Report Submitted to the Dept. of Civil & Environmental Engineering, Univ. Windsor, 47 p.

Nemerov, N.L. (1978). Industrial Water Polution: Origins, Characteristics and Treatment. Don Mills: Addison-Wesley Publ. Co.

Ravishankar, B.R., Blais, J.F., & Tyagi, R.D. (1992). Bioleaching of metals from sewage sludge: elemental sulfur recovery. J. Env. Eng., 120 (2), 462-470.

Roy, A.B., & Trudinger, P.A. (1970). The Biochemistry of Inorganic Compounds of Sulphur. Cambridge: University Printing House.

Rozek, B., Marchewczyk, E., Kuhny, A., & Konopka, E. (1978). Microbiological degradation of hydrogen sulfide from industrial water in sulfur mines. Polish Patent 98,513.

Salkinoja-Salonen, M.S., Hakulinen, R., Silakoski, L., Apajalahti, J., Backstrom, V., & Nurmiaho-Lassila, E.L. (1985). Fluidized bed technology in the anaerobic treatment of forest industry wastewaters. Wat. Sci. Tech., 17, 77-88.

SCC (1988). Water 2020: Sustainable Use for Water in the 21st Century. Ottawa: Science Council of Canada.

Sittig, M. (1978). Petroleum Refining Industry : Energy Saving and Environmental Control. Park Ridge, N.J.: Noyes Data Corp.

Stanier, R.Y., Ingraham, J.L., Wheelis, M.L., & Painter, P.R. (1986). The Microbial World (5th ed.). Englewood Cliffs, N.J.: Prentice-Hall.

Sublette, K.L. (1987). Aerobic oxidation of hydrogen sulfide by thiobacillus denitrificans. Biotechnol. Bioeng., 29, 690-695.

Sublette, K.L., & Sylvester, N.D. (1987a). Oxidation of hydrogen sulfide by continuous cultures of thiobacillus denitrificans. Biotechnol. Bioeng., 29, 753-758.

Sublette, K.L., & Sylvester, N.D. (1987b). Oxidation of hydrogen sulfide by mixed cultures of thiobacillus denitrificans and heterotrophs. Biotechnol. Bioeng., 29, 759-761.

Truper, H.G., & Fischer, U. (1982). Anaerobic oxidation of sulfur compounds as electron donors for bacterial photosynthesis. In J.R. Postgate, & D.P. Kelly (Eds.), Sulphur Bacteria (pp. 529). Great Britain: Phil. Trans. R. Soc. Lond.

Truper, H.A. (1967). Orthorhombic sulfur produced by photosynthetic sulfur bacteria. Nature, 215, 435.

Truper, H.G., & Schlegel, H.G. (1964). Sulphur metabolism in thiorhodaceae 1. quantitative measurements on growing cells of chromatium okenii. Antonie van Leeuwenhoek, 30, 225-238.

West, J.R., & Duecker, W.W. (1974). Sulfuric acid and sulfur. In J.A. Kent (Ed.), Reigel's Handbook of Industrial Chemistry (7th ed.) (pp. 62-73). Toronto: Van Nostrand Reinhold Co.

APPENDIX A

DEVELOPMENT OF METHODS OF ANALYSIS

A.1 General

A.1.1 Apparatus

All absorbance measurements were made with a Pye Unicam PU8600 UV/VIS spectrophotometer using a 10 mm quartz cuvette and are reported in Optical Density units (O.D.).

An International Equipment Co. Centra-8 centrifuge with a #269 rotor was used to centrifuge samples.

A.1.2 Common Reagents

deH$_2$O is deionized water (Type I; APHA *et al.*, 1992)

dadeH$_2$O is deaerated, deionized water. This was prepared by boiling deH$_2$O water in an erlenmeyer flask for at least five minutes. The flask was then corked and cooled in a cold water bath until tepid.

A.2 Sulfide

The methylene blue method (Truper & Schlegel, 1964) is a colorimetric method of quantifying the total sulfide (S$^-$) in solution. A sulfide sample was added to zinc acetate solution to precipitate zinc sulfide. Hence, the sulfide was preserved until a slight excess of dimethyl-*p*-phenylenediamine (DPD) could be added to form leuco-methylene blue. This compound reacted with ferric ions to form methylene blue and ferrous ions. Methylene blue is visible and its concentration was measured with a spectrophotometer. A calibration curve (Figure A.1) was generated using a sulfide solution, standardized by

135
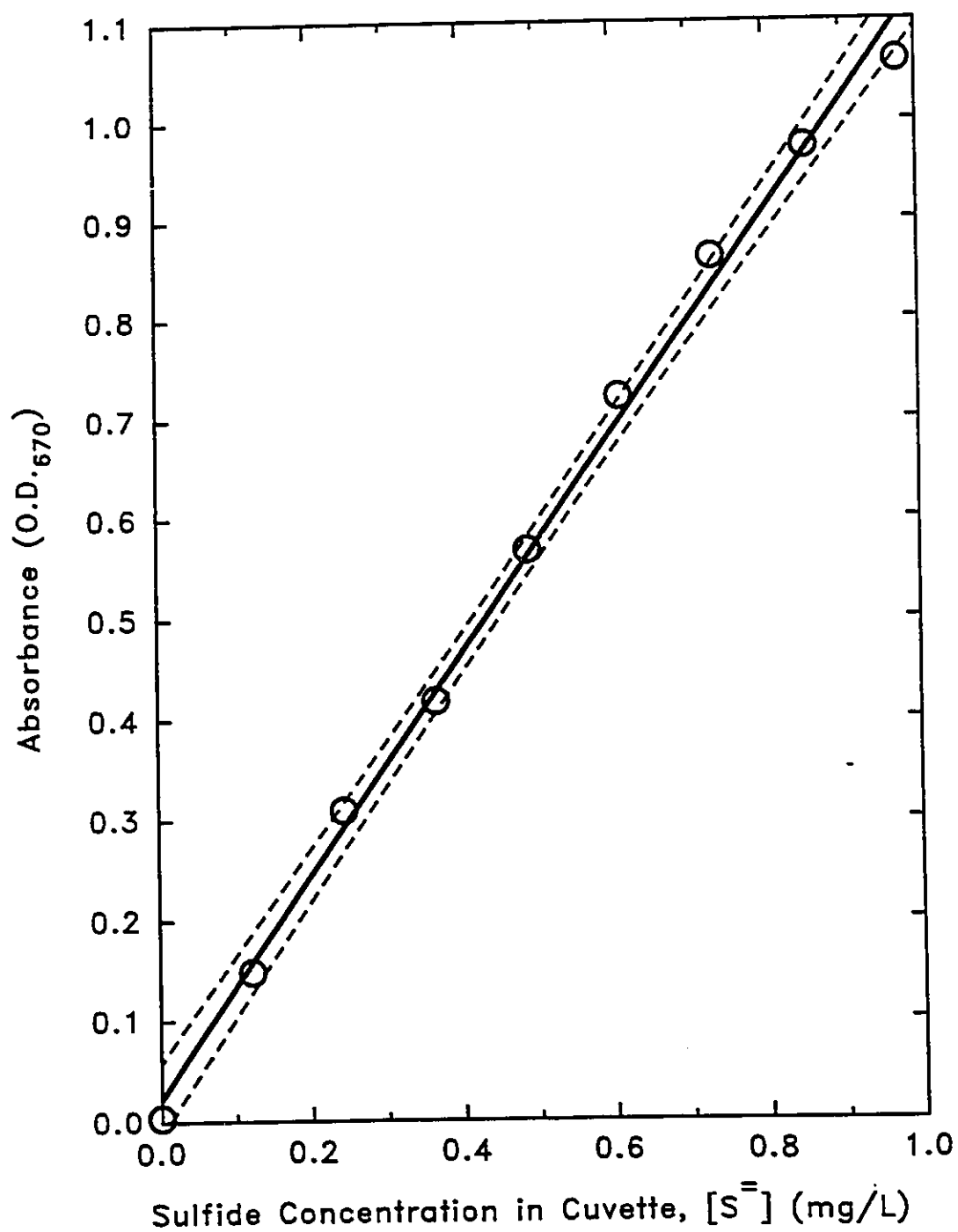
FIGURE A.1 Calibration curve for the methylene blue method of sulfide analysis

methods described previously (Henshaw, 1990). The uncertainty in sulfide concentration was calculated by taking the difference in concentrations corresponding to the two 95% confidence limits at a response of 0 and dividing by two.

A.3 Elemental Sulfur

There is no standard method for measuring elemental sulfur in water. The aqueous elemental sulfur produced in the bioreactor, at concentrations approximately one million times the solubility, was in suspension and had to be extracted into an organic solvent prior to quantification.

An elemental sulfur assay has been reported in which the aqueous sample was diluted 1:2 (Cork, 1978) or 1:40 (Maka, 1986) with 95% ethanol, extracted for two hours, centrifuged and the optical density measured at 264 nm. Unfortunately, sulfide in the sample reacts with elemental sulfur to form polysulfides (S_x^-) which shift the absorbance to 285-290 nm (Chen, 1974). Only 14% of the expected S^0 was recovered from samples containing 41 to 69 mg S^-/L (Henshaw, 1990). The addition of acid during refluxing, to shift the sulfide equilibrium to H_2S so that it may volatilize, resulted in recoveries of 130 to 138%. Because of this variable recovery, another assay was sought for elemental sulfur in aqueous suspensions.

Methods for measuring elemental sulfur (S^0) dissolved in organic liquids include colorimetry (Bartlett & Skoog, 1954) and the use of high-performance liquid chromatography (HPLC; Lauren & Watkinson, 1985).

In the colorimetric method of Bartlett and Skoog (1954), the S^0 sample dissolved in petroleum ether is converted to thiocyanate. The CSN^- thus formed reduces Fe^{3+} to

137

Fe^{2+} which is measured colorimetrically. This method was adapted to measure aqueous S^0 samples by stirring the sample, aqueous Hg^{2+} solution and petroleum ether together for sufficient time to allow the S^0 to partition into the organic phase (Henshaw, 1990). A portion of the petroleum ether layer was then carried through the above-described method.

Lauren and Watkinson (1985) performed elemental sulfur analysis using several HPLC columns. Of special interest was the use of a C_{18} reversed-phase column with methanol as the mobile phase for elemental sulfur samples dissolved in chloroform ($CHCl_3$). The HPLC method was adapted for quantifying aqueous sulfur dispersions (as found in bioreactors) by shaking the aqueous sample with chloroform to extract the S^0 into the organic phase. A portion of the $CHCl_3$ layer was then mixed with methanol in the injection vial prior to HPLC analysis.

A.3.1 Apparatus

HPLC equipment included Waters: 501 Solvent Delivery System, Intelligent Sample Processor (WISP) Model 712, Nova-Pak C18 column (3.9x150 mm), 486 Tunable Absorbance Detector, System Interface Module, and Maxima 820 software. The guard column was a Zorbak ODS (4.0x12.5 mm). The eluent was methanol (Baker HPLC grade) at 1.0 mL/min. The eluent was degassed on the day of use by filtering through a 0.5 µm pore Millipore FH filter.

A.3.2 Reagents

The four matrices tested were deH_2O, 305 mg $S^=$/L, 148 mg $S^=$/L, and the bioreactor contents.

Sulfide Matrices: Sodium sulfide nonahydrate ($Na_2S \cdot 9H_2O$; Fisher ACS grade)

crystals were rinsed in deH$_2$O, patted dry with a paper towel, weighed and then transferred to a volumetric flask. The bulk of the flask was filled with dadeH$_2$O and deH$_2$O was used to adjust the liquid level to the mark. The methylene blue method of Section 3.1.1 was used to determine the sulfide content of this stock on the day of use.

Sulfur Colloid: Approximately 200 mg of elemental sulfur (Aldrich 99.999%) was weighed and refluxed in 150 mL of 95% ethanol for one hour. The ethanol was poured hot into a 1 L volumetric flask and made up with the matrix.

Matrix/Ethanol Solution: A 15% v/v solution of 95% ethanol in matrix was prepared.

Dilute Sulfur Colloid: The sulfur colloid was diluted 1:499 with matrix/ethanol solution.

Bioreactor Contents: *C. thio.* was grown in a semi-batch reactor (Henshaw, 1990) which was fed sulfide eight days prior to use.

Dissolved Sulfur Standards: To 35 mL of CHCl$_3$ (Aldrich HPLC grade), 260.1 mg of elemental sulfur (Aldrich 99.999%) was added and refluxed for 2 hours. The mixture was made up to 50 mL with HPLC CHCl$_3$. This stock solution was serially diluted 3/25, 5/25 and 5/25.

A.3.3 Procedure

The sample was added to a screw-capped culture tube (Pyrex, no.99447, 16x125 mm) containing 2.00 mL of chloroform (Aldrich HPLC grade), 0.500 mL of 10% (v/v) nitric acid and shaken with a Burrell Wrist Action Shaker (Model 75) for 15 minutes. The sample consisted of 5.00 mL of dilute sulfur colloid or a combination of sulfur

colloid and matrix/ethanol solution totalling 5.00 mL. The tube was centrifuged at 3000 rpm (2000 gravities). One millilitre of the $CHCl_3$ layer was pipetted into a WISP vial containing 3.00 mL methanol (Baker HPLC grade). The standards were prepared by adding 1.00 mL of each to 3.00 mL of HPLC methanol in a WISP vial. The WISP vials were inverted to mix, and mounted in the WISP for injection. The run time for all injections was 5 minutes.

A.3.4 Calibration

A statistical analysis of the data from various matrices (Table A.1) indicates that the HPLC method is a precise method, with the median coefficient of variation being 1.5%. In terms of accuracy, the F test was used to compare the congruence of the line-of-best-fit in each matrix to the line-of-best-fit for the standards (no extraction). This statistical analysis reveals that the results in only two matrices (146 mg $S^=$/L and all results combined) are sufficiently close to that of the standards to be considered the same line (Figure A.2). The matrices with deH_2O and reactor contents yielded F values greater than the 99% F statistic and thus could not be considered co-linear with the line of best fit through the standards. Unfortunately, the small variation of response in a given matrix did not allow the regression lines in different matrices to be considered the same. In practice, the calibration curve used depended on the matrix. For solutions containing no reactor contents, the detector response depended on the sulfide concentration and was linearly interpolated between the deH_2O and 148 mg $S^=$/L, or 148 and 305 mg $S^=$/L lines. For measuring elemental sulfur in the bioreactor contents, a different calibration equation was used. The uncertainty in elemental sulfur concentration in each matrix was calculated

TABLE A.1 Statistical analysis of data from HPLC assay for elemental sulfur in various matrices.

Matrix	Data for Each Sulfur Concentration			All Data for Matrix	
None (stand-ards)	9.988 mg S^0/L	49.94 mg S^0/L	249.7 mg S^0/L	s= i= r^2=	8444.2 2537.6 0.9995
	$\bar{x}$= 85458 CV= 1.44 n= 5	$\bar{x}$= 425936 CV= 1.66 n= 5	$\bar{x}$= 2110734 CV= 1.85 n= 5		
deH$_2$O	0.4016 mg S^0/L	100.4 mg S^0/L	200.8 mg S^0/L	s= i= r^2= F*=	8254.8 1815.3 0.9999 9.56
	$\bar{x}$= 4168 CV= 20.9 n= 5	$\bar{x}$= 832519 CV= 0.581 n= 5	$\bar{x}$= 1658421 CV= 0.783 n= 5		
305 mg $S^=$/L	0.4012 mg S^0/L	100.3 mg S^0/L	200.6 mg S^0/L	s= i= r^2= F*=	8923.7 43423.5 0.9994 87.63
	$\bar{x}$= 42018 CV= 1.33 n= 5	$\bar{x}$= 948417 CV= 1.75 n= 5	$\bar{x}$= 1828545 CV= 1.47 n= 5		
Reactor Contents	0.4006 mg S^0/L	100.2 mg S^0/L	200.3 mg S^0/L	s= i= r^2= F*=	7741.0 1541.9 0.9999 129.7
	$\bar{x}$= 3642 CV= 17.5 n= 5	$\bar{x}$= 778800 CV= 0.632 n= 5	$\bar{x}$= 1551068 CV= 0.771 n= 5		
146 mg $S^=$/L	0.4014 mg S^0/L	100.4 mg S^0/L	200.7 mg S^0/L	s= i= r^2= F*=	8394.26 25879.2 0.9990 2.53
	$\bar{x}$= 32194 CV= 58.7 n= 5	$\bar{x}$= 862364 CV= 1.20 n= 5	$\bar{x}$= 1713541 CV= 2.12 n= 5		
All				s= i= r^2= F*=	8359.4 25739.6 0.9923 0.64

$\bar{x}$= mean response (μV·s), CV= coefficient of variation (%), n= number of data points, s= slope (μV·s/mg S^0/L), i= intercept (μV·s), r^2= coefficient of determination, F*= calculated F statistic value.
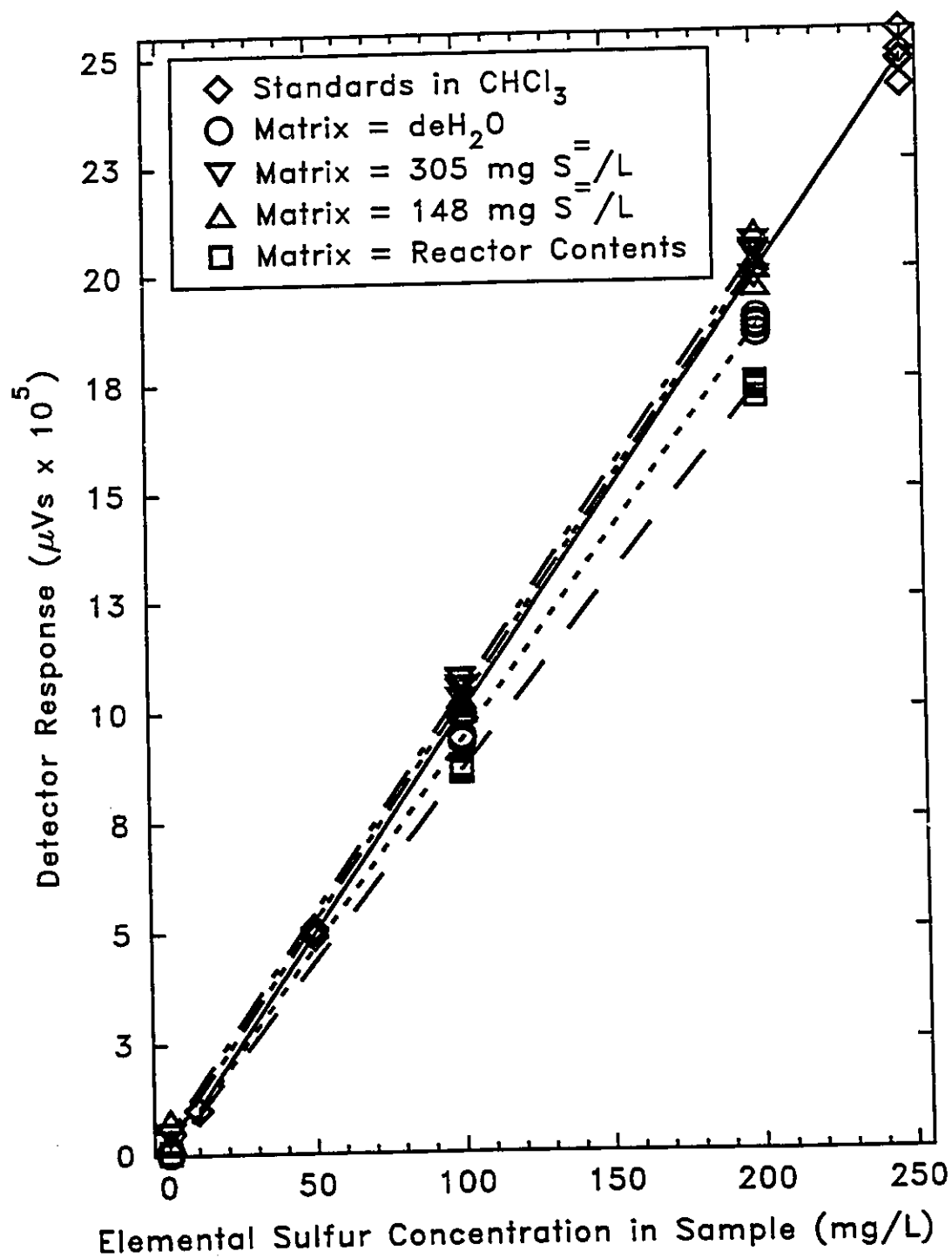
FIGURE A.2 Calibration curve for the HPLC method of elemental sulfur analysis

142

by taking the difference in concentrations corresponding to the two 95% confidence limits for that matrix at a response of 0 and dividing by two.

A.4 Sulfate

Standard Method 4500-SO_4^- E. (APHA *et al.*, 1992) describes the turbidimetric method wherein sulfate ion was precipitated in a hydrochloric acid medium with barium chloride ($BaCl_2$) so as to form barium sulfate crystals of uniform size. The turbidity of the precipitated solution was found to be linear with the concentration of the sulfate in the cuvette. Turbidity measurements were made in nephelometric turbidity units (NTU) with a Hach model 43900 Ratio/XR Turbidimeter.

Because Buffer A reacted with the sulfide and elemental sulfur in the sample, correction was made for the presence of S^- and S^0 by subtracting the turbidity of part of the sample to which $BaCl_2$ was not added (Henshaw, 1990). A calibration curve (Figure A.3) was created using a standard sodium sulfate solution.

The uncertainty in sulfate concentration was calculated by taking the difference in concentrations corresponding to the two 95% confidence limits at a response of 0 and dividing by two.

A.5 Thiosulfate

The Standard Method (APHA *et al.*, 1992) for measuring thiosulfate involves adding the sample to an iodine solution. This method was not suitable for bioreactor experiments because the iodine solution also reacts with sulfide and sulfite, which would have given a false high value for thiosulfate even when the sulfide concentration was taken into account.
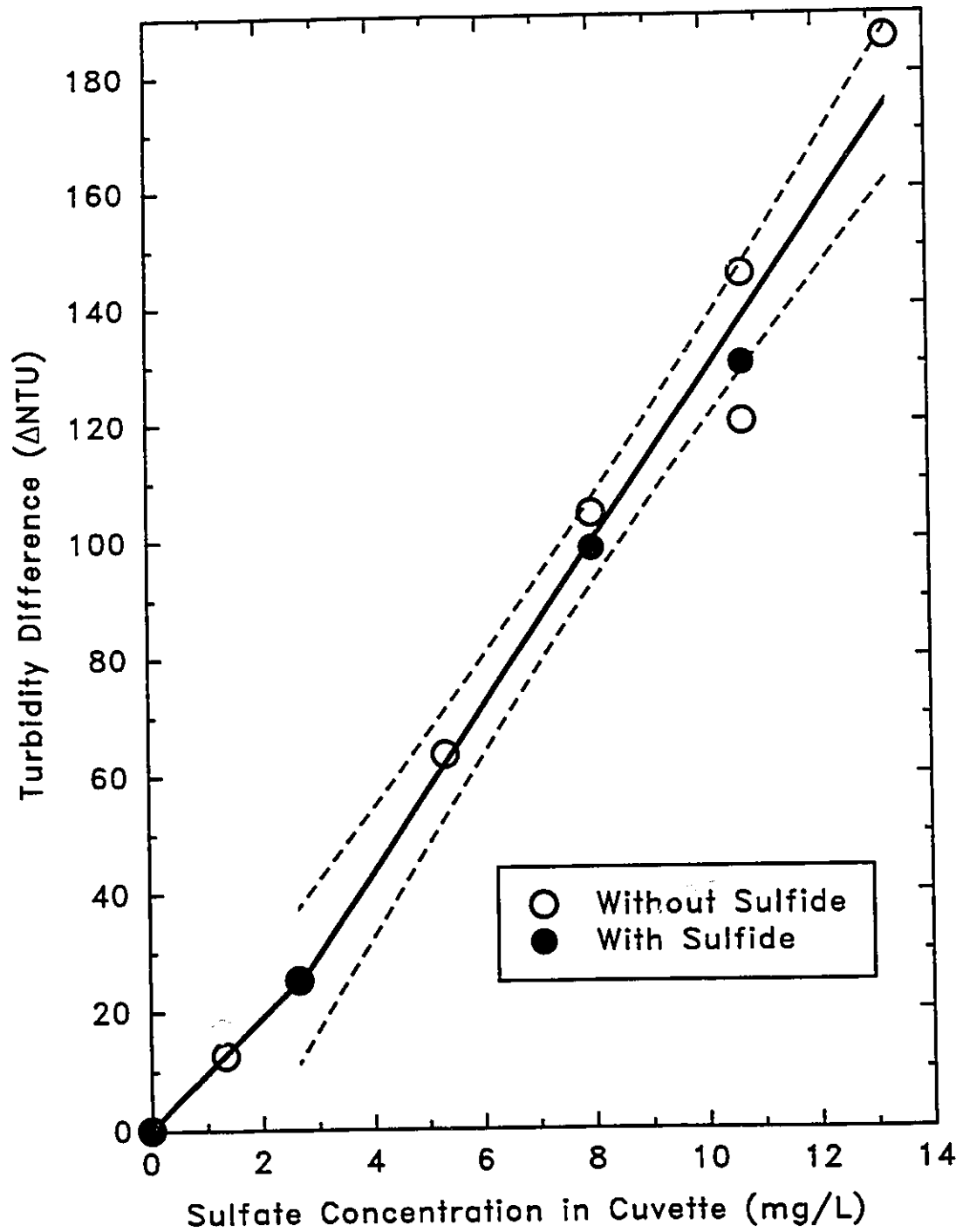
FIGURE A.3 Calibration curve for the turbidimetric method of sulfate analysis

144

The ion chromatography (IC) method for thiosulfate analysis (Hamilton, 1992) offers specificity for the analyte and low sample preparation requirements. A preliminary test was performed to determine if sulfide would interfere with the thiosulfate quantification. The procedure outlined below was used, but the eluent flow rate was 1.5 mL/min. Eight samples without S^- and 4 samples with 262 mg S^-/L were injected with concentrations of thiosulfate ranging from 0 to 142 mg $S_2O_3^-$-S/L. A plot of detector response against $S_2O_3^-$ concentration showed a linear response (correlation coefficient = 0.995) with no significant differences between those samples with and without sulfide (Figure A.4).

A.5.1 Apparatus

IC equipment included Waters: 510 HPLC Pump, Rheodyne 7161 Manual Injector, 431 Conductivity Detector, System Interface Module and Maxima 820 software. The main column was a Hamilton PRP-X100 column (4.1x150 mm), and the guard column was a Zorbak ODS (4.0x12.5 mm). The eluent was 4mM p-hydroxybenzoic acid (see Section A.5.2) at 2.0 mL/min.

A.5.2 Reagents

p-hydroxybenzoic acid: A stock solution of 4.4198 g of p-hydroxybenzoic acid (BDH) in 200 mL methanol (Baker HPLC grade) was prepared. Twenty-five millilitres of this stock solution was pipetted into a calibrated 1 L plastic bottle and made up to the mark with Milli-Q water (resistivity >18 MΩ·cm). On the day of use, the eluent was degassed by filtration through a 0.45 μm pore Millipore HA filter and the pH was adjusted to 8.5 using 1 M NaOH made up in Milli-Q water. The baseline conductivity
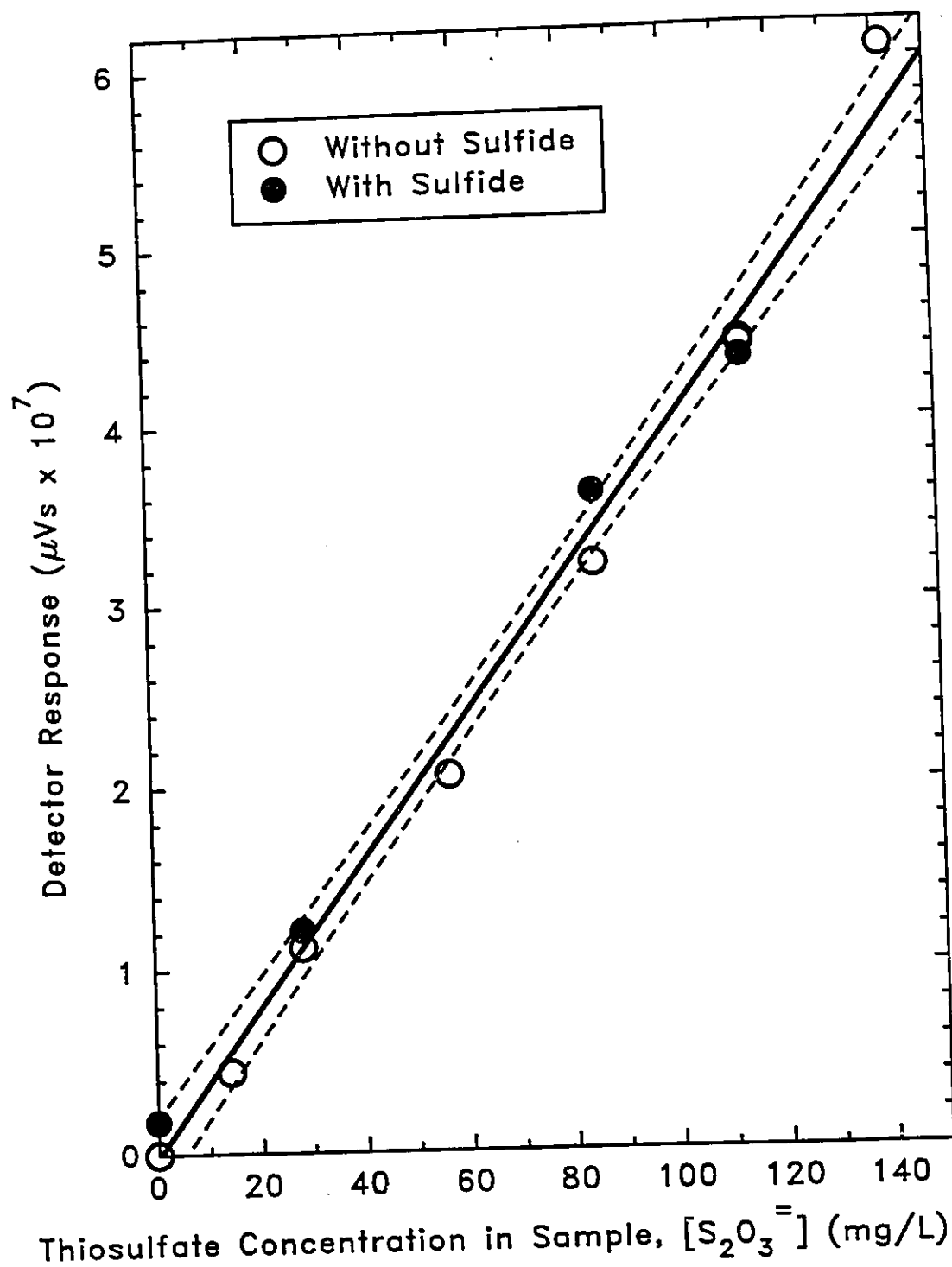
FIGURE A.4 Calibration curve for the IC method of thiosulfate analysis

146

of this eluent was 320-340 µS.

Thiosulfate Standard: On the day of use, $Na_2S_2O_3 \cdot 5H_2O$ (Fisher ACS grade) or anhydrous $Na_2S_2O_3$ (BDH) was weighed and transferred to a 500 mL volumetric flask and made up to the mark with deH_2O. The concentration of the thiosulfate was 145 to 185 mg $S_2O_3^-$-S/L. There were also two standards of 1155 and 585 mg $S_2O_3^-$-S/L.

A.5.3 Procedure

Standards were made each day that thiosulfate was measured in the reactor for Trials 9 and 10. Prior to injecting the reactor samples, standards were injected full strength, 2/5 and/or 1/5 strength into the equilibrated IC apparatus. The run time was 30 minutes.

A.5.4 Calibration

Response was a linear function of concentration from 0 to 1155 mg $S_2O_3^-$-S/L. Twenty out of twenty-two calibration points were at concentrations less than 200 mg $S_2O_3^-$-S/L, and this range of data was used in calculating the response/concentration function (Figure A.4). From this plot, it can be seen that the standards made with $Na_2S_2O_3 \cdot 2H_2O$ and $Na_2S_2O_3$ responded similarly. The uncertainty in thiosulfate concentration was calculated by taking the difference in concentrations corresponding to the two 95% confidence limits at a response of 0 and dividing by two.

A.6 Bacteria

Kakidas (1982) has reported a linear relationship between the number of cells and the mass of bacteriochlorophyll (bchl) for *C.thio.* Therefore, the extracted bacteriochlorophyll concentration was taken as an indicator of the biomass concentration.

147

She also gave data to calculate the mass of a cell as 1.8×10^{-12} g dry mass/cell. Kim (1992) used the ratio 2.7×10^{-13} g dry mass/cell. According to Kakidas' data, about 3% of the dry mass or 0.6% of the wet mass of the cell was bchl. Kim has stated that 24% of the dry weight of the cell is protein. Neave & LaRiviere (1993) found the ratio of bchl to VSS to be 3 to 6%. This seems more realistic than the values of 17 to 24% found by this researcher. These gross measures of biomass give no indication as to the numbers or mass of *active* biomass.

In this dissertation, the procedure of Maka (1986) was used but the quantities were doubled (see Section 3.1.5). The uncertainty of this measurement has been quantified previously (Henshaw, 1990). A test of S^0 was performed by dissolving S^0 (Aldrich 99.999%) in ACS methanol to a concentration of 480 mg S^0/L. The absorbance at 670 nm was zero. Therefore, S^0 in the sample had no interference in bchl observations.

APPENDIX B

HISTORY OF REACTOR OPERATION

B.1 Purpose

The purpose of this appendix is to provide a record of the problems encountered in operating a GSB bioreactor so that the experiments detailed in this dissertation can be repeated. Also, the reasons for changes in the operation and configuration of the reactor are provided.

B.2 Prior to Run 1

In the first attempt at continuous reactor operation, the configuration was similar to that depicted in Figure 3.1 except that all inlet streams were passed through a mixing coil immediately before entering the reactor. In addition, there was no air bladder on the gas outlet of the reactor, and water was used in the reactor gas trap. The purpose of the gas trap was to prevent air from entering the reactor while allowing reactor gasses to escape.

The total flow rate was about 4.6 mL/min and the [S$^-$] in the mixed inflow was 25 to 55 mg/L. Sulfuric acid (10%) was selected as the pH adjusting chemical and this caused two problems. First, at this loading, the reactor required base instead of acid, so the reactor pH drifted downward and the pH had to be neutralized manually with NaOH. Secondly, the acid dissolved the coating (or the steel) of the weighted filter at the end of the pH controller pump tubing in the bottom of the acid reservoir. This left the reservoir black/green and the weighted filter grey. The filter was removed and a weaker acid was used in the reservoir (1% H$_2$SO$_4$). After nine days of continuous operation, the mixing

149

coil became clogged, presumably with some sulfide salts. The inlet pumps were shut down.

It was noticed that the contents of the water trap was being sucked up the gas outlet line, indicating the reactor was operating under a negative pressure relative to atmospheric. On a daily basis, the gas outlet line was "pumped down" by pressurizing the reactor with CO_2.

Subsequent to the initial trials, the bacteria were maintained in the 13 L reactor by periodically adding sulfide stock solution. The volume of samples taken from the reactor balanced the additional volume of the sulfide solution. The logic of the pH controller was reversed to pump base when the pH got below 6.8. After three days the disposable pipette being used as a CO_2 bubbler in the CNS became clogged. This probably resulted in a CO_2 gas line break which caused the water trap to be sucked into the reactor. In addition, the reactor became basic due to the lack of CO_2 in the CNS.

B.3 Run 1

The gas outlet from the reactor was closed so the reactor was operated as a pressurized vessel. Also, in this and subsequent experiments, the reactor was wrapped in a shroud with windows cut in it (Appendix C) to prevent stray light from entering the reactor. The initial shroud was made of aluminum foil. The total flow was set at about 5.6 mL/min and the reactor sulfide ranged from 20 to 80 mg/L. After 5 days, the pumps began to squeak on rotation. The technician at Cole-Palmer doubted that the problem was due to brushes (these are DC motors), and more likely due to bearings or gears. After an additional day, one pump began "hiccupping". The pump would stop as though it was

seized and then suddenly rotate with a jerking motion (the whole pump hopped). The pumps were sent in for repair, ending the experiment.

B.4 Run 2

An attempt was made to grow bacteria in a reactor filled with the CNS from failed Run 1, sulfide solution, and water but no growth resulted from inoculation. The CNS was not the problem since some GSB from a new, unopened ATCC tube seemed to grow in a culture tube using the CNS. The large reactor was drained, filled and inoculated again. Two days after inoculation the glass reactor vessel was found to be cracked. Henceforth, the reactor gas outlet valve remained open and the outlet line was connected to an air bladder. The air bladder consisted of a 1 L glass vessel with a nipple at each end. One end was connected to the gas outlet line and the other was connected to a tube which was immersed in the water trap. The purpose of the bladder was to provide a buffer for the water trap liquid being sucked up the gas outlet line so that the liquid would not reach the reactor. The reactor was pressurized daily so as to "pump" the liquid back into the water trap.

The experiment was started from scratch. The contents of another ATCC tube were used to inoculate a 1 L reactor, which in turn was used to inoculate 12.5 L of growth medium in a new reactor vessel. The aluminum shroud was found to deteriorate in the water bath, so a metallized mylar shroud was substituted. A new CNS was autoclaved and saturated with CO_2 and the inflow and outflow pumps were started. Things ran smoothly for 5 days, then the pH controller display began to flicker from 7.0 to 7.6. After another three days, sulfide began showing up in the reactor effluent. The

pH electrode/controller was found to be reading low by 0.8 pH units. An independent

measure of the reactor pH revealed it to be 7.7 while the pH controller indicated 7.0. The

pH electrode was regenerated by briefly immersing the tip in 10% HF. After calibration,

and independent measurement of the reactor solution, the pH electrode/controller was

found to be reading low only by 0.3 pH units. The tip was immersed two more times in

10% HF for 1 minute each time, then soaked in the diaphragm cleaning solution

overnight. After calibration, the electrode/controller seemed to be functioning properly.

Overnight, the reactor outlet pump had been accidentally turned off and the reactor filled

and leaked. This experiment was ended but the reactor was not drained.

B.5 Run 3

Some pumps that had been "chirping" during Run 2 were replaced with new

pumps and Run 3 was initiated with a complete set of reactor and feed measurements.

At this time, the thiosulfate test had not been developed so only $S^=$, S^0 and $SO_4^=$ were

measured. In addition, the pH electrode/controller was calibrated daily. At roughly 173

to 194 hours, the CO_2 bubbling in the CNS had stopped. This was probably due to

minerals (carbonates?) clogging the glass tube used for a bubbler, as this occurred

regularly. A "+" shaped tube was used when subsequent batches of CNS were made up

so that if one outlet became clogged, two others were available for bubbling. Sometime

after 221 hours, but before 238 hours, the sulfide solution ran out. A new solution was

immediately brought on-line so that the total time of sulfide interruption was probably

less than 20 hours. The measured sulfide concentration in the SSS was found to

fluctuate, so a magnetic stirrer was used at low speed to mix the solution in this and all

future experiments. This experiment ran successfully for 13 days.

B.6 Run 4

After measurements were taken for Run 3, a stronger sulfide solution was used for Run 4. This experiment ran successfully for 16 days. After 14 days, the reactor shroud seemed to become transparent around the windows. A temporary shroud of aluminum foil was placed on the lit side of the reactor and secured with rubber bands while the reactor was in operation.

B.7 Run 5

After measurements were taken for Run 4, a stronger sulfide solution was used for Run 5. At this sulfide loading, either the reactor was not producing acid as in Runs 3 and 4 *or* the greater concentration of $S^=$ (which was basic) in the feed was causing the pH in the reactor to rise. Consequently, the reactor needed acid to neutralize it so the controller logic was reversed six days after the start of the run. On the last day of the run, the CNS pump was calibrated and found to be operating at only 10% of its expected flowrate. From the daily volume observations, it was concluded that either the calibration was in error or the CNS pump became clogged only in the last day of operation.

After Run 5 was completed, the reactor was allowed to sit in batch mode for 8 days without liquid input or output and without pH control. Feed solutions were made as in previous runs and fed into the reactor but the bacteria did not grow.

B.8 Trial 1

Sixteen days after the end of Run 5, the 1 L batch reactor was inoculated but poor growth resulted. Typically, the inoculated reactor turned cloudy and yellow after one day.

After three to four days, the yellow gave way to a deep green colour. In Trial 1, the reactor achieved a bright yellow colour after two days and never turned to deep green. There was some grey growth at the neck of the 1 L flask. Five days later, a Gram stain of the reactor contents revealed chains of bacteria with a barred appearance (some Gram positive and some Gram negative sections).

B.9 Trial 2

The 1 L reactor was refilled and inoculated with a pure culture directly from ATCC which unfortunately had spent 6 days, in transit before it could be subcultured. After three days the 1 L reactor was cloudy yellow and the Gram stain showed chains of bacteria or filaments with a barred appearance. Contamination by filamentous bacteria was suspected but not confirmed.

It was observed that the ferrous chloride (used to make the TES) from a new source was yellow and granular as opposed to hard brown chunks which had been previously used. Although there had not been a problem in previous growth medium batches, some new $FeCl_2 \cdot 4H_2O$ was added to the 1 L reactor. This proved unable to revive the bacteria.

B.10 Trial 3

Again a 1 L reactor was prepared, but this time it was autoclaved as in the preparation of sterile culture tubes. In addition, a new TES using the new $FeCl_2 \cdot 4H_2O$ was used. After four and eight days growth was pale yellow.

B.11 Trials 4 and 5

Non-sterile 1 L reactors were inoculated without successful growth. The lack of

growth may have been due to stirring. The holder for the 1 L reactor was designed for a 300 mL reactor and as such the 1 L reactor was higher in elevation (and further from the magnetic stirrer) than the 0.3 L reactor. Stirring was adjusted but could not be maintained more than a few hours. As such the reactor was only well-stirred once a day. However, lack of stirring did not seem to adversely affect the growth of bacteria in the culture tubes. Prior to starting Trial 6, the IC method for measuring $S_2O_3^-$ was calibrated.

B.12 Trial 6

After subculturing the *C. thiosulfatophilum* for 5 months in sterile culture tubes, successful batch growth was achieved in the 1 L reactor and the 12 L reactor. In this configuration, the bicarbonate and mineral salts solutions were kept separate to avoid precipitation of carbonate salts. Carbon Dioxide and nitrogen were bubbled through the bicarbonate and mineral salts solutions respectively. Rotameters were added to all inlet streams to provide a secondary check on flowrate. However, the accuracy of the rotameters was poor and timing of pump rotations was used to set the pump flow rates. The reactor was operated with the bladder outlet tube immersed in a zinc acetate trap so as to trap any H_2S coming from the reactor. After starting the input and output pumps, the concentration of bacteria (as measured by bchl) slowly decayed to zero. It was thought that oxygen entering the reactor might be the problem, so the oxidation-reduction potential (ORP) of a sample from the reactor was measured and found to be -160 mV. This measurement was repeated after two days and found to be -300 mV, indicating anaerobic conditions. In addition, the reactor pressure was only once negative relative to atmospheric, so it was unlikely that oxygen was being sucked into the reactor.

155

B.13 Trial 7

Trial 6 was repeated, with the same results. The bearing in the reactor headplate was found to leak nitrogen under positive pressure and could be a source of oxygen if the reactor pressure was negative. The bearings were adjusted to stop leakage.

B.14 Trial 8

Trial 6 was repeated. Growth in 1 and 12 L batch reactor was good. Under continuous operation, the bacteria were maintained at a high concentration. After six days, the stirrer drive belt broke, causing the pH to drop to 6.4. Stirring resumed and the pH was brought back up to 7.0.

In all the experiments, the outlet pump was actuated by a time delay relay which was actuated by the level controller. When the reactor liquid level reached the probe, the relay circuit was actuated, and after 3 minutes, the pump ran for about 1 minute. It was thought that negative pressures in the reactor could have been caused by the outlet pump running too fast. Slowing down the pump rotational speed reduced the negative pressure in the reactor. In this trial, the "gas out" line (to the bladder) was clamped shut to eliminate another possible source of oxygen contamination.

After the stirring belt failure, the bacteria concentration slowly decreased. Some grey material was found in the tube between the mineral salts reservoir and the mineral salts pump. This material grew on a TSA plate and indicated the presence of fungus (most of which are aerobic) and aerobic bacteria. Therefore, the mineral salts solution was the source of GSB-inhibiting oxygen in spite of the fact that N_2 was being bubbled through it.

In a side experiment, bubbling nitrogen (High Purity) through 5 L of water in a jar caused the dissolved oxygen (DO) to go from 3.1 mg/L to 1.7 mg/L in 21.5 hours. On reducing the volume of water to 2 L and reducing the N_2 flow rate, the DO increased to 6.1 mg/L. It was concluded that N_2 bubbling did not adequately remove O_2 from the feed solution.

To ensure anaerobic conditions, the loading was adjusted daily to maintain a low concentration (10 to 30 mg/L) of sulfide in the reactor. Also, the feeds were reconfigured to two solutions: a nutrient medium with enough sulfide to keep it anaerobic ($\approx$100 mg $S^=$/L), and a sulfide stock solution.

B.15 Trial 9

Trial 9 was started from a 1 L batch reactor and ran for 70 days. Six days after inoculation, the sulfide loading to the reactor was increased from 1.9 to 3.5 mg/h·L in order to ensure anaerobic conditions in the reactor. At the same time, the HRT was increased from 60 to 100 hours to decrease the rate of removal of bacteria from the reactor by flushing. The logic of the pH controller was reversed after 7 days to pump acid. At nine days after inoculation, the reactor sulfide concentration was too high (38 mg/L) so the sulfide loading was decreased to 1.4 mg/h·L. The HRT was increased to 170 hours at this time. Reactor conditions stabilized, but the HRT was kept at a high value throughout the experiment, although sulfide loading was subsequently increased (Table 3.2).

Even though the concentrations of soluble and suspended substances were not very different between the top and bottom of the reactor (Appendix D), the outlet site within

the reactor was changed from the bottom of the reactor to about 50 mm below the surface of the reactor 12 days after inoculation. If there was any settling of biomass in the reactor, pumping from the top would remove less biomass than pumping out of the bottom sampling tube. As in Run 2, there were fluctuations in the pH controller readout. However, the readout was steady when the electrode was in calibration solutions. Immersing the electrode in diaphragm cleaning solution overnight seemed to have helped. These problems were worked out after 49 days.

B.16 Trial 10

Trial 10 was started from 1 and 12 L batch reactors as the biomass from Trial 9 could not be revived after 10 days. The experiment ran for 43 days, after which the upper light was unplugged. The reactor was then operated for an additional 8 days.

APPENDIX C

MEASUREMENT OF LIGHT ENTERING THE REACTOR

C.1 Materials and Methods

The top of the fermenter was substituted with a plastic ring to hold the reactor vessel in place while the fermenter was immersed in the fermenter drive assembly water bath. The sensor of an International Light IL 1700 Research Radiometer (Newburyport, MA) was positioned *inside* the empty reactor and normal to the light source at 18 locations as shown in Figure C.1. The projected area of each window in the reactor shroud was divided into 9 sub-windows of equal area. The light intensity was measured with the sensor positioned at the centre of each sub-window and the values averaged to determine the total irradiance (W/cm²). This value was multiplied by the window area to arrive at the total light energy (radiant flux) received in the reactor (W).

The sensor could detect various qualities of light depending on the filter combination used. The TFRD filter blocked light outside the range 700 to 975 nm, giving a measurement of the infrared light in W/cm². The F filter allowed the sensor to give an even response to light anywhere in the broad band of 400 to 1,000 nm. The ratio of the broad band irradiance to the infrared irradiance is constant for a given light source. In the case of the Philips IR 175 Watt R-PAR bulbs used in these experiments, the average ratio was 2.24:1. The irradiance was either measured with the F/W filters or measured with the TFDR/W filters and converted to a broad band measurement by the ratio.

C.2 Results

Tables C.1, C.2, and C.3 summarize the measurements of light irradiance.
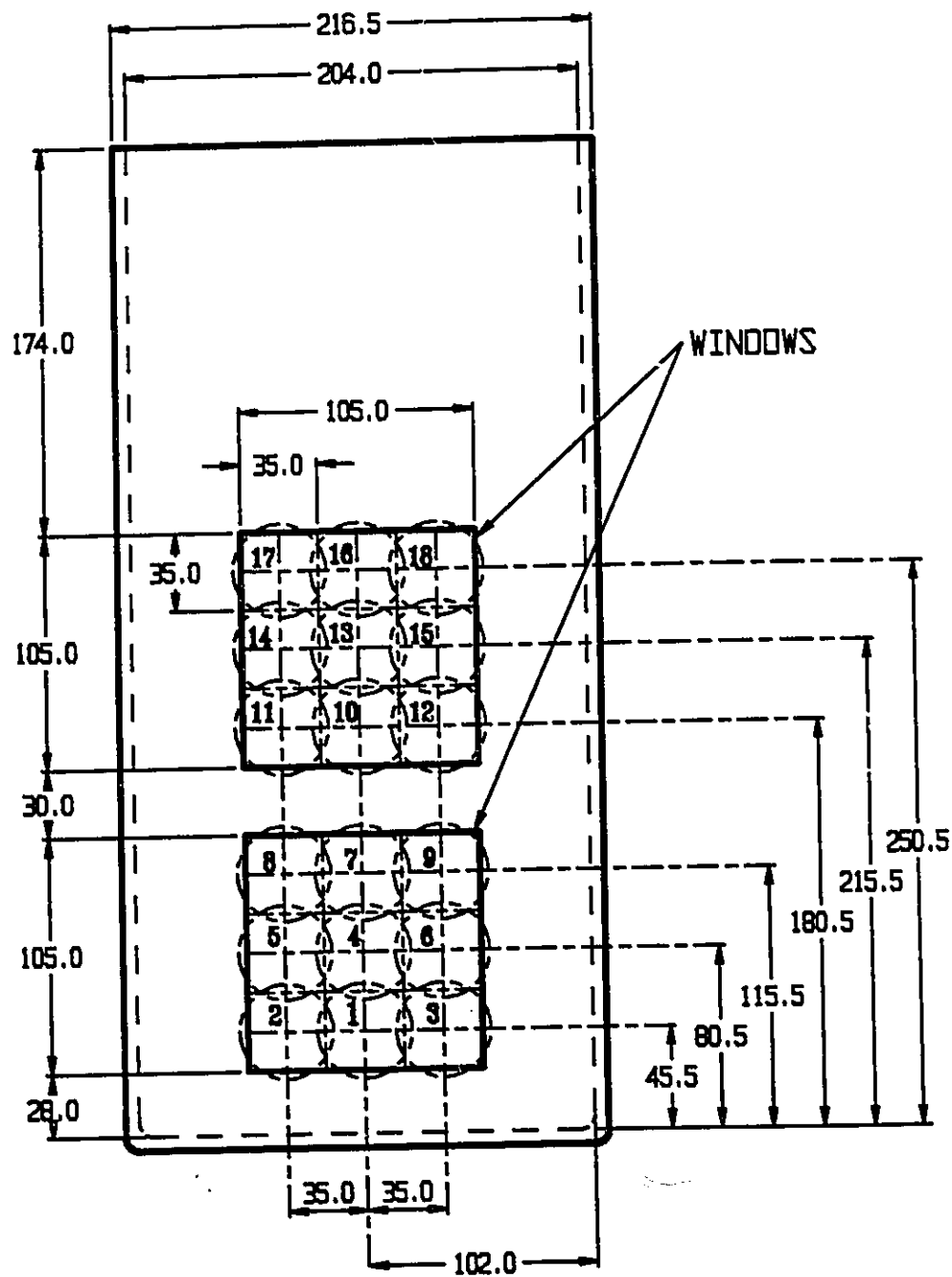
FIGURE C.1 Front view of the bioreactor showing the sensor locations (phantom circles). All dimensions are in mm.

160

TABLE C.1 Irradiance measurements with both lights ON.

Date	Infrared Irradiance (W/cm^2)	Broad Band Irradiance (W/cm^2)
Jan. 12, 1993	0.0120	0.0269*
Nov. 17, 1993	0.0115	0.0258*
Jan. 13, 1994		0.0268
Aug. 11, 1994		0.0235
Average Coeff. Variation		0.0258 6.2%

*= measured with infrared filter and converted to broad band, Coeff.Variation= coefficient of variation (standard deviation/mean).

TABLE C.2 Irradiance measurements with only lower light ON.

Date	Infrared Irradiance (W/cm^2)	Broad Band Irradiance (W/cm^2)
Jan. 12, 1993	0.00576	0.0129*
Aug. 11, 1994		0.0109
Average Coeff. Variation		0.0119 12%

*= measured with infrared filter and converted to broad band, Coeff.Variation= coefficient of variation (standard deviation/mean).

TABLE C.3 Calculation of radiant flux.

Lights ON	Broad Band Irradiance (W/cm^2)	Total Window Area (cm^2)	Radiant Flux (W)
Both	0.0258	220.5	5.69
Lower	0.0119	220.5	2.62

C.3 Factors Affecting Light Penetration into the Reactor

A brief study was undertaken to determine the factors responsible for the very low radiant flux reaching the reactor. Two 175 W bulbs had a total output of 350 W, and yet only 5.7 W were received by the reactor. Thus, only 1.6% of the energy input to the bulbs entered the reactor. One factor was that the light from the bulbs had spread out and the intensity decreased with the square of the distance between the bulb and the reactor.

The radiometer was fitted with the F/W filter combination and held in the centre of each of the reactor windows while a reading was taken. The sensor and bulb were positioned as listed in Table C.4, and readings from the top and bottom window were averaged. The irradiance was measured at only two positions and it was assumed that, had a full set of 18 measurements been taken and the radiant flux calculated, the normalized ratios would be the same.

Table C.4 shows that the reduction in radiance due to the presence of the reactor vessels and the waterbath was 67%. The remaining reduction (to 2%) was due to the factor of distance. Put another way, 4.9% of the light energy input to the bulbs would have reached the sensor if there were no vessels or water. An additional reduction to 1.6% occurred because of the reflective and refractive effects of the vessels in the water. Therefore the effect of distance was the main factor in radiant energy reduction.

162

TABLE C.4 Effects of reactor vessels and waterbath on irradiance.

No.	Configuration	Avg. of 2 Readings (W/cm^2)	Readings Normalised to No. 4
1	• bulb to sensor distance = 118.5 mm • sensor in reactor • bulb in reactor • waterbath full	0.039	33
2	• bulb to sensor distance = 118.5 mm • sensor in reactor • bulb in reactor	0.105	85
3	• bulb to sensor distance = 118.5 mm • bulb in reactor	0.102	85
4	• bulb to sensor distance = 118.5 mm	0.120	100

C.4 The Incandescent Bulb

Kim *et al.*(1991, 1992, 1993) used incandescent bulbs to irradiate their reactors and measured the illuminance in units of lux. The luminous efficacy or ratio of the illuminance to irradiance was given as 20 lux·m^2/W for this light source. The measured value of illuminance was 24,000 lux. This would convert to 1,200 W/m^2 using their conversion factor. The area of the reactor was 0.249 m^2, making the radiant flux equal to 299 W. This is an incredible efficiency considering that two 150 W bulbs were used! The calculated radiant flux from Kim *et al.*(1992) was also high.

An investigation was carried out to confirm the luminous efficacy of a local incandescent source by comparing the illuminance with the irradiance of an incandescent

light source using the radiometer sensor clamped to a retort stand. The incandescent light source was measured in lux (using the Y filter) and W/m² (using the F filter). The luminous efficacy was 49.4 lux·m²/W, over twice that reported by Kim *et al.*(1991). With this factor, the irradiance of two 150 W bulbs was still very high at 122 W, and for this reason these data do not appear on the plot of the van Niel curve (Figure 2.3).

APPENDIX D

VERIFICATION OF THE ASSUMPTION OF UNIFORMITY
IN THE REACTOR

D.1 The Assumption

The operation and analysis of results for the bioreactor, used in this research, was

based on the assumption that the reactor is completely mixed. As such, the following

assumptions for a continuous stirred-tank reactor (CSTR) were applied:

- No spatial variations in the concentration of any chemical species in the reactor;

- Concentration of any chemical at the exit point of the reactor was equal to the

   concentration within the reactor (Fogler, 1986).

D.2 Spatial Variations Within the Reactor

On two days during Trial 9, soluble and insoluble (suspended) parameters were

measured from the top and bottom of the reactor. Samples from the top of the reactor

were taken by pressurizing the reactor with N_2, opening the septum port and inserting a

25 mL wide-mouthed glass pipette to withdraw a sample at 45 mm below the liquid

surface. Samples from the bottom of the reactor were taken by pressurizing the reactor

with N_2, opening the bottom sampling tube valve, discarding first approximately 100 mL

volume, and collecting the sample from the subsequent discharge from the tube. It should

be noted that, in the reactor configuration used in Trials 9 and 10 (Figure 3.2) the bottom

sampling tube was not used for the effluent, and the nutrient medium tubing had to be

disconnected while taking these samples.

Table D.1 shows that the values of soluble parameters taken from top and bottom

were equal within the error of the measurement. The sulfur concentrations at the bottom were slightly higher than those taken from the top. The difference lies outside of the uncertainty of the measurement, but is relatively small, being only 3 to 4% of the value of the measurement. The specific gravity of sulfur is greater than unity, which would favour higher sulfur concentrations at the bottom. One would expect the bchl concentration to be higher at the bottom as well, since the bacteria are strongly associated with sulfur granules and are slightly more dense than water. Bacteriochlorophyll concentrations were equal on March 22 but the bottom bchl concentration was less on March 29. Based on these limited observations, the assumption of good mixing in the reactor is reasonable.

TABLE D.1 Comparison of measurements taken at the top and bottom of the reactor during Trial 9

Date	Soluble Parameters				Suspended Parameters			
	$S^=$ (mg/L)		$SO_4^=$ (mg/L)		S^0 (mg/L)		bchl (mg/L)	
	Top	Bot.	Top	Bot.	Top	Bot.	Top	Bot.
Mar. 22, 1994	56 ±4	56 ±4	48 ±18	55 ±18	270 ±2	280 ±2	5.4 ±0.7	5.4 ±0.7
Mar. 29, 1994	8 ±4	8 ±4	-	-	483 ±1	497 ±1	8.7 ±0.7	6.8 ±0.7

D.3 The Effect of Sampling Location

Early in Trial 9, it was noticed that chunks of green slime would intermittently emerge while sampling from the effluent sampling tube. Tests were performed to determine if the pumped reactor effluent had the same concentrations as the

reactor contents. In Trials 9 and 10, the pumped effluent was drawn from a point 45 mm below the reactor liquid surface. One hundred mL of reactor contents was discarded to clear the sampling tube before the pumped sample was collected. Direct samples were collected by pressurizing the reactor with N_2, opening the septum port, and pipetting 10 mL from 45 mm below the liquid surface.

Because the concentrations of dissolved and suspended parameters varied from day to day, the best way to compare the pumped samples with the direct samples was to normalize them by dividing the pumped value by the direct value. Then, the normalized values were averaged and compared to unity by the t test (Tables D.2 and D.3). If there was sulfide oxidation in the effluent tube, one would expect normalized values to be higher than unity for bchl, elemental sulfur and sulfate, and less than unity for sulfide. The null hypotheses for the t tests were that the (pumped concentration)/(direct concentration) = 1. The alternative hypotheses were that the ratio was >1 for bchl, S^0 and $SO_4^=$ and was <1 for $S^=$.

The critical values for $t_{c,n-1}$ at the 95% confidence level are 2.015 for n=6 and 2.353 for n=4. For sulfide, the calculated T, -0.1, is not less than -2.015 so the null hypothesis cannot be rejected. In the case of the other parameters, $T < t_{\alpha,n-1}$ therefore, the null hypothesis cannot be rejected. Therefore, in all cases, the pumped sample concentration and directly sampled concentration were not statistically different.

TABLE D.2 Comparison of pumped and direct-sampled soluble parameter measurements from the reactor in Trial 9

Date	S= (mg/L)				SO$_4$= (mg/L)			
	Dir.	Pump	P/D	T	Dir.	Pump	P/D	T
Mar. 22, 1994	56	31	0.55		-	-	-	
Mar. 29, 1994	8	7	0.88		-	-	-	
Apr. 22, 1994	3	2	0.67		27	31	1.13	
Apr. 26, 1994	23	23	1.00		29	35	1.22	
May 4, 1994	27	28	1.04		34	29	0.87	
May 6, 1994	21	30	1.43		33	28	0.84	
	average = std. dev. =		0.93 0.31	-0.1	average = std. dev. =		1.01 0.19	0.03

Dir. = sampled directly from reactor, Pump = sampled from pumped effluent, P/D = ratio of pumped concentration to directly sampled concentration, T = calculated t test statistic.

168

TABLE D.3   Comparison of pumped and direct-sampled suspended parameter measurements from the reactor in Trial 9

Date	S^0 (mg/L)				bchl (mg/L)			
	Dir.	Pump	P/D	T	Dir.	Pump	P/D	T
Mar. 22, 1994	270	545	2.02		5.4	7.4	1.37	
Mar. 29, 1994	483	541	1.12		8.7	8.7	1.00	
Apr. 22, 1994	1054	557	0.53		3.7	3.8	1.03	
Apr. 26, 1994	971	1505	1.55		3.2	3.3	1.03	
May 4, 1994	623	1145	1.84		2.6	2.9	1.12	
May 6, 1994	615	940	1.53		2.7	3.1	1.15	
	average = std. dev. =		1.43 0.54	0.33	average = std. dev. =		1.12 0.14	0.36

Dir. = sampled directly from reactor, Pump = sampled from pumped effluent, P/D = ratio of pumped concentration to directly sampled concentration, T = calculated t test statistic.

APPENDIX E

CALCULATION OF THE MINIMUM HYDRAULIC RETENTION TIME

An initial estimate of the HRT was needed to select pumps and operate the reactor. If the HRT selected was too short, the biomass would have been flushed out of the reactor faster than it could grow.

A continuous reactor operated without recirculating the biomass, as used in this dissertation, is sometimes referred to as a once-through reactor, or a chemostat. For the once-through bioreactor, the HRT equals the cell residence time. When steady state operation is reached, the cell residence time equals the inverse of the specific growth rate, μ, of the biomass (Gaudy & Gaudy, 1980).

The net specific growth rate, μ', of C. thiosulfatophilum in batch reactors has been determined (Henshaw, 1991):

$$\mu' = \frac{\mu_m S K_s}{(K_s + S)^2} - k_d S \qquad \text{[E-1]}$$

where μ_m is the maximum specific growth rate = 0.558 h^{-1}
S is the reactor sulfide concentration (mg/L)
K_s is the saturation constant = 94.1 mg/L
k_d is the endogenous decay coefficient = 0.000262 L/mg·h

Wash-out of the reactor contents occurs when the reactor $S^=$ concentration, $[S^=]$, equals the influent $S^=$ concentration, $[S^=]_i$. At washout, when $[S^=]_i$ = 100 mg/L, $[S^=]$ = 100 mg/L, μ' = 0.113 h^{-1}, and HRT_{min} = 1/(0.113 h^{-1}) = 8.8 hours. At an HRT less than 8.8 hours, the biomass would be flushed-out of the reactor. The minimum HRT is multiplied by a safety factor of 2 to 20 to determine the operating HRT (Metcalf & Eddy, 1991).

A safety factor of 5 was used. Thus, the operating HRT for Run 3 was 5(8.8)= 44 hours.

APPENDIX F

INTERPRETATION OF FEED SOLUTION CONCENTRATIONS

F.1 Sulfide

For each feed solution (NM or SSS) daily readings of sulfide concentration were taken and used to calculate the $S^=$ loading to the reactor. The condition of the reactor was assessed at that time and a new loading was determined. The sulfide concentration of each feed solution over the next day was estimated, assuming a slight decrease in $S^=$ concentration with time. Then, the pumps were adjusted to provide this loading. The estimated concentrations were only as good as the $S^=$ measurement on that day.

A particular day's sulfide concentration measurement of the feed solution could be higher or lower than the previous days. However, in general, the concentration of sulfide decreased with time (Figure F.1). The best approximation of the *true* sulfide concentration would be a curve of best fit through the daily sulfide measurements. The question arises about the nature of the curve, *i.e.* it could be a linear, logarithmic or some other function of time.

Two approaches were investigated. The first and simplest was to plot the $S^=$ concentration against time for each batch of solution and try to fit various curves to this plot. The second approach was to perform a mass balance on the vessel containing the solution and replace the differential in the accumulation term with a finite difference. This could then be used to predict the sulfide concentration at the next time step if the flow rate was known. Calculations were performed on the data from Trials 9 and 10 because these experiments had the greatest number of batches of nutrient medium (NM)
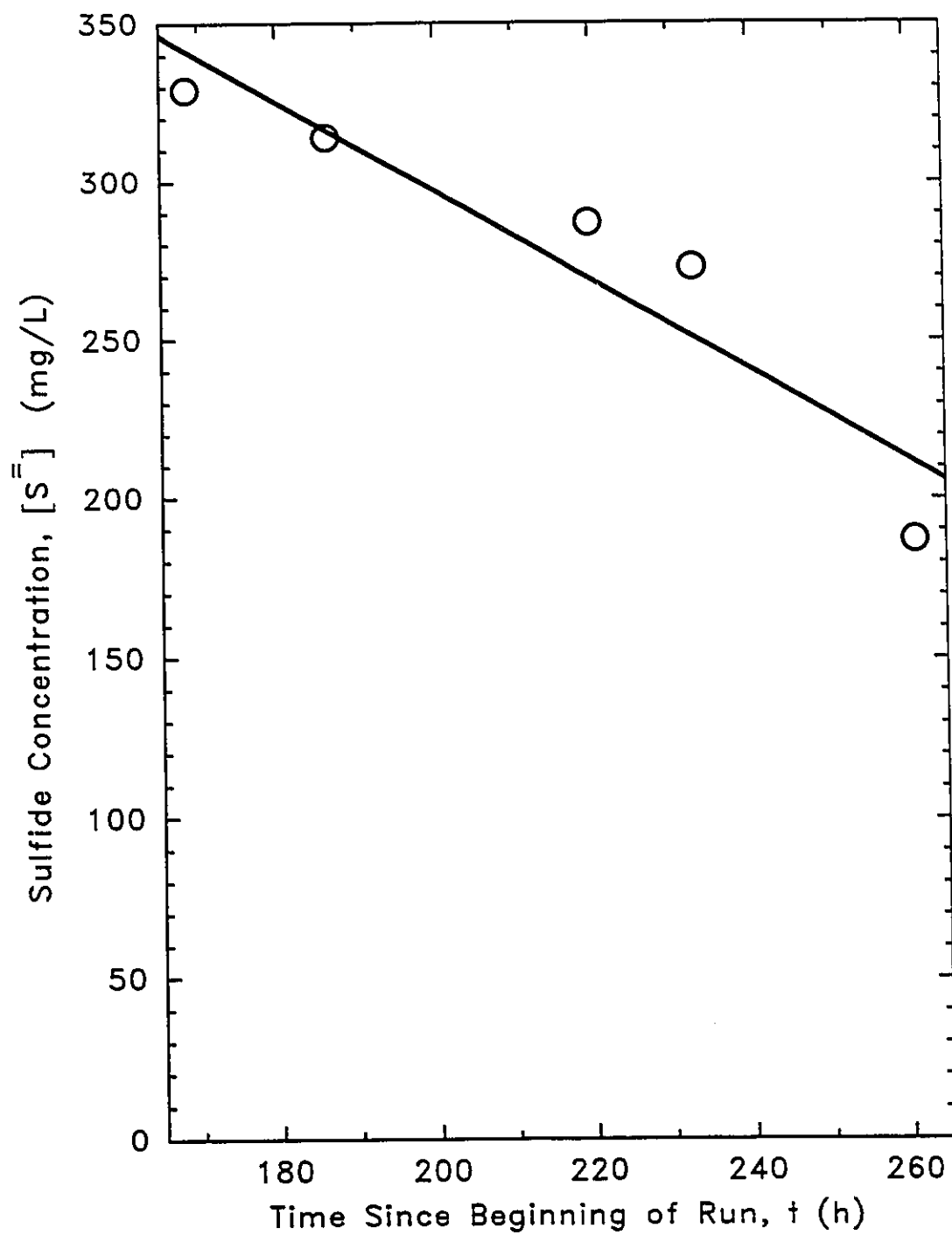
FIGURE F.1 Typical decay of sulfide in the nutrient medium

173

and sulfide stock solution (SSS).

F.1.1 Concentration versus Time

Four predictive equations of $S^=$ concentration against time were tested: zero order

(linear), first order, Chen's equation and differential analysis.

F.1.1.1 Zero Order (Linear)

This equation assumes that the rate of change in sulfide concentration is constant:

$$\frac{d[S^-]}{dt} = m \qquad\qquad \text{[F-1]}$$

Which integrates to:

$$[S^-] = [S^-]_0 + mt \qquad\qquad \text{[F-2]}$$

So that the $S^=$ concentration is a linear function of time.

F.1.1.2 First Order

This prediction assumes that the rate of change in sulfide concentration is

proportional to the $S^=$ concentration at that time:

$$\frac{d[S^-]}{dt} = k[S^-] \qquad\qquad \text{[F-3]}$$

Which integrates to:

$$\ln[S^-] = \ln[S^-]_0 - kt \qquad\qquad \text{[F-4]}$$

So that ln([S$^=$]) is a linear function of time.

F.1.1.3 Chen's Equation

Chen (1972) observed that the rate of change of total sulfide in solution was a

function of total sulfide and oxygen concentrations:

$$\frac{d[S^-]}{dt} = -k_c[S^-]^{1.34}[O_2]^{0.56} \qquad \text{[F-5]}$$

Assuming $[O_2]$ is constant in the feed solution vessel, the equation integrates to:

$$[S^-]^{-0.34} = k_c't + [S^-]_0^{-0.34} \qquad \text{[F-6]}$$

where: k_c' is $0.34 \cdot k_c \cdot [O_2]^{0.56}$

Thus, $[S^-]^{-0.34}$ is a linear function of time.

F.1.1.4 Differential Analysis

This is a method of determining the order of the reaction, without assuming any relationship, by integrating and testing the data in the integrated form. The generalized rate equation:

$$-r_A = k[A]^n \qquad \text{[F-7]}$$

is evaluated at two different times, 1 and 2, resulting in the following two equations:

$$(-r_A)_1 = k[A]_1^n \qquad \text{[F-8]}$$

$$(-r_A)_2 = k[A]_2^n \qquad \text{[F-9]}$$

Dividing Equation F-8 by F-9 gives:

$$\frac{(-r_A)_1}{(-r_A)_2} = \left(\frac{[A]_1}{[A]_2}\right)^n \qquad \text{[F-10]}$$

Taking the natural logarithm of both sides results in:

$$\ln\left[\frac{(-r_A)_1}{(-r_A)_2}\right] = n \cdot \ln\left(\frac{[A]_1}{[A]_2}\right) \qquad \text{[F-11]}$$

Thus, a plot of the logarithm of the ratio of reaction rates against the logarithm of the

ratio of concentrations should give a straight line with slope "n". The batches of nutrient medium in Trial 10 typically lasted 3 to 4 days, so there were 3 to 5 readings of concentration and 2 to 4 calculated rate values. For some batches, the rate of $S^=$ consumption between two points may be positive but the subsequent rate may become negative, because of the fluctuations in concentration. Since the logarithm of a negative value is undefined, the differential analysis was not applied in such cases.

F.1.1.5 Tabulation

Different functions between rate and concentration, outlined in Sections F.1.1.1 to F.1.1.4 were calculated and linear regressions were performed using the time from the beginning of the experiment as the independent variable and the concentration function as the dependant variable. The coefficient of determination (R^2) was calculated and tabulated.

In Tables F.1 to F.4 the zero order (linear) approximation shows the highest coefficient of determination in 15 out of 30 batches of NM in Trials 9 and 10. Since the linear approximation is the simplest to use, and gave better correlation in half of the cases, it was chosen for use in Runs 3 to 5. As for the SSS, the zero order rate equation fit the data best in 10 out of 19 batches in Trials 9 and 10. In some cases, the sulfide stock solution concentration decreased rapidly on the last day of use. For these cases, the above analysis was performed on the first part of the batch and the concentration between the last and second last days was calculated by linear interpolation.

There were insufficient data to compute the order of reaction by the differential analysis method in Trial 10. Tables F.1 and F.2 show that only three batches of NM had

176

TABLE F.1 Predictive equations in the nutrient medium of Trial 10

Batch No.	No. Pt.	Concentration vs Time					Diff. Anal. n	Mass Balance				
		Zero Order (Linear)			Chen Eqn. R^2	First Order R^2		$-r_{LOSSES}$ vs [S⁻]			Dev. from Data	
		Slope	Inter.	R^2				Slope	Inter.	R^2	Linear	Mass B
1	3	-0.1994	97.69	0.16	0.11	0.12	U	0.1015	0.3	0.01	14	25
2	4	-0.07483	78.21	0.06	0.08	0.07	U	-0.06014	3.2	0.17	10	13
3	3	-0.5894	308.5	0.77	0.70	0.72	U	0.2039	-11.0	0.72	15	10
4	3	-0.3233	210.0	1.00	1.00	1.00	1.46	0.1202	-5.1	0.89	1	11
5	4	-0.5571	374.5	0.76	0.74	0.75	U	0.2515	-14.5	0.55	16	14
6	3	-0.02287	77.14	0.28	0.29	0.29	U	-1.723	11.1	0.22	2	8
7	4	+0.1436	-41.27	0.46	0.50	0.49	U	-	-	-	-	-
8	3	-0.5911	503.1	0.63	0.64	0.64	U	0.3212	-10.3	0.48	23	35
9	4	-0.3443	344.0	0.68	0.64	0.65	U	0.1707	-7.8	0.29	10	18
10	4	-0.3941	423.0	0.74	0.76	0.75	14.6	0.3256	-18.4	0.71	12	11
11	3	-0.4387	487.5	0.61	0.48	0.52	U	-0.1671	9.0	0.54	18	19
12	5	-0.5752	669.9	0.92	0.95	0.94	U	0.2015	-10.0	0.87	5	3
13	3	-0.2110	297.4	0.99	1.00	1.00	3.15	0.1796	-9.4	0.82	1.6	1.8
14	4	-0.06117	120.6	0.23	0.24	0.24	U	-0.04123	2.0	0.01	32	60

No.Pt. = number of measured points in the batch, Inter. = intercept, R^2 = coefficient of determination, Chen Eqn. = Chen's equation, Diff. Anal. n = value of "n" from differential analysis, Dev. form Data = deviation of predicted values from actual, Linear = zero order equation, Mass B. = mass balance, U = undefined.

177

TABLE F.2 Predictive equations in the sulfide stock solution of Trial 10

Batch No.	No. Pt.	Concentration vs Time						Mass Balance				
		Zero Order (Linear)			First Order R^2	Chen Eqn. R^2	Diff. Anal. n	$-r_{LOSSES}$ vs $[S^=]$			In Each Batch	
		Slope	Inter.	R^2				Slope	Inter.	R^2	Mean	Std.Dev.
1	4	-2.147	1100	0.30	0.35	0.37	U	0.007050	0.6	0.06	6.05	6.4
2	4*	-0.6093	2327	0.03	0.03	0.03	U	-0.00670	18.9	0.16	1.76	11.9
3	7	-5.972	5986	0.83	0.72	0.70	-7.0	0.1021	-226.0	0.06	0.54	46.8
4	7*	-2.054	4355	0.74	0.73	0.73	20.9	0.02241	-62.6	0.08	6.22	9.8
5	4*	-0.8878	2975	0.38	0.37	0.37	U	-0.09295	213.4	0.08	4.66	12.0
6	8	-4.284	6462	0.44	0.42	0.42	U	0.00596	-14.0	0.02	0.88	18.4
7	7	-4.915	7896	0.50	0.50	0.50	U	-0.01996	43.8	0.36	0.24	17.3

No.Pt. = number of measured points in the batch, Inter. = intercept, R^2 = coefficient of determination, Chen Eqn. = Chen's equation, Diff. Anal. n = value of "n" from differential analysis, In Each Batch = mean and standard deviation of all of the rate of loss value from each batch, * = an additional point was measured but not used in fitting these curves, U = undefined (logarithm of a negative number).

178

TABLE F.3 Predictive equations in the nutrient medium of Trial 9

Batch No.	No. Pt.	Concentration vs Time			
		Zero Order (Linear)			Chen's Equation R^2
		Slope	Intercept	R^2	
1	2	-0.8770	238.0	1.00	-
2	5	-1.405	578.1	0.87	0.80
3	5	-0.5522	377.2	0.63	0.62
4	5	-1.442	654.6	0.79	0.85
5	4	-0.4995	291.0	0.90	0.94
6	4	-0.1988	161.7	0.35	0.35
7	4	-0.6558	446.9	0.97	1.00
8	5	-0.7971	618.1	0.83	0.82
9	5	-0.5530	482.5	0.92	0.87
10	7	-0.07408	124.0	0.39	0.37
11	6	-0.2737	346.7	0.72	0.73
12	5	-0.5096	632.6	0.90	0.86
13	6	-0.2574	377.5	0.51	0.55
14	7	-0.2454	405.8	0.54	0.49
15	4	-0.09019	191.6	0.22	0.18
16	5	-0.2573	490.6	0.82	0.81

No.Pt. = number of measured points in the batch, R^2 = coefficient of determination.

TABLE F.4 Predictive equations in the sulfide stock solution of Trial 9

Batch No.	No. Pt.	Concentration vs Time			
		Zero Order (Linear)			Chen's Equation R^2
		Slope	Intercept	R^2	
1	2	0.08511	657	1.00	-
2	12	-2.495	2825	0.54	0.55
3	7	-0.8966	2480	0.04	0.06
4	11	-6.289	9622	0.46	0.46
5	6	-3.611	5824	0.24	0.20
6	5	-0.8908	3741	0.52	0.51
7	6	-6.074	9553	0.40	0.40
8	9	-3.844	7703	0.56	0.58
9	7	-2.958	6920	0.53	0.51
10	3	10.71	-14060	0.83	0.84
11	4	-10.74	20774	0.95	0.96

No.Pt. = number of measured points in the batch, R^2 = coefficient of determination.

sufficient data to yield a value for the order, and these values ranged from 1.5 to 14.6. Similarly, there were insufficient or poor SSS data, and only two values were obtained for "n", -7.0 and 20.9.

F.1.2 Mass Balance

In this approach, a mass balance on sulfide (Equation 4-1) was applied to the vessels containing sulfide stock solution or nutrient medium in Trial 10. The input flowrate to the vessel was zero. The rate of formation term was replaced by the rate of losses (through chemical reaction with the oxygen in the water or volatilization):

$$\begin{pmatrix} Rate\ of \\ Accumulation \\ of\ S^- \end{pmatrix} = - \begin{pmatrix} Rate\ of \\ Output \\ of\ S^- \end{pmatrix} - \begin{pmatrix} Rate\ of \\ Loss \\ of\ S^- \end{pmatrix} \qquad [\text{F-12}]$$

Where the rate of accumulation of $S^=$ is:

$$\begin{pmatrix} Rate\ of \\ Accumulation \\ of\ S^- \end{pmatrix} = \frac{[S^-]_2 V_2 - [S^-]_1 V_1}{t_2 - t_1} \qquad [\text{F-13}]$$

and the rate of output is:

$$\begin{pmatrix} Rate\ of \\ Output \\ of\ S^- \end{pmatrix} = \frac{0.06(f_1[S^-]_1 + f_2[S^-]_2)}{2} \qquad [\text{F-14}]$$

Therefore the loss at each time step can be calculated.

For the NM there was a correlation ($R^2 > 0.54$) between the rate of loss and the S^- concentration in 6 out of 13 batches (Table F.1). The slopes and intercepts of those batches with a good correlation were averaged, and a predictive equation was derived from the mass balance equation using the average slope and intercept:

$$[S^=]_2 = \cfrac{\cfrac{[S^=]_1 V_1}{t_2 - t_1} - \cfrac{0.06[S^=]_1 f_1}{2} - intercept}{\cfrac{V_2}{t_2 - t_1} + \cfrac{0.06 f_2}{2} + slope} \qquad [\text{F-15}]$$

This equation was used to predict the $S^=$ concentration at the "next step" (t_2) where the concentration at the "present" time (t_1) was known. The $[S^=]$ was predicted in this step-wise manner for each day of the nutrient medium batch. In order to compare this method with the linear approximation from Section F.1.1, the predicted values of concentration were subtracted from the daily measured values, the result squared, and the squares summed over the duration of the batch. The square roots of the sum of squares are listed in Table F.1 as "Dev. from Data". As this table shows, the deviation calculated for the mass balance method was greater than that from the linear method in 9 out of 13 cases.

For the SSS, there was neither a correlation between the losses from the solution vessel and the $S^=$ concentration in the vessel, nor a constant average loss for all of the batches (Table F.2). Thus, there was no basis for a predictive model using mass balance in the case of the sulfide stock solution. This was surprising since the sulfide stock solution was the simpler of the two vessels, having no gas trap or N_2 blanket.

F.1.3 Conclusion

The assumption that $S^=$ concentration was a linear function of time was the best way of predicting the $S^=$ concentration in the nutrient medium and sulfide stock solution in Trials 9 and 10. To that end, the values of slope and intercept in Tables F.1 to F.4 were used in place of measured concentrations in the spreadsheets used to tabulate the concentration of all species. For Runs 3 to 5, the $S^=$ concentration in each batch of SSS

was assumed to be a linear function of time, and the slope and intercept of the line of best fit through the raw data were used in the spreadsheets.

F.2 Sulfate and Elemental Sulfur

In Runs 3 to 5, the $SO_4^=$ and S^0 concentrations were measured at the beginning and end of each SSS batch. The values increased with time because $SO_4^=$ and S^0 are products of $S^=$ oxidation. Values at times between these measures were determined by linear interpolation between the beginning and end points. Where only one point in a batch was available, it was used throughout the batch.

Throughout the duration of each CNS batch, two to four measurements of sulfate concentration in the CNS or combined CNS and water were made in Runs 3 to 5. Although these values did not change much, the $SO_4^=$ concentration was predicted by linear regression through the measured values.

Values of $SO_4^=$ and S^0 concentrations in the feed solutions were typically measured only at the times of the sulfur species characterizations in Trials 9 and 10. These values were assumed to be constant around the time of the characterization.

APPENDIX G

CALCULATION OF BIOMASS PARAMETERS FROM LITERATURE

G.1 Introduction

Maka and Cork (1990) operated a gas-fed batch reactor in experiments lasting 17 hours. In terms of bacteria, there was no input or output so the mass balance Equation 4-3 simplifies to:

$$\frac{dX}{dt} = r_x = \mu X \qquad \text{[G-1]}$$

Maka and Cork used the term k instead of r_x. k was calculated as $\Delta X/\Delta t = (X_{17} - X_0)/(17$ hours), where X_{17} and X_0 are the bchl concentrations at 17 and zero hours respectively. Separate specific growth rates were calculated at the beginning and end of each experiment:

$$\mu_0 = \frac{k}{X_0} \qquad \text{[G-2]}$$

$$\mu_{17} = \frac{k}{X_{17}} \qquad \text{[G-3]}$$

Strictly speaking, the value of μ is calculated by integrating Equation G-1:

$$\mu = \frac{dX}{X\,dt} = \frac{lnX_2 - lnX_1}{t_2 - t_1} = \frac{ln\left(\dfrac{X_2}{X_1}\right)}{t_2 - t_1} \qquad \text{[G-4]}$$

Which is often approximated as:

$$\mu = \frac{\Delta X}{\bar{X} \, \Delta t} = \frac{X_2 - X_1}{\left(\dfrac{X_2 + X_1}{2}\right)(t_2 - t_1)} = \frac{2(X_2 - X_1)}{(X_2 + X_1)(t_2 - t_1)} \qquad \text{[G-5]}$$

Franklin (1978) provides a series to calculate the logarithm:

$$\ln(x) = 2\left[\frac{x-1}{x+1} + \frac{1}{3}\left(\frac{x-1}{x+1}\right)^3 + \frac{1}{5}\left(\frac{x-1}{x+1}\right)^5 + \dots\right] \qquad \text{[G-6]}$$

Substituting X_2/X_1 into the first term of this series gives:

$$\ln\left(\frac{X_2}{X_1}\right) = 2\left[\frac{\dfrac{X_2}{X_1} - 1}{\dfrac{X_2}{X_1} - 1}\right] = 2\left[\frac{X_2 - X_1}{X_2 + X_1}\right] \qquad \text{[G-7]}$$

so that Equation G-5 approximates the analytical solution (Equation G-4) for the first term of the series.

G.2 Calculating the Average Bacterial Concentration

Maka and Cork reported only the values of μ_0 and μ_{17}. It was necessary to calculate the bchl concentration in order to plot the modified form of the van Niel curve (Section 4.2.4). If Equation G-2 is divided by Equation G-3, then:

$$\frac{\mu_0}{\mu_{17}} = \frac{X_{17}}{X_0} \qquad \text{[G-8]}$$

This was substituted into the expression for the average bacteria concentration:

$$\bar{X} = \frac{X_0 + X_{17}}{2} = \frac{\dfrac{X_0}{X_0} + \dfrac{X_{17}}{X_0}}{\dfrac{2}{X_0}} = X_0\left(\frac{1 + \dfrac{\mu_0}{\mu_{17}}}{2}\right) \qquad \text{[G-9]}$$

185

The X versus time plots in Maka and Cork's work show that the initial value of X, X_0 was typically 25 mg/L. Thus, the value of $\overline{X}$ was calculated from Equation G-9.

G.3 Calculating the Average Specific Growth Rate

For fitting the data to the models discussed in Chapter 5, the average value of the specific growth rate was required. This was calculated from the μ_0 and μ_{17} values as follows. Using the approximation of Equation G-5:

$$\mu = \frac{k}{\overline{X}} = \frac{2k}{X_0 + X_{17}} \qquad \text{[G-10]}$$

Inverting:

$$\frac{2}{\mu} = \frac{X_0 + X_{17}}{k} = \frac{X_0}{k} + \frac{X_{17}}{k} \qquad \text{[G-11]}$$

Using the relationships in Equations G-2 and G-3:

$$\frac{2}{\mu} = \frac{X_0}{\mu_0 X_0} + \frac{X_{17}}{\mu_{17} X_{17}} = \frac{1}{\mu_0} + \frac{1}{\mu_{17}} = \frac{\mu_0 + \mu_{17}}{\mu_0 \mu_{17}} \qquad \text{[G-12]}$$

Therefore the average specific growth rate can be calculated:

$$\mu = \frac{2\mu_0 \mu_{17}}{\mu_0 + \mu_{17}} \qquad \text{[G-13]}$$

186

APPENDIX H

CARBON DIOXIDE AS A NON-LIMITING SUBSTRATE

H.1 Assumption

Carbon dioxide is the substrate for *C. thiosulfatophilum*, and sulfide is the primary electron donor. The experiments in this dissertation dealt with the effect of sulfide on the metabolism of GSB, and to that end, the supply of CO_2 could not limit the metabolism of the bacteria. The reduction of the carbon in CO_2 to a valence of zero requires 4 electrons. Therefore, 2 moles of $S^=$ must be oxidized to S^0 for each mole of CO_2 assimilated (Equation 2-2).

H.2 Calculation

The available CO_2 in the CNS (Runs 3, 4, and 5) and the NM (Trials 9 and 10) was calculated as follows.

H.2.1 Concentrated Nutrient Solution (CNS)

Sources of CO_2:

1. 15 L of deH_2O saturated with CO_2

   •solubility of CO_2 in water at 25°C = 0.145 g/100 mL   (CRC, 1980)

   (15 L x 1.45 g CO_2/L)/(44.0 g CO_2/mole)   = 0.50 mole CO_2

2. 150 g of $NaHCO_3$

   (150 g $NaHCO_3$)/(84.0 g $NaHCO_3$/mole)   = 1.78 mole $NaHCO_3$
   = 1.78 mole CO_2

Total: (0.50 + 1.78) mole CO_2 = 2.28 mole CO_2

Sulfide that could have been utilized:

$$2.28 \text{ mole } CO_2 \times 2 \text{ mole } S^=/\text{mole } CO_2 = 4.56 \text{ mole } S^=$$

Equivalent concentration of $S^=$:

$$(4.56 \text{ mole } S^= \times 32.0 \text{ g } S^=/\text{mole})/15 \text{ L} = 9.73 \text{ g } S^=/L$$

The CNS was diluted by 1/5 in the reactor influent:

$$(9.73 \text{ g } S^=/L)/5 = 1.95 \text{ g } S^=/L = 1950 \text{ mg } S^=/L$$

Therefore, the CNS had enough CO_2 to oxidize an effective inlet $S^=$ concentration of 1950 mg $S^=/L$. In Runs 3, 4, and 5 the highest $[S^=]_i$ was 260 mg $S^=/L$ (Table 3.2), so the CO_2 was more than adequate.

H.2.2 Nutrient Medium (NM)

Sources of CO_2:

1. 3.6 L of deH_2O saturated with CO_2

   •solubility of CO_2 in water at 25°C = 0.145 g/100 mL   (CRC, 1980)

   $$(3.6 \text{ L} \times 1.45 \text{ g } CO_2/L)/(44.0 \text{ g } CO_2/\text{mole}) = 0.12 \text{ mole } CO_2$$

2. 20.0 g of $NaHCO_3$

   $$(20.0 \text{ g } NaHCO_3)/(84.0 \text{ g } NaHCO_3/\text{mole}) = 0.24 \text{ mole } NaHCO_3$$
   $$= 0.24 \text{ mole } CO_2$$

Total: $(0.12 + 0.24) \text{ mole } CO_2 = 0.36 \text{ mole } CO_2$

Sulfide that could have been utilized:

$$0.36 \text{ mole } CO_2 \times 2 \text{ mole } S^=/\text{mole } CO_2 = 0.72 \text{ mole } S^=$$

Equivalent concentration of $S^=$:

$$(0.72 \text{ mole } S^= \times 32.0 \text{ g } S^=/\text{mole})/9.0 \text{ L} = 2.56 \text{ g } S^=/L$$

The NM was diluted by 1/1.11 in the reactor influent:

$$(2.56 \text{ g } S^=/L)/1.11 = 2.31 \text{ g } S^=/L = 2310 \text{ mg } S^=/L$$

Therefore, at the beginning of a batch of NM, the CO_2 in the NM could have supported an effective inlet sulfide concentration of 2310 mg $S^=/L$. However, N_2 was used to pressurize the headspace of the reactor and this may have carried away some CO_2 as well as H_2S. Two assumptions were made to predict the CO_2 loss into the headspace gas:

1. The loss of CO_2 was proportional to the loss of H_2S.

2. The decrease in H_2S in the NM was entirely due to volatilization into the headspace. This was a conservative assumption since chemical oxidation was also taking place in the NM.

The greatest decrease in $S^=$ concentration in the nutrient medium occurred in batch number 4 of Trial 9 (Table F.3). The rate of $S^=$ decrease was 1.44 mg $S^=/h \cdot L$. The measured $S^=$ concentration decreased from 202 mg/L to 48 mg/L, a 76% reduction. Following the assumptions above, the CO_2 in the NM also decreased by 76%. Therefore, the CO_2 at the end of the batch required (2310 mg $S^=/L$)x(1 - 0.76) = 554 mg $S^=/L$. The highest $[S^=]_i$ in Trials 9 and 10 was 490 mg/L (Table 3.2) which means that CO_2 was non-limiting.

VITA AUCTORIS

NAME   Paul Henshaw

PLACE OF BIRTH   Windsor, Ontario

YEAR OF BIRTH   1961

EDUCATION   Centennial Secondary School, Windsor, Ontario
                        1974-1979

                        University of Western Ontario, London, Ontario
                        1979-1982 B.Sc. (Chemistry)

                        University of Western Ontario, London, Ontario
                        1982-1985 B.Eng.Sc. (Mechanical)

                        University of Windsor, Windsor, Ontario
                        1988-1990 M.A.Sc. (Environmental)

                        University of Windsor, Windsor, Ontario
                        1990-1995 Ph.D. (Environmental Engineering)